AD 740852

RHEOLOGY OF FRICTION-REDUCING POLYMER SOLUTIONS

by

P. I. Gold

and

P. K. Amar

DEPARTMENT OF MECHANICAL ENGINEERING

March, 1971

Reproduced by
NATIONAL TECHNICAL
INFORMATION SERVICE
Springfield, Va 22151

DDC
RECEIVED
APR 28 1972
B

CALIFORNIA STATE COLLEGE
1947
LOS ANGELES

APPROVED OR PUBLIC RELEASE: DISTRIBUTION UNLIMITED.

173

RHEOLOGY OF FRICTION REDUCING POLYMER SOLUTIONS

by

P. I. Gold

and

P. K. Amar

Department of Mechanical Engineering
California State College, Los Angeles

This research was conducted under the sponsorship of the Naval Undersea Research and Development Center, Pasadena California, under contract No. N68001-70-C-0723.

Abstract

Stress decay characteristics of concentrated (0.14% - 1.03%) PEO solutions were measured. Apparent viscosity loses of up to 50% were recorded at 30°C. Shear rates ranged up to 1370/sec^{-1}. Limiting viscosities were found to be relatively independent of solution history. Moreover, limiting viscosities could be correlated by a power-law model over a four decade shear rate range.

Disk flow was used to investigate the phenomenon of turbulent drag reduction and subsequent mechanical degradation of dilute aqueous solutions of polyethylene oxide. The relationship of drag reduction and degradation to the molecular weight, solution concentration and temperature was investigated. Reduced viscosity measurements (which are a measure of molecular weight of polymer) were carried out directly on the dilute solutions tested.

It was found that the extent of initial drag reduction, except for very low concentrations, is essentially independent of the polymer molecular weight for this particular apparatus. In addition, lower molecular weight polymers degraded more slowly than higher molecular weight polymers if comparison was made in terms of degradation of reduced viscosity rather than in decrease of percent drag reduction. The results also indicated that the drag reduction depends primarily on the high molecular weight components of the distribution. The failure of reduced viscosity to correlate with drag reduction degradation was also noted. The rate of degradation of drag reduction was found to be very severe at higher temperatures.

It was determined that the shearing of concentrated solutions did not cause any measurable change in drag reduction effectiveness and degradation characteristics of subsequently diluted forms.

Table of Contents

		page
	Abstract	ii
1.0	Introduction	1
2.0	Summary of Results	3
2.1	Concentrated Solution Rheology	3
2.2	Friction Reduction in Dilute Solutions	4
3.0	Experiment Techniques and Procedures	6
3.1	Polymers Studied	6
3.2	Solution Preparation Techniques	6
3.2.1	Vortex Mixer Method	6
3.2.2	Boiling Water Method	8
3.3	Stress Decay and Viscosity Measurements in Concentrated Solutions	8
3.4	Turbulent Flow Rheometer	14
3.5	Characterization of Dilute Polymer Solutions	15
3.5.1	Viscometer	15
3.5.2	Capillary Flow Relations	16
3.5.3	Intrinsic Viscosity and Molecular Weight Relations	18
	Figures	22
4.0	Rheology of Concentrated Solutions	31
4.1	General	31
4.2	Rheology of Concentrated PEO Solutions	34
4.2.1	Stress Decay Characteristics of Concentrated PEO Solutions	36
4.2.2	Step Sequence Experiments	52
	Figures	58
5.0	Frictional Drag Reduction in Dilute PEO Solutions	83
5.1	Introduction	83
5.1.1	Preliminary Remarks	83
5.1.2	Theories of Drag Reduction	84
5.1.3	Polymer Degradation	87
5.1.4	Enclosed Disk Flow	89
5.1.5	Objectives of the Present Investigation	91
5.2	Effect of Shearing Thick Solutions on Drag Reduction Effectiveness and Mechanical Degradation	92
5.3	Mechanical Degradation of Dilute Solutions of PEO in a Turbulent Field	95
5.3.1	Theoretical Background	95
5.3.2	Experimental Results	98
5.4	The Effect of Temperature on Drag Reduction and Mechanical Degradation	107
5.5	Effect of Static Storage of Master Solutions on Drag Reduction	110
5.6	Static Viscosity Degradation of Dilute Solutions	111
	Figures	112

		page
6.0	Conclusions and Recommendations	136
6.1	Recommendations for Continuing Efforts	139
7.0	Bibliography	141
8.0	Appendix I. End Corrections for Filled Cup-Newtonian Fluid	145
9.0	Appendix II. Kinetic Energy Correction	148
10.0	Appendix III. Wall Shear Rate of Capillary Viscometer . . .	149
11.0	Appendix IV. Data Tables	150
12.0	Appendix V. Power Law Analysis of Miscellaneous Preliminary Data	166

1.0 Introduction.

Many of the physical characteristics of solutions of polyethylene oxide are sensitive to mechanical degradation effects encountered in mixing and handling processes. In particular, rheological properties have proved to be strongly dependent upon the mode of solution preparation (28, 29).[1] That is shearing action due to agitation during preparation can influence the measured rheological properties of a solution. This sensitivity to mechanical effects is due largely to the rather complex molecular structure of these solutions. Thus, even in relatively dilute solutions, a high degree of molecular entanglement exists between and within long chain polymer molecules. Coupled with the existence of relatively weak and easily ruptured inter-chain hydrogen bonds and the possibility of actual polymer chain scission under the action of shearing forces this leads to the so-called "viscosity loss" so often observed in concentrated solutions.

The principal objective of this research has been the determination of the critical rheological properties of aqueous solutions of polyethylene oxide and the development of a molecular interpretation of these properties, particularly as they may relate to the friction reducing characteristics of very dilute solutions.

In the next section, a brief summary of the results of the research conducted during this program is presented. Section 3.0 provides a detailed description of instrumental techniques and experimental procedures. The results of the study of the rheological characteristics of concentrated

---

[1] Numbers in parentheses refer to references listed at the end of this report.

solutions are described in Section 4.0. An extensive investigation of the friction reducing characteristics of very dilute solutions is contained in Section 5.0. Emphasis here is placed upon the influence of mechanical degradation of friction reduction. A review of the principle conclusions steming from these results, as well as recommendations for future efforts is provided in Section 6.0. A number of analytical developments and data summaries are relegated to the appendices at the end of this report.

2.0 Summary of Results.

The principal efforts of this research were directed along two distinct channels. First, was the study of the viscometric characteristics of concentrated solutions, with particular emphasis on time-dependent rheology. The second area of emphasis was centered about the investigation of turbulent flow friction reducing characteristics of very dilute solutions. In this case, the influence of mechanical degradation on polymer molecular weight and friction reduction capability received primary attention.

These topics are treated in detail in the following sections. The purpose of this section is to provide a brief summary of the essential results of these studies.

2.1 Concentrated Solution Rheology.

A key factor in describing the rheological characteristic of concentrated polyethylene oxide solutions is the recognition of the importance of time dependence of those characteristics. In this work, relatively unsheared "fresh" solutions were prepared using the vortex mixer described in section 3.0. Solutions in the concentration range of 0.14% - 1.03% (by weight) of polymer were prepared. Each solution was sheared at a series of constant shear rates ranging from 25 sec^{-1} to 1370 sec^{-1}, and the time-dependent shear stress response was recorded until a steady-state shear stress response obtained. At that point, a series of steady-state shear stress readings at successively lower shear rates were obtained. All experiments were conducted at 30°C ± 0.1°C.

The stress decay experiments revealed that limiting apparent viscosities obtained after long periods of shear were from 25 - 50% lower than that

observed at the start of shearing. Stress decay rates, being due to complex molecular rate processes, however, did not correlate with simple mechanical models for viscoelasticity. A comparison of limiting viscosities obtained after each stress decay experiment revealed that limiting viscosity is essentially independent of the shear rate at which the fluid is "worked" during stress decay, but depends only upon the shear rate at which it is measured. This conclusion, of course, is restricted to the shear rate range covered. The limiting viscosities indicated that concentrated polyethylene oxide solutions can be considered to be power-law fluids in which shear stress is given by the relation

$$\tau = KD^n$$

where τ is the shear stress in dynes/cm , D the Newtonian shear rate in sec^{-1}, and K and are constants. Values of n were found to be generally in the range 0.5 - 0.6 for a wide variety of concentrations and polymer samples, even those with vastly different viscous properties.

2.2 Friction Reduction in Dilute Solutions.

Friction reduction studies in this program emphasized the determination of the effects of mechanical degradation or the loss of friction reducing capability. Degradation of friction reduction was observed in a thermostated rotating disk assembly for samples of WSR-205, WSR-301, and coagulant grades of polyethylene oxide as a function of polymer concentration and solution temperature.

Except for very low concentrations, initial (time zero) friction reduction was found to be virtually independent of polymer grade and solution

concentration. On the other hand, the friction reducing capability of the lower molecular weight grade, WSR-205, was found to degrade much more rapidly than the higher molecular weight homologs.

Initial drag reduction increased as a function of temperature in the range 30°C to 60°C, however the rate of degradation of drag reduction was found to be very severe at the higher temperatures.

Additional experiments were conducted to determine the effect of shearing concentrated solutions upon the drag reduction effectiveness and degradation characteristics of subsequently diluted forms. In all cases, dilute solution drag reduction characteristics were found to be independent of the solution history imposed upon the concentrated solution.

3.0 Experimental Techniques and Procedures

3.1 Polymers Studied

Three grades of Union Carbide's Polyox were obtained for these experiments: Coagulant, WSR-301 and WSR-205. All were samples of industrial blends donated by the Union Carbide Company and were used as received, without purification and fractionation. All polymer tests described in this study have been conducted with the following grades and blends of Polyox:

Grade	Blend	Approximate Molecular Weight
WSR-205	1214-A-09	900,000
WSR-301	1227-A-01, 1006-A-01	3,200,000
Coagulant	8258-R	3,500,000

The molecular weights given above are based on the intrinsic viscosity measurements made in this study which are described later.

3.2 Solution Preparation Techniques

Two methods for preparing the concentrated "Master" solutions were used. These were the Vortex mixer method and the boiling water method.

3.2.1 Vortex Mixer Method

This method proved to be suitable for the preparation of concentrated PEO solutions in bulk amounts (30-40 lbs). The system is shown schematically in Figure 1. A photograph of the system is given in Figure 2. The entire system is mounted on casters for portability.

Plastic piping is incorporated in the system to elimate any metallic degradation effect on the polymer. An orifice meter is included to provide a measure of control of the water flow rate. In addition, the holding tank is calibrated in gallons. The principal element of the system is the vortex mixer unit depicted in Figure 3. This unit was donated by the Naval Undersea Research and Development Center, Pasadena, California and modified slightly to adapt to the system. The method of preparation involved the simultaneous controlled flow of water and the addition of a calculated amount of PEO powder through the vortex mixer. Both operations were performed for one minute. Care was taken that powder was added at a uniform rate during the mixing process to provide a homogeneous solution.

The system is capable of preparing master solutions in the concentration range of 0.1% to 1%. Since PEO solutions prepared with ordinary tap water are not suitable for making reproducible physical property determinat s because of possible chemical degradation effects (15), distilled water was used in all cases. Immediately after the mixing, isopropyl alcohol (0.5%) was added to the solutions as a degradation retardant (17). Solutions were then stirred gently by a 12" diameter propeller at 10-15 rpm. for one hour. The concentrated solutions were allowed to stand for at least a 24 to 48 hour period in order to insure complete solution homogeneity of the solutions, several samples were withdrawn from various levels of the holding tank and viscometrically compared. The results indicated solution uniformity.

3.2.2 Boiling Water Method

In this technique, solutions were prepared according to manufacturer's specifications (17) with some modifications. A slurry of a weighed amount of PEO (6 grams) in 40 ml. of anhydrous isopropyl alcohol was first prepared. The slurry was stirred in a 1000 ml. stainless steel beaker using a three-bladed impeller positioned as shown in Figure 4. A prescribed quantity of boiling distilled water (594 grams) was then added immediately and at one time. The mixture was stirred at 600 rpm. for one minute. At this point, the speed of agitation was reduced to 150 rpm. and maintained for ten minutes or until the mixture developed a sufficient viscosity to exhibit the so-called Weissenberg (or rod-climbing) effect. Finally, the speed was brought down to 75 rpm. and a dissolving time of about one hour was found necessary to insure complete solution. Approximately 600 ml. of a 1% master solutions are prepared in this fashion. These solutions were also allowed 24 to 48 hour period to insure homogenization.

3.3 Stress Decay and Viscosity Measurements in Concentrated Solutions

All viscometric measurements obtained in this program were made with a Haake Rotating Viscometer (Rotovisco). The Rotovisco is a Couette flow type viscometer (cup and bob system) with a circular gap between co-axial concentric cylinders. The inner cylinder rotates while the outer one is stationary. The arrangement of bob and cup is shown in Figure 5. A recorder is incorporated into the system in order to study the time-dependent behavior of the viscometric characteristics

of PEO solutions, i.e., the decay of shear stress (or viscosity) as a function of time at a constant shear rate.

Preliminary experiments were performed to establish the range of shear rates obtainable using the Rotovisco, the particular problem being related to the tendency of these concentrated solutions to be drawn out of the gap because of their viscoelastic character. It was decided to extend this range by employing the bob and cup combination with the cup completely filled with fluid and capped (see Figure 5) in order to obtain shear rates high enough to adequately illustrate stress-decay. Naturally, this change in geometry leads to possible errors in the form of end effects, flow field perturbations, etc.

A check with a viscous, Newtonian fluid, glycerin, indicated that the effect using the MVI system was negligible up to a shear rate of about 1370 $sec.^{-1}$ The results of this experiment are listed in Appendix I where the viscosity of glycerin determined with the apparatus filled normally is compared to that with the cup completely filled and capped. In addition, calculations (see Appendix I) show possible end effects to be no greater than on the order of 3% in the case of Newtonian fluids.

These determinations cannot, on the other hand, be automatically assumed to apply to the non-Newtonian, viscoelastic fluids of primary interest here. It has been shown, for example, that suppression of the Weissenberg effect by enclosing the sample leads to the development of certain secondary flows (40). Such perturbations to the simple

Couette-flow essential to the interpretation of the experimental data in terms of fundamental units could lead to unacceptable errors. In order to shed further light upon the extent of the problem associated with completely enclosing the sheared sample, a plexiglass model of the RV cup was constructed to allow direct visualization of the flow field.

The flow characteristics of the system where studied by suspending droplets of the dye Rhodamine B at various locations throughout the system and photographically observing the dispersion of the dye subsequent to the start of shearing. Some typical photographs illustrating the dye dispersion and the flow field are shown in Figure 6. The primary feature noted is that within the annular gap between the outer stationary cylinder and the inner rotating cylinder the flow is <u>essentially</u> Couette-flow. This is effectively illustrated by the dye patterns visible in the Figure. There are, however, secondary flows observed which do not show up in the photographs. Dye originally placed above or below the bob is immediately drawn into the gap when the bob is rotated. That this is not simply a starting transient is confirmed by the occasional movement of small stray bubbles into and out of the gap during the entire course of the experiment. The significance of these secondary flows especially with regard to their influence upon the stress decay measurements will be discussed in Section 4.0.

Each experiment was performed in the following manner:

a. A solution was prepared in the vortex mixer as previously described.

b. Each sample was then sheared at a selected rate.[1] After some period of time, the applied shear rate was reduced in steps to the minimum rate yielding a measureable shear stress. Each sequence proceeded according to Table 1.

c. Each sequence was performed on a fresh (unsheared) sample prepared in the vortex mixer.

d. The initial rate runs were designed to provide a quantitative measure of the stress decay characteristics over a fairly wide range of shear rates.

e. The step sequence runs, most of which were free of stress decay were included to illustrate the influence of shear history on apparent solution viscosity.

f. All runs were conducted at 30.0°C ± 0.1°C.

The results of these experiments are discussed in detail in Section 4.0.

The effect of shearing concentrated solutions on the frictional drag reducing characteristics of their subsequently diluted forms is discussed in some detail in Section 5.0.

The concentrated solutions studied in this fashion were sheared in the Rotovisco as described above. In this case, however, the temperature range for all tests was 22.5°C to 24°C, depending upon room temperature.

---

[1] Shear rates are estimated assuming Newtonian behavior.

Table 1

Applied Shear Rate Sequences

Sequence	Initial Rate Rate (sec^{-1})	Step Sequence Rates (sec^{-1})
1	1370	685,457,228,152,76,51,25,17,8
2	685	457,228,152,76,51,25,17,8
3	457	228,152,76,51,25,17,8
4	228	152,76,51,25,17,8
5	152	76,51,25,17,8
6	76	51,25,17,8
7	51	25,17,8
8	25	17,8
9	17	8
10	8	-

3.4 Turbulent Flow Rheometer

The turbulent flow rheometer (TFR), shown schematically in Figure 7, was constructed for the study of polymer solution drag reducing and degradation characteristics. A photograph of the system is given in Figure 8. The main dimensions of the TFR are shown in Figure 9. The apparatus consists of a smooth and polished disk made of brass, rotating in a closed housing of 10" I.D. and 6.4" in depth, with a volume capacity of 8.2 liters of solutions. The disk rotates in a plane symmetrically in the middle of the housing. Two disks were used; a 5" diameter disk at 1800 rpm. and a 6" diameter disk at 1700 rpm.. The first disk was used for most of the tests, while the second disk was used in the latter part of the program to study the temperature effects on the drag reduction and degradation characteristics. Corresponding Reynolds numbers were 9.6×10^5 and 1.29×10^6 (based on physical properties of water at 30°C).

The principal element of this system is a Master Servodyne laboratory mixer (supplied by the Cole-Parmer Instrument Company). The unit consists of a motor and a control unit. The maximum torque output of the unit is 48 inch-ounce. The control unit is provided with a visual torque indicator calibrated in millivolt output. The unit has the built-in capacity to deliver a variable torque equal to the demand rate of the load while maintaining a preset speed at a constant level. The system includes a potentiometric recorder.

The mixer is mounted on a heavy duty stand to reduce vibrational interference. A mercury thermometer incorporated in the system is used to determine solution temperature during each test. Solution temperature is controlled by circulating water in a jacket surrounding the closed test chamber. The temperature of circulating water is regulated by a constant temperature bath provided with a thermoregulator. The inner housing containing the test solution is made of bronze to ensure good heat transfer characteristics.

The experimental procedure consisted of setting the disk into motion at the required speed (1700 rpm. for the 6" diameter disk and 1800 rpm. for the 5" diameter disk). Initially the housing contained pure distilled water at a particular temperature (30°, 45°, or 60°C). As in the preparation of master solutions, distilled water was used for drag reduction tests, to eliminate the possibility of chemical degradation occurring simultaneously with mechanical degradation. As the steady state was reached (which took 10 to 15 minutes), the torque reading for distilled water was recorded. The desired polymer concentration was then obtained by injecting the required quantity of concentrated solution into the test chamber through a fitting at the top of housing. The instantaneous decrease in drag and the degradation of this effect was recorded for a period of time.

The temperature for all tests was controlled to an accuracy of $\pm$ 1°C. After each test the test chamber was emptied easily through a drain-cock in the bottom of the test chamber. The housing was then

flushed twice with water to ensure complete removal of the polymer solution before another test was made.

The effectiveness of injecting master solutions into the test chamber was evaluated by conducting two identical tests with 100 wppm. of Polyox WSR-301. One of the solutions was made by injecting the master solution as described above. The other solution was prepared outside in a polyethylene vessel. The drag reduction and degradation characteristics of these two solutions were found to be identical.

Samples for the measurement of intrinsic viscosity (which is described in Section 3.5) were withdrawn through the injection fitting. The samples were withdrawn from the TFR using a clean plastic syringe. The samples withdrawn represented a radially averaged sample by virtue of the turbulent mixing occurring in the rheometer. On the average, four to five samples were taken, each sample having a volume of about ten ml.. Thus the total volume of samples taken out was less than 0.5% of the total volume of the test solution (8.2 liters) in the test chamber. Each time a sample was taken out, it was replaced through another syringe with an equal amount of distilled water so that the chamber was completely filled at all times. This had a negligible effect on the solution concentration.

3.5 Characterization of Dilute Polymer Solutions

3.5.1 Viscometer

A Cannon-Fenske routine type capillary viscometer was used to measure the viscosities of dilute PEO solutions. The viscosities of

the dilute polymer solutions varied between 0.8 and 1.1 centipoise. The ASTM Standard Method of Test (2) recommends a size 50 viscometer for viscosities ranging from 0.8 to 4 and, accordingly, a size 50 was used for this study.

The capillary viscometer was immersed in a constant temperature "Temp-Trol" Viscosity Bath. The bath was filled with Nujol heavy mineral oil. The temperature was controlled with a thermoregulator, which gave an accuracy of .025°C. The vertical alignment of the viscometer was done by eye.

A Hewlett-Packard Auto Viscometer along with a photocell-lamp detector assembly was used to automatically measure efflux times of liquid samples in the capillary viscometer. The times were recorded with an accuracy of .01 second. The two photocell detectors were installed on the two etched marks on the capillary viscometer. The use of photocells eliminated manual errors in measuring the flow times in the viscometer. The Autoviscometer also operated a pneumatic pump which supplied a very small pressure for automatic influxing of the sample. After each measurement, the viscometer was immersed in a solution of technical acetone and dried with dehumidified air before the next use.

3.5.2 Capillary Flow Relations

The Hagen-Poiseuille law for laminar flow of Newtonian fluids in a capillary is given by:

(1) $$\eta = \frac{\Delta P \, \pi \, R^4 t}{8 \, QL}$$

where L = capillary length

Q = volumetric flow through the capillary during time t

R = radius of capillary

The pressure drop ΔP is due to the difference in the hydrostatic heads, which varies continuously as the test sample flows down. Therefore, the mean logarithmic difference must be used when the drop is computed from the hydrostatic heads. Thus:

(2) $$\Delta P_{avg} = \frac{h_2 - h_1}{\ln \frac{h_2}{h_1}} \rho g$$

Since the flow rate of water is greater than that of the polymer solution for the same applied gravity driving head, a greater proportion of this driving head is used up in accelerating the water from rest than in the case of polymer solutions. This necessitates the application of "Kinetic energy correction". For the liquid sample tested the Kinetic energy correction was negligible as shown in Appendix II.

Equation (1) can then be written as:

(3) $$\eta = A \, t$$

where

$$A = \frac{\frac{h_2 - h_1}{\ln \frac{h_2}{h_1}} \pi R^4 g}{8QL}$$

Since measurements were made on dilute solutions the difference in densities between water and polymer solutions was small enough to ignore. The relative viscosity, η_r, is from (3);

$$\eta_r = \frac{\eta_p}{\eta_s} = \frac{t_p}{t_s} \tag{4}$$

where subscripts p and s are for polymer solution and water, respectively.

3.5.3 Intrinsic Viscosity and Molecular Weight Relations

The viscosity method of molecular weight determination was chosen because it is the simplest of all the methods available. The parameter used to measure the viscosity effect of a polymer is the Intrinsic Viscosity, defined as:

$$[\eta] = \lim_{\substack{D \to 0 \\ C \to 0}} \frac{\eta_p(D) - \eta_s}{C\eta_s} \tag{5}$$

where $\eta_p(D)$ = polymer solution viscosity at shear rate D

η_s = solvent viscosity at the same temperature

C = concentration of solute (gm./dl.)

D = shear rate for viscosity measurement in (Sec.$^{-1}$)

Since the concentration is usually expressed in gm./dl., $[\eta]$ has the units of dl./gm.

The intrinsic viscosity is taken as a measure of the hydrodynamic influence of the dissolved polymer molecules on the flow of

solvent. It represents the force necessary to drag the molecule through the solvent, and hence the larger the molecule, the higher the intrinsic viscosity.

Paterson (16) states "the limit of zero shear rate should be taken to eliminate the effect of shear rate on the deformation and orientation of the random coil since this deformation and orientation changes the solution viscosity." He found a strong shear rate dependence of viscosity of dilute PEO solutions at very low shear rates (less than 100 Sec.$^{-1}$). Various investigators have expressed different opinions on the subject of shear dependence of viscosity of dilute PEO solutions. Available reports conflict with one another. Fabula (7) observed shear dependence for WSR-301 only above concentrations of 100 wppm. using a particular viscometer with an approximate wall shear rate range of 130 to 1250 Sec.$^{-1}$. However using a different type of viscometer, which gave much lower shear rates, he found that the intrinsic viscosity increased. Virk (27) observed the shear independence of viscosity for 500 wppm. of WSR-301 in the shear rate range of 1-1000 Sec.$^{-1}$. The available instrument capabilities were limited and the phenomenon of shear dependence at very low shear rates could not be established. The approximate shear rate was 1216 Sec.$^{-1}$, as shown in Appendix III.

Paterson (16) also states that an extrapolation to zero concentration is not required to find $[\eta]$ if measurements of the reduced

viscosity, $\frac{\eta_p - \eta_s}{\eta_s C}$, are made at sufficiently low concentrations. A small correction is applied for the fact that the measurements are made at small but finite concentrations. The corrected and uncorrected values of intrinsic viscosity are related by the relation (16):

(6) $$100\,([\eta]_u - [\eta]_c)/[\eta]_c = 40C[\eta]_c$$

where $[\eta]_u$ = uncorrected intrinsic viscosity

$[\eta]_c$ = corrected intrinsic viscosity

Reduced viscosity values in this study have been corrected as described above, the extrapolation to zero concentration not having been made. However, because of the possible shear rate dependence of viscosity of dilute PEO solutions at very low shear rates, the values obtained for reduced viscosity may not be reliable.

Flory (8) shows that linear polymers obey an intrinsic viscosity-molecular weight relation of the form:

(7) $$[\eta] = KM^a$$

Where M is the molecular weight of the solute and K and a are constants for a given polymer-solvent system at a given temperature. If the polymer is heterogeneous, i.e., a wide spectrum of molecular weight distribution exists, then an average molecular weight should be substituted for M in the above equation. By definition, this is the viscosity average molecular weight denoted by $\overline{Mv}$. The method of light scattering (24) gives the weight average molecular weight $\overline{Mw}$, which can be related to the intrinsic viscosity by the relation:

(8) $$[\eta] = K\bar{M}w^{a}$$

In the above equation K and a would be different from the values in equation (7). The results of Shin (23) and Bailey (4) for Polyox in distilled water are:

(9) $$[\eta] = 1.03 \times 10^{-4}\ \bar{M}w^{0.78}$$ (Shin, at 25°C)

(10) $$[\eta] = 1.25 \times 10^{-4}\ Mw^{0.78}$$ (Bailey, at 30°C)

The constant found by Shin is thus slightly lower than the value obtained by Bailey. As different commercial unfractionated samples of Polyox were used by the two investigators, the difference in Constant, K, may be due to the different molecular weight distributions. Shin's relation was used in this study.

Paterson (16) shows experimentally that Shin's relation is also valid for degraded solutions. The samples in this study were taken directly from the TFR for molecular weight measurements. In this respect this study is similar to Paterson's work except that his system involved pipe flow instead of disk flow. This procedure of taking the sample directly out of the rheometer permitted the study of the process of polymer degradation in the turbulent flow and its effect on drag reduction.

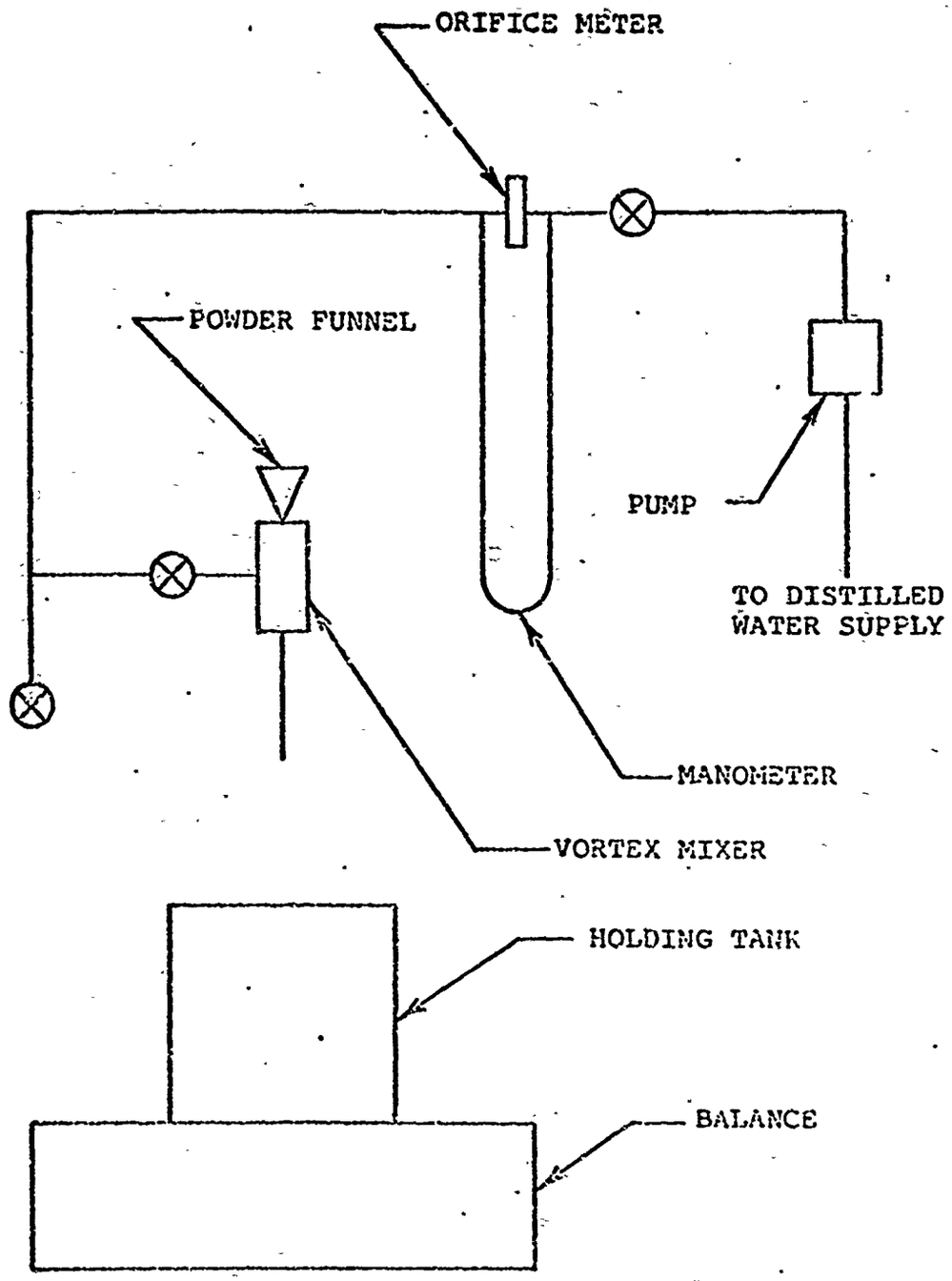

FIGURE 1

VORTEX MIXER ASSEMBLY

Reproduced from best available copy.

Figure 2

Vortex Mixer

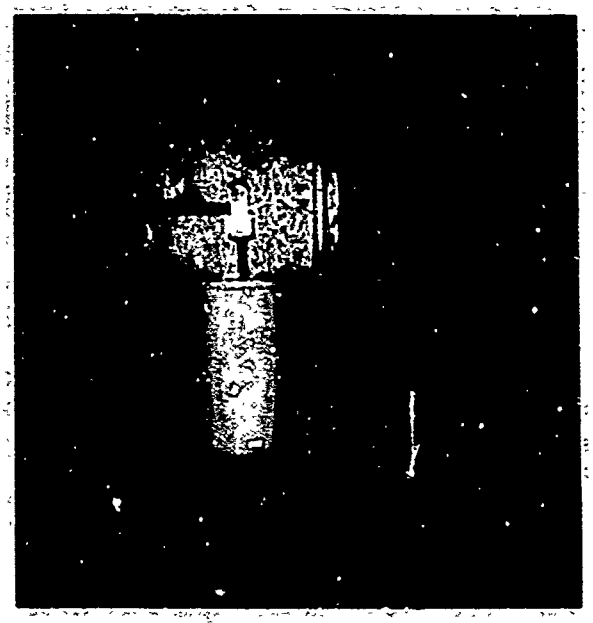

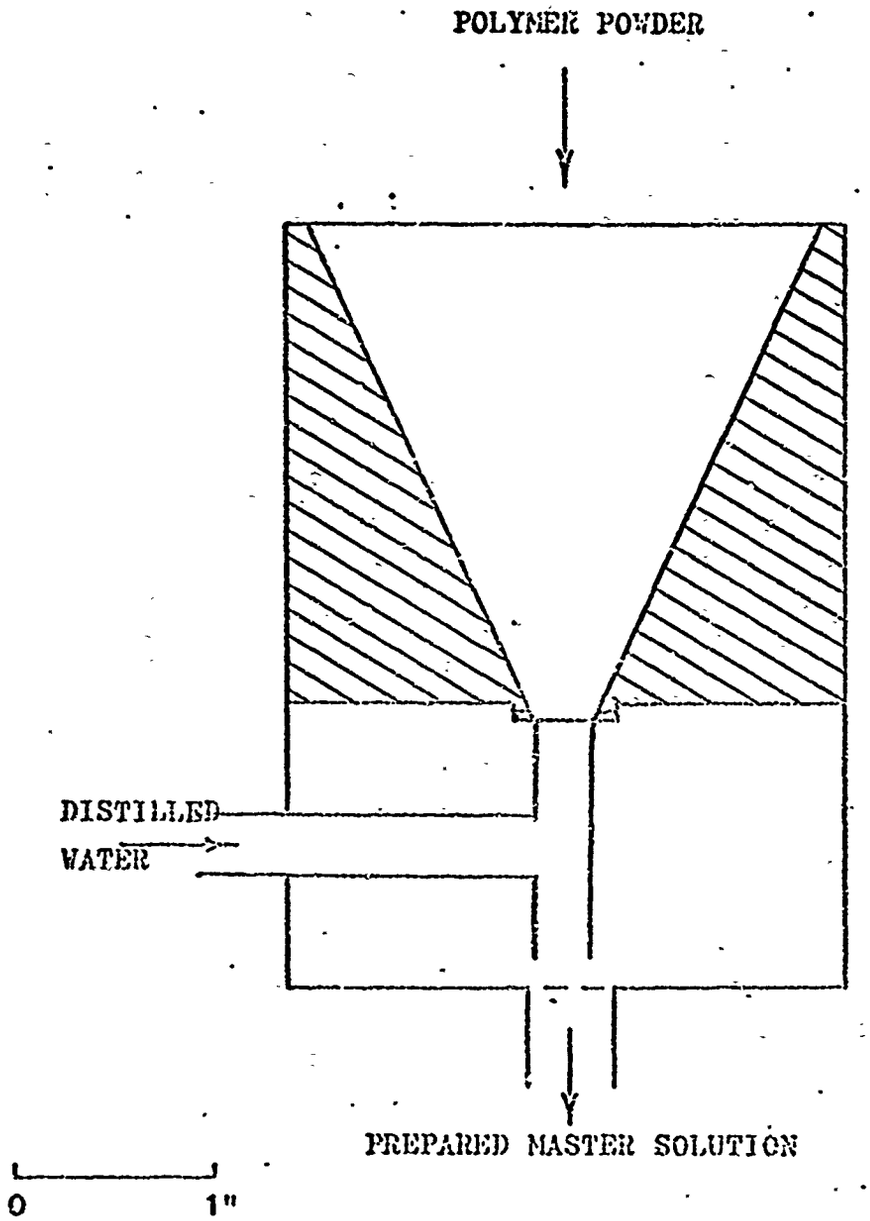

FIGURE 3
VORTEX MIXER UNIT

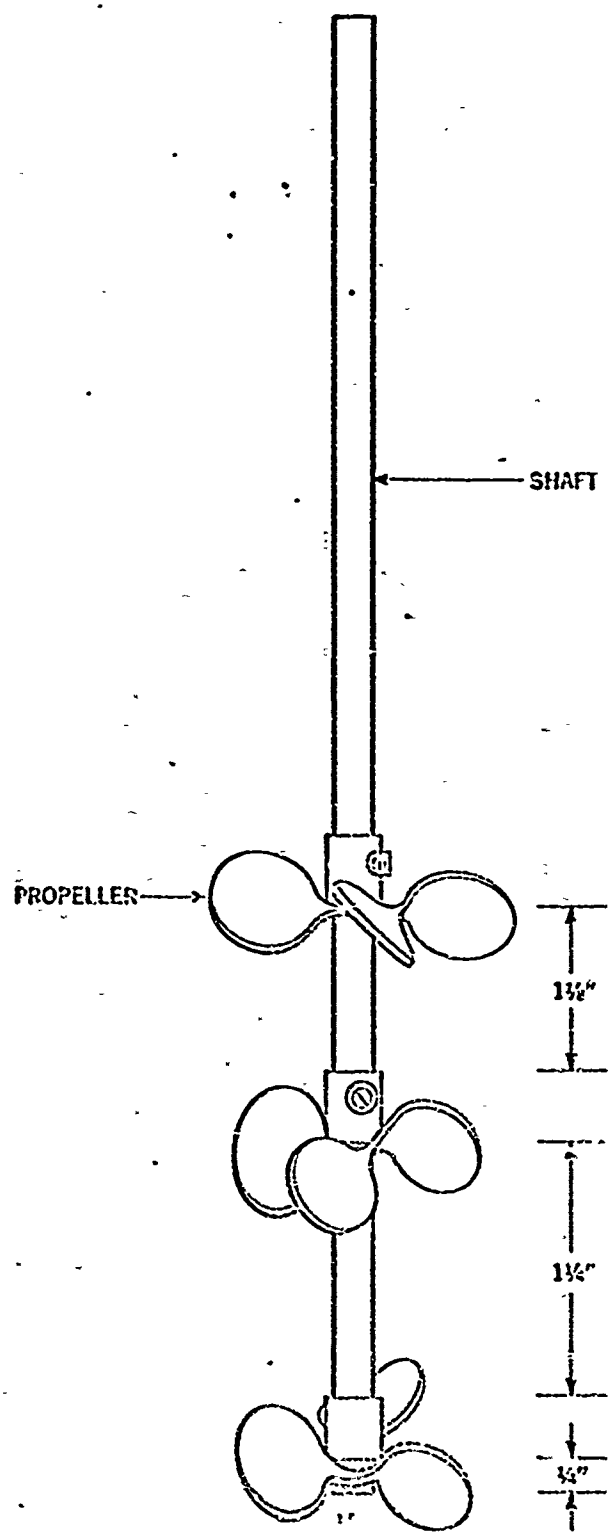

FIGURE 4
THREE-BLADED STIRRER

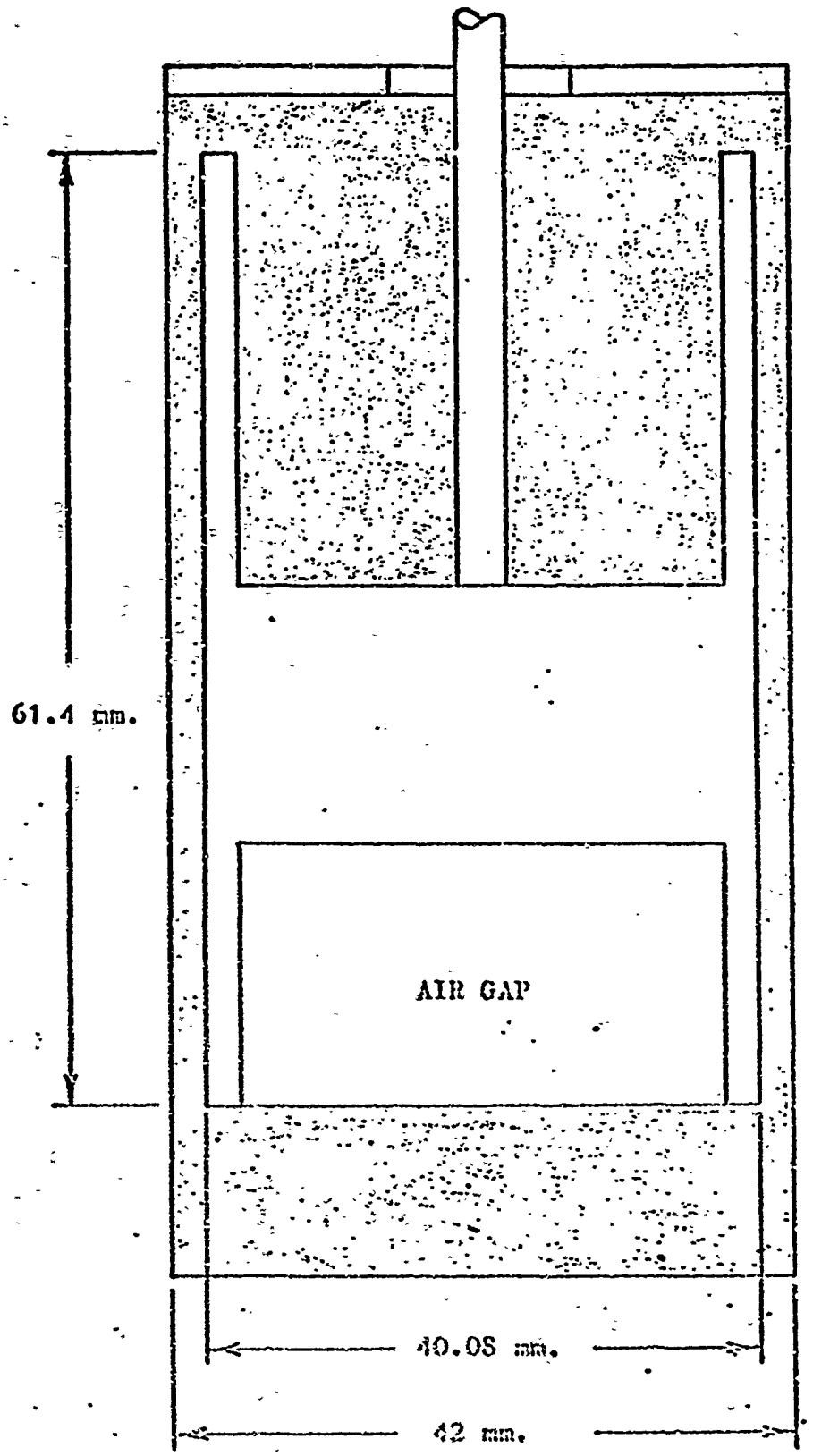

FIGURE 5: ROD AND CUP ARRANGEMENT

Figure 6
Flow Visualization

Reproduced from best available copy.

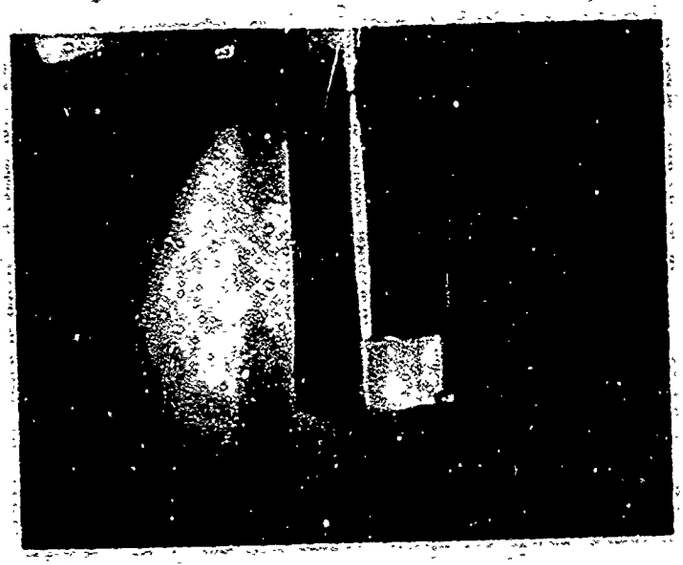

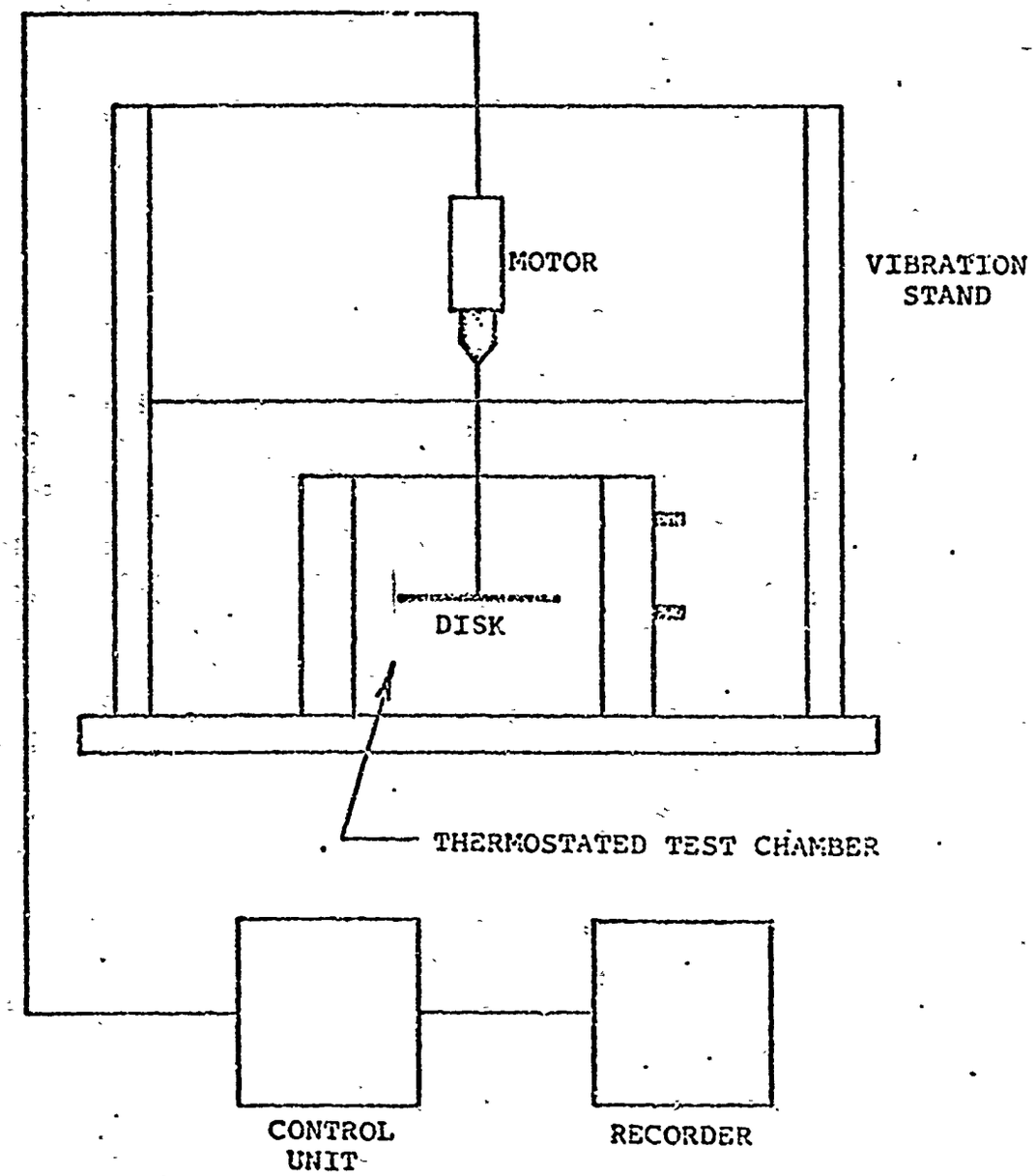

FIGURE 7

TURBULENT FLOW RHEOMETER

Figure 8

Turbulent Flow Rheometer

Reproduced from best available copy.

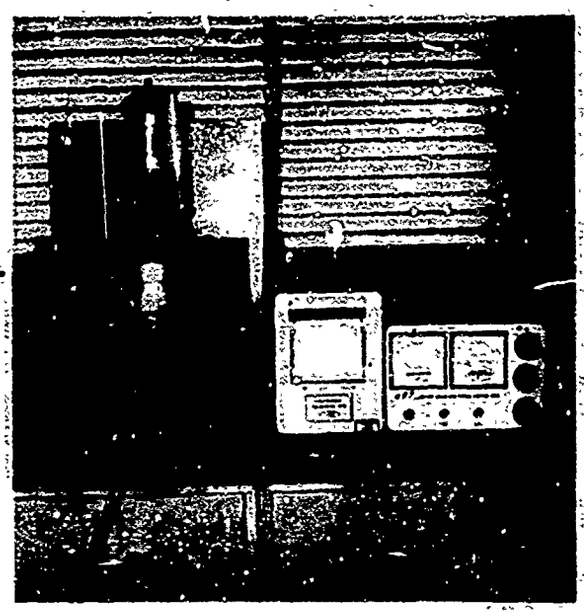

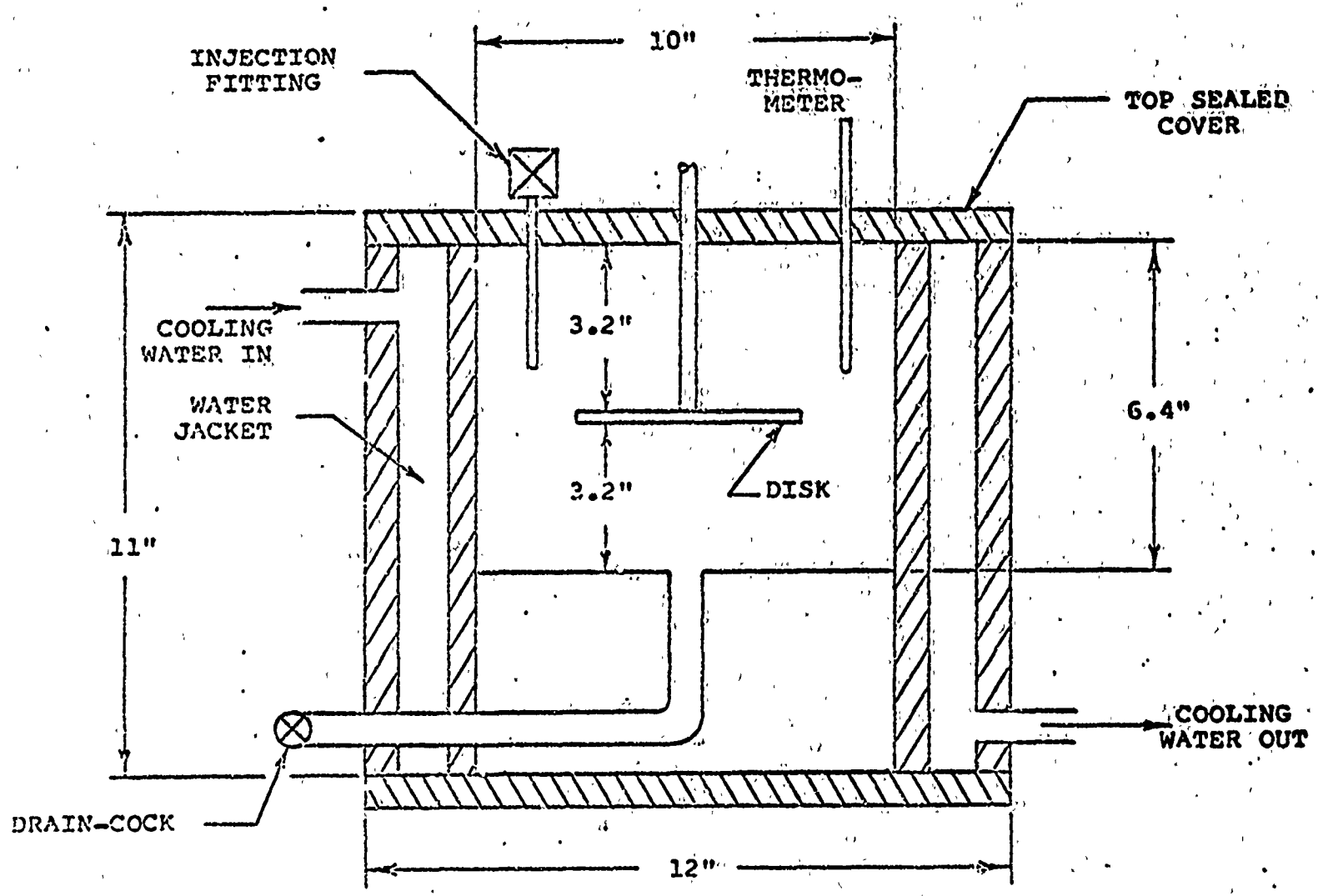

FIGURE 9 - TEST CHAMBER

4.0 Rheology of Concentrated Solutions.

4.1 General.

Rheological data have been obtained over very wide ranges of shear stress and shear rate for high polymers. Typical flow curves for various ideal rheological bodies exhibiting no yield stress are presented in Figure 10. Line A represents the Newtonian fluid for which the viscosity is constant, independent of shear rate. For many polymeric materials, the relationship between shear stress and shear rate can be represented by a "power law" of the form

$$\tau = KD^n \qquad (1)$$

over a wide range of shear stresses and shear rates, where τ is the shear stress in dynes/cm^2, D is the shear rate in sec^{-1}, K is a constant, and n is a constant less than unity. Such a relationship is depicted by curve B, and a fluid exhibiting this behavior is called pseudoplastic or shear-thinning. For a few fluids, n is greater than unity (curve C). These fluids are termed dilatant or shear-thickening. For a Newtonian fluid, of course, n is unity and K is the ordinary Newtonian viscosity. The apparent viscosity, which is the ratio of the total shearing stress to total shear rate at a given rate of shear is exemplified by the dotted line shown on Figure 10. Hence, for a case in which Equation (1) applies, the apparent viscosity, η, may be written

$$\eta = \frac{\tau}{D} = KD^{n-1} \qquad (2)$$

The curves A, B, and C of Figure 10 refer to steady-state effects and are considered independent of time. However, many polymeric fluids exhibit time-dependent flow effects that can be either reversible or irreversible. Materials whose flow effects are reversible are said to exhibit thixotropy. The apparent viscosity of a thixotropic fluid decreases with time from an initial value, η_0, to a final limiting value, η_∞. Flow curves such as those depicted in Figure 10 can be constructed from the dependence of either η_0 or η_∞ as a function of shear rate.

Figure 11 (a) (26, 35) shows a recorder trace of stress decay at a constant rate of shear obtained on a pseudoplastic emulsion in a rotational viscometer. Figure 11 (b) reveals that the shear stress-time relationship is a logarithmic one. This logarithmic stress decay behavior represents a first order decay rate and is quite commonly observed in thixotropic fluids (26) Figure 12 (26, 35) shows the variation with shear rate of the apparent viscosities corresponding to zero time and to infinite time of shearing for the same system depicted in Figure 11.

In general, the apparent viscosity of a thixotropic substance is reduced from η_0 to η_∞ in some variable amount of time. The characteristic reversibility of thixotropic substances is manifested by the complete recovery of the apparent viscosity from η_∞ back to η_0 after some other, unspecified, period of time. Subsequent shearing reproduces the identical result with no hysteresis. In the example cited above and depicted in Figures 11 and 12, the apparent viscosity is reduced from η_∞ to η_0 in several seconds, while about 8 hours were needed for complete recovery.

On a microscopic or molecular level, orientation of molecular chains, as well as disengagement and reformation of molecular entanglements plays an important role in pseudoplastic flow. Thixotropy undoubtedly involves similar phenomena as well as the rupture of weak secondary bonds (such as hydrogen bonds) between molecules. Furthermore, the combination of these events is such as to require a finite time. This effect must of necessity be a highly complex one, since the number, distribution, and relative strength of these bonds must vary throughout the fluid. The existence of a limiting viscosity, η_∞, can be taken to imply that at a given rate of shear, there exists an appreciable number of such bonds (and other configurational barriers to further stress decay) whose strength is equal to or greater than the applied steady-state stress.

Thixotropy is frequently discussed in the literature, and techniques have been developed to provide a semi-quantitative description of thixotropic changes (36). Irreversible time-dependent effects, however, are infrequently treated. The irreversible decrease in viscosity noted in some polymer fluids subjected to high shear environments is usually associated with chain scission (4, 37). On the other hand, viscosity also drops as a result of disentanglement and the reversibility of the entanglement-disentanglement process is by no means established (37, 38). It has been pointed out (39) that there is no obvious cause for reentanglement at rest to be as marked as in the polymerization process, or as severe as disentanglement under shear.

Elastic behavior of some polymer fluids is also the cause of a number of time-dependent effects. A viscoelastic fluid is one which possesses a certain elastic character in addition to its usual viscous

properties. The well-known tendency for viscoelastic fluids to flow in a direction normal to the direction of shear stress--the Weissenberg Effect--is an example of such behavior due to the creation of normal stresses within the fluid. Another example occurs when a viscoelastic material enters a capillary. Elastic stresses develop as the fluid converges at the inlet which relax as the fluid flows through the capillary. The magnitude of the stresses and the relaxation time depends upon the fluid and the geometry of the capillary. Stress relaxation phenomena in general occur when a viscoelastic substance is suddenly brought to a given deformation. The stress required to maintain this deformation decreases with time. The microscopic factors listed above can also be used to explain, qualitatively, the viscoelastic behavior of polymer fluids.

Thus, viscometric data represent the joint contribution of several effects, among which must be included those which are manifested by the time dependency of these data. The above discussion has been limited to several specific rheological phenomena. In the next section, the concentrated solution rheology of polyethylene oxide WSR-301 is discussed in the light of these phenomena.

4.2 Rheology of Concentrated PEO Solutions

Interest in the viscous characteristics of aqueous solutions of the homologous series of polyethylene oxide polymers has been high for many years. Bailey and his co-workers (28) reported rheograms[1] for PEO WSR-301

---

1. A diagram illustrating the shear stress response in a sample as a function of shear rate is sometimes called a rheogram.

water solutions up to about 3% (by weight) polymer over a range of shear rates from 0.001 to about 10,000 sec^{-1}. Rodriguez and Goettler (32, 33) obtained data up to about 15,200 sec^{-1} for PEO WSR-35, -205, -301, and "Coagulant" water solutions as high as 10% (by weight) polymer. They used their data to test a number of models for pseudoplastic flow and to develop a two-parameter model yielding a good fit to the data over five decades of shear rate. Hoyt and Fabula (14) reported rheograms for PEO (MW $4x10^6$) in water over a low shear rate range (0.1 -10 sec^{-1}, 0 -0.1% polymer), and a high shear rate range (10,000 -1,000,000 sec^{-1}, 0 -0.01% polymer).

In addition, various workers (4, 5, 10, 16, 28, 29, 30, 34) have noted the influence of mechanical agitation on the viscous characteristics of contrated PEO solutions. Primarily it is noted that measured viscosity levels are strongly dependent upon the mode of solution preparation and that the viscosity of a solution can be altered by stirring, pumping, and other forms of agitation. It is also well known that fresh, unstirred samples of concentrated PEO solutions exhibit the classical characteristics of highly viscoelastic fluids such as rod climbing, elastic recovery, die swell, etc. Furthermore, these are observed to decrease as a result of continued agitation of the solution. These observations introduce another more complex element into the rheological characterization of concentrated solutions. Thus, although the non-Newtonian (shear thinning or pseudoplastic) behavior seems to be fairly thoroughly documented as noted above the time-dependent and viscoelastic flow characteristics implied by the apparent influence of mechanical agitation on solution viscosity and viscoelastic properties has only been qualitatively noted.

It is clear, therefore, that a complete rheological characterization of concentrated PEO solutions must include a thorough delineation of these time-dependent effects. It is also important to note that the quantitative pseudoplastic flow properties alluded to above probably represent the steady-state limiting viscometric data--a fact which is not explicitly established in the references cited. In addition, it must be recognized that even such limiting viscometric data could be influenced by the shear history experienced by the solution during the preparation and handling procedures prior to the viscometric measurements. This is particularly true if the shear environment during preparation and handling is more severe than that in which the viscometric measurements are conducted. This last factor will be discussed in some detail later.

In the following sections, the results of the research conducted during this program directed towards the resolution of these questions and the delineation of the concentrated solution rheological characteristics of PEO are presented.

4.2.1 Stress Decay Characteristics of Concentrated PEO Solutions

A detailed description of the instrumental techniques and experimental procedures utilized in this study of the stress decay characteristics of concentrated PEO solutions has been provided in Section 3. In summary, the purpose of these experiments was to develop a description of the concentrated aqueous solution rheology of PEO WSR-301 with particular attention to time-dependent effects.

The first point which must be firmly established in any such analysis is the significance of time "zero". Clearly, if the rheological properties

change with time under shear, then any such shearing during preparation or handling may alter the rheological state of the fluid. Under these circumstances, a sample undergoing a stress-decay experiment possesses a "solution history", and the state of the fluid at the initiation of the experiment is some (unknown) function of that history. Because of this uncertainty, all solutions used in stress decay experiments were prepared by the vortex mixer method also described in Section 3. This method provides for the rapid dispersion and dissolution of polymer powder with a minimum of mechanical agitation. Of all the preparation techniques described in the literature, the vortex mixer method probably comes the closest to yielding a final product solution which can be considered "unsheared". Therefore, the stress decay properties reported in this section are considered to be characteristic of previously unsheared solutions.

The bulk of the stress decay experiments were conducted in two sequences. In the first sequence, stress decay measurements were made on PEO solutions at concentrations of 0.24%, 0.36%, 0.41%, 0.63%, 0.91%, and 0.94% (by weight) of polymer over a shear rate range of 1370 sec^{-1} down to as low as 25 sec^{-1}.[1] All solutions in this sequence were prepared with Union Carbide PEO powder lot WSR-1006-A-01. The results of these measurements are depicted in Figures 13 through 18 as the decay of shear stress as a function of time under shear. As indicated in these figures, selected runs were allowed to proceed until an apparent steady-state shear stress response had been achieved. Because of the considerable time required, most runs were terminated at some intermediate time. The second sequence of stress decay

---

1. Unless otherwise specified, the shear rates reported were determined on the basis of the Newtonian assumption, and are, therefore, only approximate.

experiments were conducted with solutions of 0.14%, 0.41%, 0.70%, and 1.03% (by weight) of polymer over the shear rate range of 1370 sec^{-1} down to 152 sec^{-1} using Union Carbide PEO powder WSR-1227-A-01. These stress decay measurements are shown in Figures 19 through 22. In the second sequence, all runs were permitted to continue until a steady-state shear stress response was obtained. In each case, temperature was controlled to 30°C ± 0.1°C. All of these stress decay curves show only the "smoothed" data. Examples of actual stress decay curves for some typical runs will be discussed presently. Data tables for these figures are provided in Appendix IV.

Qualitatively, the stress decay curves are observed to display some common characteristics. Each curve is characterized by the attainment of a certain stress level followed by a more or less steadily decreasing stress response. A distinct maximum is observed in some of the curves. These are particularly noted at higher concentrations and lower shear rates. Compare, for exan , Figure 13 (0.24%) and Figure 17 (0.91%). The maximum is not observed at lower concentrations and higher shear rates. The typical behavior of a viscoelastic fluid subjected to the instantaneous imposition of a rotational shearing flow is depicted qualitatively in Figure 23. Probably, in those cases in which the maximum disappears, it is simply shifted so close to time t = 0 that it is obscured by the instrumental time constant.

Figure 24 represents a composite of actual recorder output obtained during stress decay experiments on samples of PEO WSR-301 (WSR-1006-A-01) solutions consisting of 0.63% (by weight) of polymer. These curves illustrate a varying degree of fluctuation superimposed on the stress-time relationship. The magnitude of the fluctuations increases with shear rate.

The obvious necessity to explain the significance of these fluctuations lead to the flow visualization experiments outlined in Section 3.0. The important characteristics of the fluctuations are that:

a. They always appear in the initial stress decay measurements on fresh solutions.

b. They do not disappear if the solution is aged by "standing".

c. They are not observed in the steady-state stress response evidenced after the stress decay has ceased.

d. They are not observed when solutions which have been sheared at some high for some time are then sheared at a lower rate.

The flow visualization studies have shown that:

a. The flow in the viscometer is essentially Couette-flow.

b. A secondary flow is observed in which a slow movement of fluid to and out of the gap occurs.

c. These secondary flows do not diminish with time.

It would appear that the fluctuations are caused by the secondary flows which continuously feed solution into the viscometer gap. Any such solution placed into the gap would not be expected to generate the same shear stress response as the element of fluid being replaced, since their shear histories would probably be different. The fluctuation would, therefore, be expected to continue until a steady-state shear stress level had been reached by all the fluid in the viscometer.

This explanation is a plausable one. Except for an uncertainty in the readings (especially near time zero), the fluctuations cause no particular difficulty in following the course of the over-all stress decay curve.

The stress decay curves shown in Figures 13 through 22 effectively depict the marked change from the initial shear stress response to that exhibited in the steady-state after long periods of shear at some steady rate. This can also be illustrated in terms of apparent viscosity. Table 1 lists the apparent viscosities η_0 and η_∞ based on the Newtonian shear rate D and Equation (2)[1] for the stress decay sequence on lot number WSR-1227-A-01. The shear stresses at t = 0 are obtained from the data by extrapolation (see the data tables in Appendix IV). The limiting apparent viscosity is obtained from the steady-state shear stress achieved after long periods of shear at the corresponding constant shear rate. Table 2 lists only η_0 for the corresponding sequence for lot number WSR-1006-A-01 since most of these runs were terminated prior to attainment of the steady-state shear stress response. It is striking to note that percent reductions in apparent viscosity (% η_R) of up to 50% were observed.

At this juncture it is useful to digress briefly to discuss some general guidelines for the evaluation of these results. A complete quantitative interpretation would be composed of several elements:

a. Initial apparent viscosity or shear stress response.

An indicated above, η_0 and τ_0 are, by definition, representative of the initial (t = 0) response of the previously unsheared solution. As such, therefore, they are independent of "solution history" (there being none at t = 0), and depend

[1] Van Wazer (26) points out that this should be more properly termed the "apparent", apparent viscosity since the shear rate used in Equation (2) is itself obtained by assuming Newtonian flow.

Table 1
Initial and Limiting Apparent Viscosities from Stress Decay Measurements
(WSR-1227-A-01)

Shear Rate (sec^{-1}) \ Concentration	1.03%			0.70%			0.41%			0.14%		
	η_0 (cp)	η_∞ (cp)	$\%\eta_R$	η_0 (cp)	η_∞ (cp)	$\%\eta_R$	η_0 (cp)	η_∞ (cp)	$\%\eta_R$	η_0 (cp)	η_∞ (cp)	$\%\eta_R$
1370	63	38.5	38.9	32	18.7	41.5	23	10.7	53.5	9.5	5.8	39.0
585	78	51	34.6	43	25.3	41.2	25	12.1	49.6	8.8	5.0	43.2
457	78	58	25.6	53	30.2	43	27	13.8	49.0	9.8	4.8	51.0
228	121	89.5	26.0	68	42.5	37.5	35	18.9	46.0			
152	156	110	29.5									

Table 2
Initial Apparent Viscosities from Stress Decay Measurements
(WSR-1006-A-01)

Shear Rate (sec^{-1}) \ Concentration	0.94%	0.91%	0.63%	0.41%	0.36%	0.24%
	η_o (cp)	η_o (cp)	η_o (cp)	η_o (cp)	η_o (cp)	η_o (cp)
1370			62.5	32.5	25.5	19
685	110	94	58	30.6	33	21.6
457	127	115	77	41.5	36	23.6
228	167	141	90	50	44.5	
152	194	159	102	57	48	
76	283	297				
51	355	290				
25		384				

only upon solution concentration and shear rate.

b. Limiting apparent viscosity or shear stress response.

The limiting values must be treated somewhat more cautiously. If the limiting values at a specific shear rate are defined as those values toward which η and τ tend while the fluid is being sheared at that same rate (the case described by the stress decay curves), then no ambiguities arise, and η_∞ and τ_∞ depend only on concentration and shear rate. On the other hand, a fluid can be expected to encounter a variety of shear rates during its handling and processing. It is of significance to inquire into the influence of these encounters on the limiting values at a particular shear rate.

c. Stress decay

Stress decay leads to a decrease of apparent viscosity from its initial value η_0 to its limiting value η_∞. Quantitatively, therefore, stress decay can be described as a rate process and is completely specified only when the instantaneous shear stress is known as a function of time, as well as concentration and shear rate. Again, however, such an analysis is strictly applicable only in those cases for which the shear rate is maintained at some constant value. Shearing a solution for some period of time at a given rate and then changing to a different rate presents an entirely different problem. The stress decay at the second rate is subject to the influence of the "solution history" imposed by the prior shearing at the initial rate.

d. Quality control.

One important parameter has been thus far omitted from consideration. This can best be described as quality control. More specifically, factors such as reproducability of measurements, aging effects, and polymer lot variations must be evaluated. This last factor is particularly compelling in view of the dispersion in molecular weight distribution reported by the manufacturer in the PEO WSR series, and significant variations in properties for different lots of the same WSR grade (see for example reference 16).

It is convenient at this point to consider those factors described in paragraph d., above. It is obvious that any quantitative interpretation of stress decay data cannot be made independently of a satisfactory demonstration of their reproducability. Figures 25 through 29 portray several examples of multiple runs which were conducted to test the reproducability of these results (see also the data tables in Appendix IV). These runs were made at various shear rates. Repeated runs were made on a "same day" basis and 24 hours subsequent to the initial runs. No significant differences due to aging effects are noted, and the runs seem to be reproducable to better than about ±5%. Figure 25 also illustrates one example of a number of tests which were conducted to demonstrate the inherent irreversibility of the stress decay process. In this example, the run described was suspended after 75 minutes. The sample was then allowed to rest undisturbed for 17.5 hours. No recovery was noted when the shearing was resumed. Additional tests showed that concentrated solutions

stabilized with isopropyl alcohol could be safely stored for various periods while awaiting tests[1] without any significant viscosity loss. The results of these tests confirm the adequacy of the precautions taken in the preparation, handling, and storage of concentrated solutions to eliminate possible external causes of degradation.

The final factor in paragraph d. which remains to be evaluated is the influence of batch variations on the experimental parameters. In this case, experience and the conclusions of other workers (16, for example) did not give cause for optimism. Significant lot-to-lot variations in the PEO WSR series have been repeatedly demonstrated. Whether this is a direct result of some inherent factor in the manufacturing process or is due to a lack of quality control, it is not known. It is sufficient to note that broad differences are found. These differences are illustrated in the case of this program by Figure 30, where stress decay curves for lots (WSR-1006-A-01) and (WSR-1227-A-01) are compared at a common concentration (0.41%) and two different shear rates (1370 sec^{-1} and 228 sec^{-1}). These differences are charactdristic of those encountered at all levels of comparison of the two lots.[2]

One other possible contribution to the existence of apparent batch variations stems from the occurrence of degradation of the polymer powder itself. Several opportunities were available to check on this possibility during the course of the program. Figure 31 describes a portion of the

---

[1] Some tests occured up to one week after preparation. See also Section 5.6 describing static storage tests on dilute solutions.

[2] The exception is in the study of turbulent flow friction reduction characteristics of dilute solutions where no substantial differences were noted. These studies were conducted in disk flow with a Reynolds number of about 10^6.

stress decay curves for three separate cases: (WSR-1006-A-01, 0.84%, powder stored 8 months), (WSR-1006-A-01, 0.63%, fresh powder), and (WSR-1006-A-01, 0.91%, fresh powder). Powder used prior to the manufacturer's recommended expiration date is classified as fresh powder. The decreased effectiveness of the powder after eight months storage is noted. Although the mechanism by which this degradation has proceeded is uncertain, it is of interest to note that several tests were conducted of the influence of long term storage of concentrated solutions on the friction reducing capability of their subsequently diluted forms. These tests are described in more detail in the following section. Briefly, however, they revealed that the concentrated solutions stabilized with 0.5% isopropyl alcohol exhibited no discernible decrease in friction reducing capability after 8 months storage.

It seems reasonable to expect degradation of the polymer to proceed more rapidly in solution than in the dry powder state. According to the observed results, however, the slow degradation process was effectively stopped by the addition of an oxidation retardant. Presumably, therefore, some deleterious residue of the manufacturing process remains in the powder leading to long term degradation.

The ramifications of these facts are clear. The determination and comparison of physical properties of PEO solutions on the basis of manufacturer's grade specifications is not, in general, valid. These grade specifications purport to describe the average molecular weight of the product. No estimate of the batch-to-batch distribution of actual molecular weights about this average is given by the manufacturer. Yet, these are just the factors upon which comparisons between samples must be made. It

is important to know, as accurately as possible, the molecular weight distribution of any sample being investigated.

Intrinsic viscosity represents one measure of the average molecular weight of a polymer in solution. Efforts made in this program to obtain an approximate value of the intrinsic viscosity of the PEO solutions studied are discussed in Section 3.0 and 5.0. These results indicated that intrinsic viscosity (or average molecular weight) is simply not a sensitive enough indicator of the molecular weight distribution to correlate friction reduction data. No effort was made to apply it to the present problem of comparing concentrated solution properties. Some comments and suggestions for additional efforts along these lines are included in Section 6.0.

The results of the present program, therefore, are applicable (on a quantitative basis) only to the specific lot numbers tested. Extrapolations to include WSR-301 samples in general must be made cautiously and with a full understanding of the inherent dangers.

The complex molecular factors which play a role in stress decay have already been described. A number of quantitative examples of actual stress decay processes in concentrated solutions have been presented. It is now appropriate, in the light of the comments which have just been made, to formulate an interpretation of these results in terms of the fundamental processes involved.

It has already been pointed out that stress decay in thixotropic substances is often observed to exhibit a logarithmic stress-time relationship of the form

(3) $$\ln (\tau - \tau_\infty) = - A t + B$$

where τ is the instantaneous shear stress at time t, τ_∞ is the limiting shear stress, and A and B are constants. This type of relationship is often encountered in the literature dealing with rate processes, particularly in the field of chemical kinetics. In the commonly used terminology, the time rate of change of a property C can be written as

(4) $$\frac{dC}{dt} = - k C^N$$

where k is a rate constant whose units depend upon the constant N. Comparing (3) and (4), it can be seen that (3) can be written in differential form as

(5) $$\frac{d(\tau - \tau_\infty)}{dt} = - A (\tau - \tau_\infty)$$

from which it can be seen that N = 1, and B is the constant of integration when proceeding from (5) to (3). Since the form of equation (4) which corresponds to the stress decay process requires that N = 1, the process is termed first order.

There exists considerable evidence to suggest that stress decay in viscoelastic fluids such as concentrated PEO solutions might well be described by a relationship of the form (3). In treating viscoelastic behavior, it is common practice to use mechanical models. The simplest mechanical model of a system exhibiting both viscous and elastic characteristics is the Maxwell model in which the elastic components are

represented by a Hookean spring in series with a Newtonian dashpot representing the viscous components. For such a simple mechanical system, the strains are additive and the stress on the spring is equal to that on the dashpot. Hence, for the Maxwell model for shear,

(6) $$\frac{d\alpha}{dt} = \frac{\tau}{\eta_M} + \frac{1}{G_M}\frac{d\tau}{dt}$$

where α is the strain, η_M is the coefficient of viscosity and G_M is the elastic modulus.

In the present study, the strain rate, $\frac{d\alpha}{dt}$ is kept constant at D for time greater than zero, hence

(7) $$\frac{d\tau}{dt} = -\frac{G_M}{\eta_M}\tau + G_M D$$

letting $\frac{\eta_M}{G_M} = \lambda$, and integrating,

$$-\int \frac{d\tau}{\tau - G_M D\lambda} = \frac{1}{\lambda}\int dt$$

(8) $$\ln(\tau - G_M D\lambda) = -\frac{t}{\lambda} + c$$

where c is a constant of integration. The boundary conditions which must be met by (8) are

(9) $$\tau(t = 0) = \tau_o$$

$$\tau(t = \infty) = \tau_\infty$$

Hence,

$$\tau_\infty - G_M D\lambda = 0$$

(10) $$G_M D\lambda = \tau_\infty$$

and

(11) $$c = \ln(\tau_o - G_M D\lambda) = \ln(\tau_o - \tau_\infty)$$

Inserting (10) and (11) into (8),

(12) $$\ln(\tau - \tau_\infty) = -\frac{t}{\lambda} + \ln(\tau_0 - \tau_\infty)$$

which has the same form as (3). Rearranging,

(13) $$\ln\left(\frac{\tau - \tau_\infty}{\tau_0 - \tau_\infty}\right) = -\frac{t}{\lambda}$$

According to (13), λ has the form of a time constant and can be obtained by plotting the dimensionless term $\ln\left(\frac{\tau - \tau_\infty}{\tau_0 - \tau_\infty}\right)$ as a function of t. If the model is appropriate to the case under consideration, a straight line will result whose slope is λ. The coefficients G_M and η_M follow immediately from the definition of λ and (10).

Unfortunately, few polymeric systems can be represented by a single relaxation time, because of the complexity of the molecular structure. For this reason, a generalized Maxwell model involving a spectrum of Maxwell elements in parallel is used. The equation for this model is suggested by the exponential form of (13). That is,

(14) $$\frac{\tau}{D} = G_1 e^{-t/\lambda_1} + G_2 e^{-t/\lambda_2} + \ldots$$

If a constant strain rate results in the appearance of a steady-state stress response after a long period of time (as is the case here), then one of the relaxation times is equal to infinity and (14) should be written

(15) $$\frac{\tau - \tau_\infty}{D} = G_1 e^{-t/\lambda_1} + G_2 e^{-t/\lambda_2} + \ldots$$

Additional refinements to the treatment, such as the assumption of a continuous spectrum of relaxation times, are possible. Furthermore, numerous other models and approaches have been postulated.

The analysis of the stress decay characteristics of the concentrated PEO solutions examined in this program in terms of clear-cut models of the type just described is complicated by several factors. First, because of the complex nature of the physical processes involved, it is not likely that a single time constant will suffice to explain the data. On the other hand, an analysis of the type implied by equation (14) wherein the data are simply forced to fit by the inclusion of a sufficient number of terms, tends to obscure the physical interpretation of the relaxation times. In addition, such an analysis requires a fairly high degree of prescision in the data. Unfortunately, it will be recalled, the fluctuations noted in the stress decay curves result in some uncertainty in the magnitudes of the stress levels at short times. In addition, since the fluctuations presumably result from a slow secondary circulation of fluid, there tends to be a distortion of the time scale (at long times) from that which would be expected if no circulation occurred.

As an example, the stress decay characteristics previously depicted in Figure 21 for a 0.7% solution are shown again in Figure 32. In this case, however, the function $(\tau - \tau_\infty)$ is plotted logarithmically as a function of time for shear rates of 1370, 685, 957, and 228 sec^{-1}. If the Maxwell model were applicable, these data would fall in a straight line, and a single relaxation time would suffice to describe the stress decay process at each shear rate. That this is not the case is clear from the Figure. Although they are not shown, similar plots of stress decay in the other solutions studied fail to follow the Maxwell model.

Any further effort to analyze these data in terms of more complex models will not be attempted here. The anomalies present in the data, especially at long times, are evident in Figure 32. These are characteristic of the data for the other concentration studied and result from the factors alluded to above.

4.2.2 Step Sequence Experiments.

The operations involved in the concentrated solution viscosity measurements are described in Section 3.0. It will be recalled that each stress decay experiment was followed immediately by a stepping-down, in sequence (according to Table 1 in Section 3.0), of the shear rate. Thus, the stress-decay experiment provides a solution with a well defined solution history whose instantaneous apparent viscosity (or shear stress) is determined as a function of shear rate by the subsequent sequence. Figure 33 represents a composite of actual recorder output illustrating the relationship of the step sequence runs to the corresponding stress decay experiments. The essential characteristics of these curves has already been discussed.

The limiting viscosities obtained at the end of each stress decay experiment are given in Tables 3 through 5. In each case, the shear rate at the head of each column represents a stress decay experiment. The limiting values η_∞ and τ_∞ appear immediately below. The following sequence of numbers in each column represents the limiting viscosities obtained in the corresponding step sequence. The shear rates at which the stress decay runs were made vary by as much as a factor of 8 (10 for the 1.03% solution). The corresponding step sequence limiting viscosities are surprisingly

Table 3
Step Sequence Limiting Viscosities
(WSR-1227-A-01)
1.03%

Stress Decay Shear Rate (sec^{-1})	1370	685	457	228	152	
η_∞(cp)	38.5	51	58	89.5	110	η_∞(avg) (cp)
$\tau_\infty(\frac{dynes}{cm^2})$	526.5	348.3	264.2	203.9	167	
Step Sequence Shear Rate (sec^{-1})						
1370						38.5
685	52					51.5
457	57.5	61				59
228	83.6	85.8	80.5			85
152	101.5	105	97	108		104
76	142	146	134	146	146	143
51	180	180	167.5	180	177	177
25	256	268	244	284	246	252
16	311	320	284	311	302	306
8.5	439	475	402	438	421	435

Table 4
Step Sequence Limiting Viscosities
(WSR-1227-A-01)
0.7%

Stress Decay Shear Rate (sec^{-1})	1370	685	457	228	
η_∞(cp)	18.7	25.3	30.2	42.5	
$\tau_\infty(\frac{dynes}{cm^2})$	256.5	173.0	137.5	97.3	η_∞(avg) (cp)
Step Sequence Shear Rate (sec^{-1})					
1370					18.7
685	22.7				24
457	26.5	29.4			28.7
228	35.2	39.6	40.6		39.5
152	42.7	47.2	49.2	51.3	47.6
76	55	62	65	67	62
51	67	76	79	82	76
25	92	111	107	99	102
16	106	135	120	135	128
8.5	110	146	136	164	139

Table 5
Step Sequence Limiting Viscosities
(WSR-1227-A-01)
0.41%

Stress Decay Shear Rate (sec^{-1})	1370	685	457	228	
η_∞(cp)	10.7	12.1	13.8	18.[illegible]	η_∞(avg) (cp)
$\tau_\infty(\frac{dynes}{cm})$	146	83.5	63.4	42.5	
Step Sequence Shear Rate (sec^{-1})					
1370					10.7
685	11.8				11.9
457	13.2	13.2			13.4
228	16.9	17.0	15.8		17.2
152	17.3	16.3	16.0	20.3	17.5
76	22.6	22.4	22.4	25.4	23.4
51	25.7	27.3	28.8	30.7	28.1
25	30.9	30.9	30.9	35.5	32.1

unaffected by these differences. There appear to be several exceptions to this "rule", especially for the 0.7% solution, but, they occur primarily at the lower shear rates, where it is expected that errors would be greatest.

A tentative conclusion, therefore, is that at least within the range of shear rates and concentrations studied, the limiting viscosities measured at each shear rate are independent of the shear rate at which the stress decay is imposed. Although these results cannot be considered conclusive, it is tempting to speculate upon their meaning in terms of an explanation of the molecular mechanisms involved in the stress decay process. In particular, they would appear to rule out any extensive molecular scission as a major contributor to the stress decay. Surely, of all the possible molecular processes taking place during stress decay (disentanglement, molecular orientation, molecular scission, etc.) scission, which involves the definable "energy of activation" necessary to break bonds, would be expected to be strongly dependent upon the rate of mechanical energy input to the fluid. Studies of the effect of stress decay in concentrated solutions on the friction reducing ability of corresponding diluted solution are described in the next section. Friction reduction was found to be virtually independent of the concentrated solution history. Friction reduction is a rough measure of molecular weight, being primarily affected by the longer chain molecules in the molecular weight distribution. Since these longer molecules should be even more susceptible to mechanical degradation, these studies confirm the findings of this section.

One additional interesting characteristic of the limiting viscosity-shear rate relationship is illustrated in Figure 34 where the limiting

viscosities from Tables 3, 4, and 5 are plotted versus shear rate on log-log coordinates. The resulting straight lines verify the power-law behavior of PEO solutions over a wide range of shear rates and concentrations. The applicable power law relations are, from Figure 34,

For 1.03% PEO: $\tau = 12.2D^{0.51}$ (8.5 - 1370 sec^{-1})

For 0.70% PEO: $\tau = 4.4D^{0.55}$ (16 - 1370 sec^{-1})

For 0.41% PEO: $\tau = 0.83D^{0.71}$ (25 - 1370 sec^{-1})

Additional confirmation of the power-law relation is detailed in Appendix V, where some preliminary data obtained during the early part of the program is summarized.

Figure 10
Flow Curves for Various Ideal Rheological Bodies

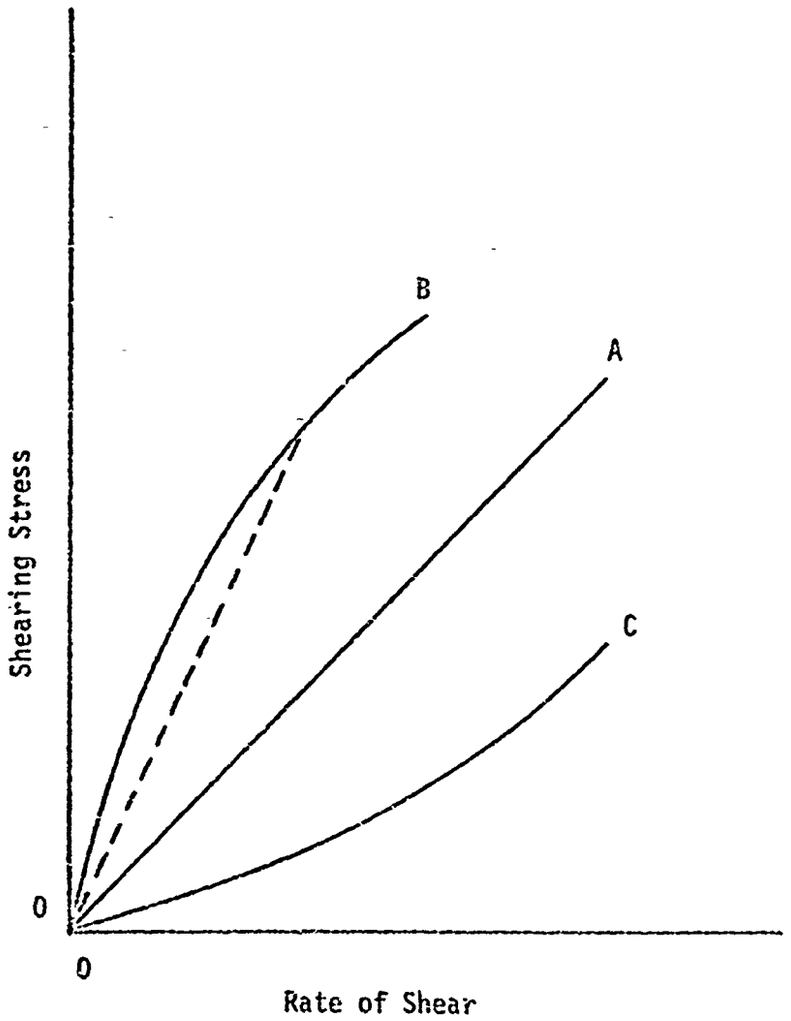

Figure 11
Thixotropy in a Pseudoplastic Emulsion of Soaps and High Polymers in Gasoline at 25°C (26,35)
(a)

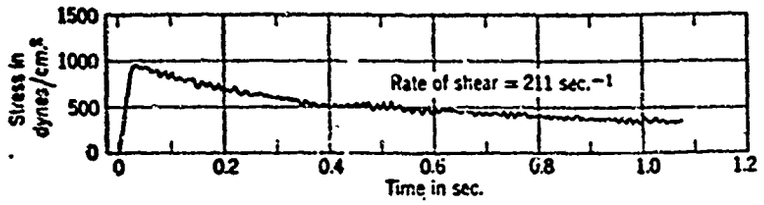

(b)

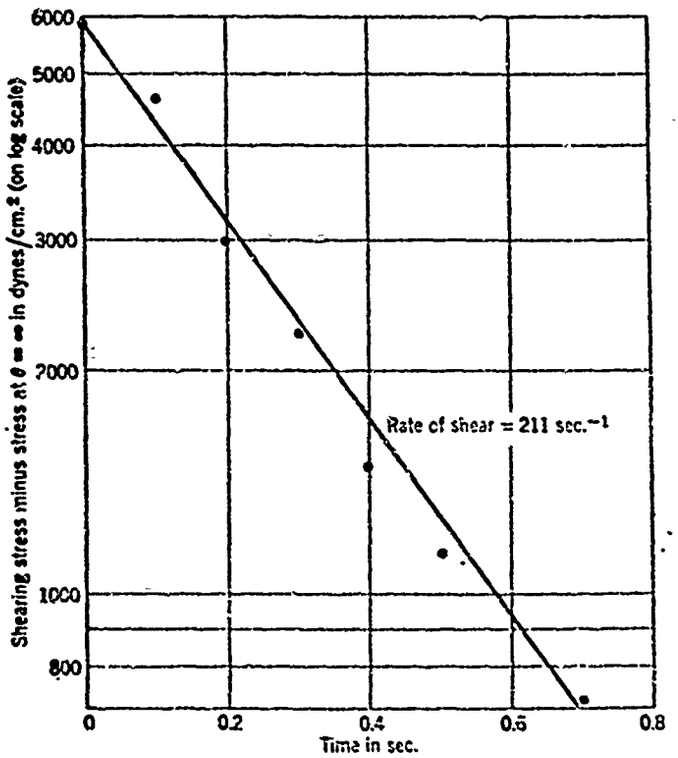

Figure 12
Variation of Initial and Final Apparent Viscosities
at 28°C of the Thixotropic System of Figure 11

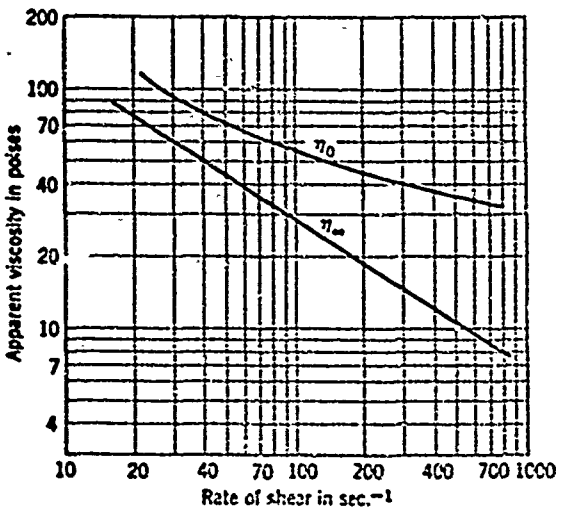

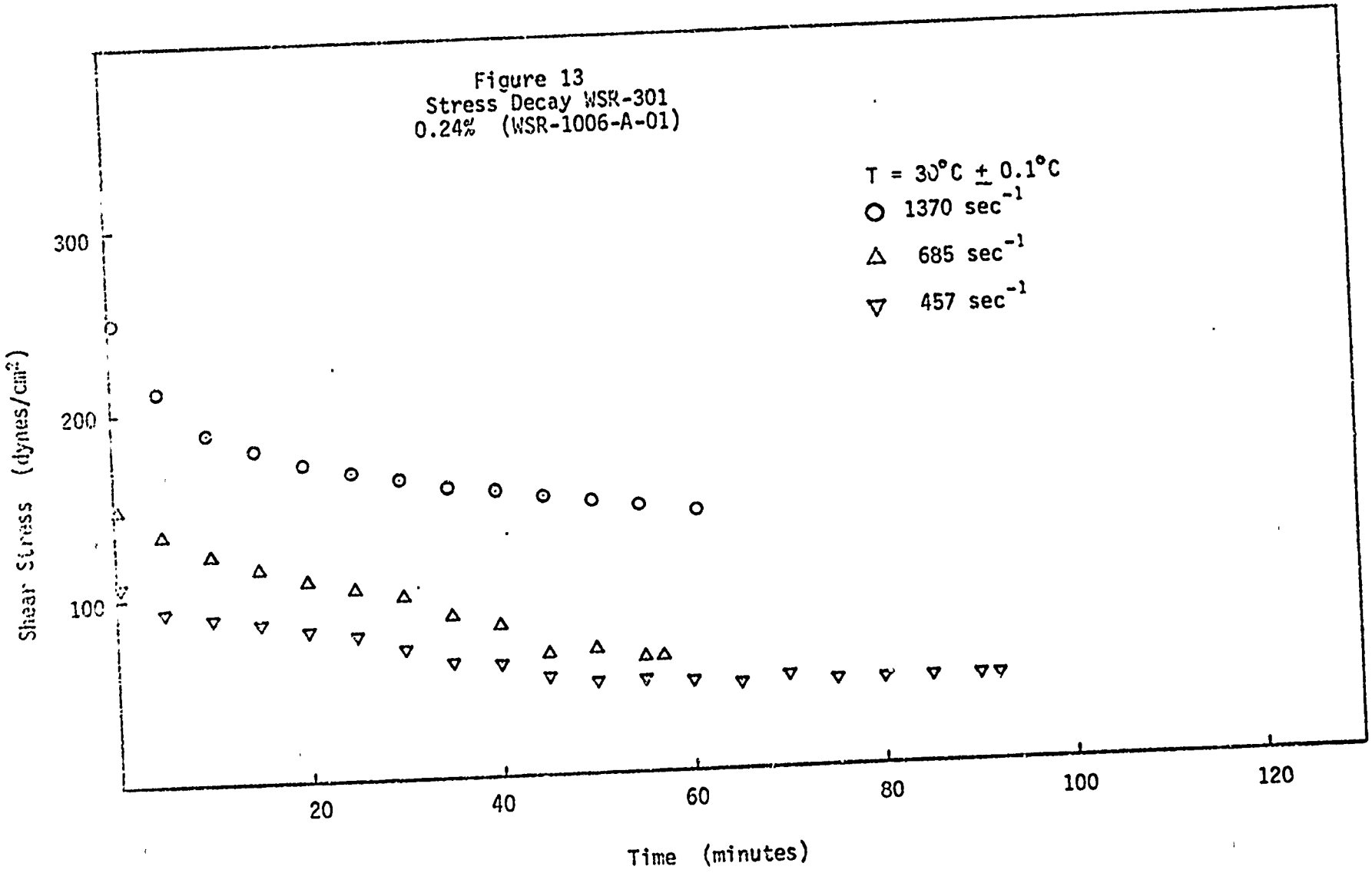

Figure 13
Stress Decay WSR-301
0.24% (WSR-1006-A-01)

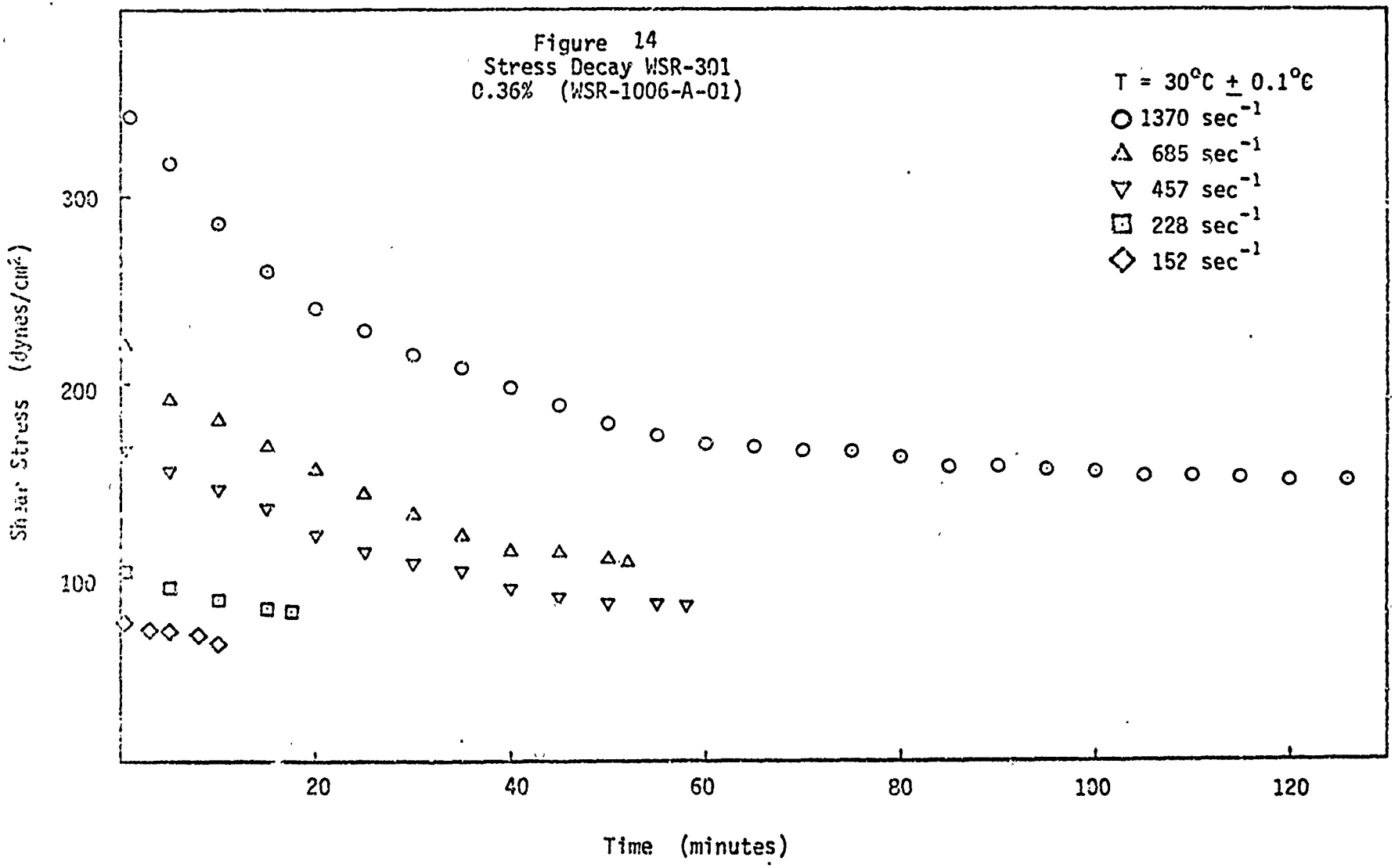
Figure 14
Stress Decay WSR-301
0.36% (WSR-1006-A-01)
T = 30°C ± 0.1°C
1370 sec⁻¹
685 sec⁻¹
457 sec⁻¹
228 sec⁻¹
152 sec⁻¹
Shear Stress (dynes/cm²)
300
200
100
20
40
60
80
100
120
Time (minutes)

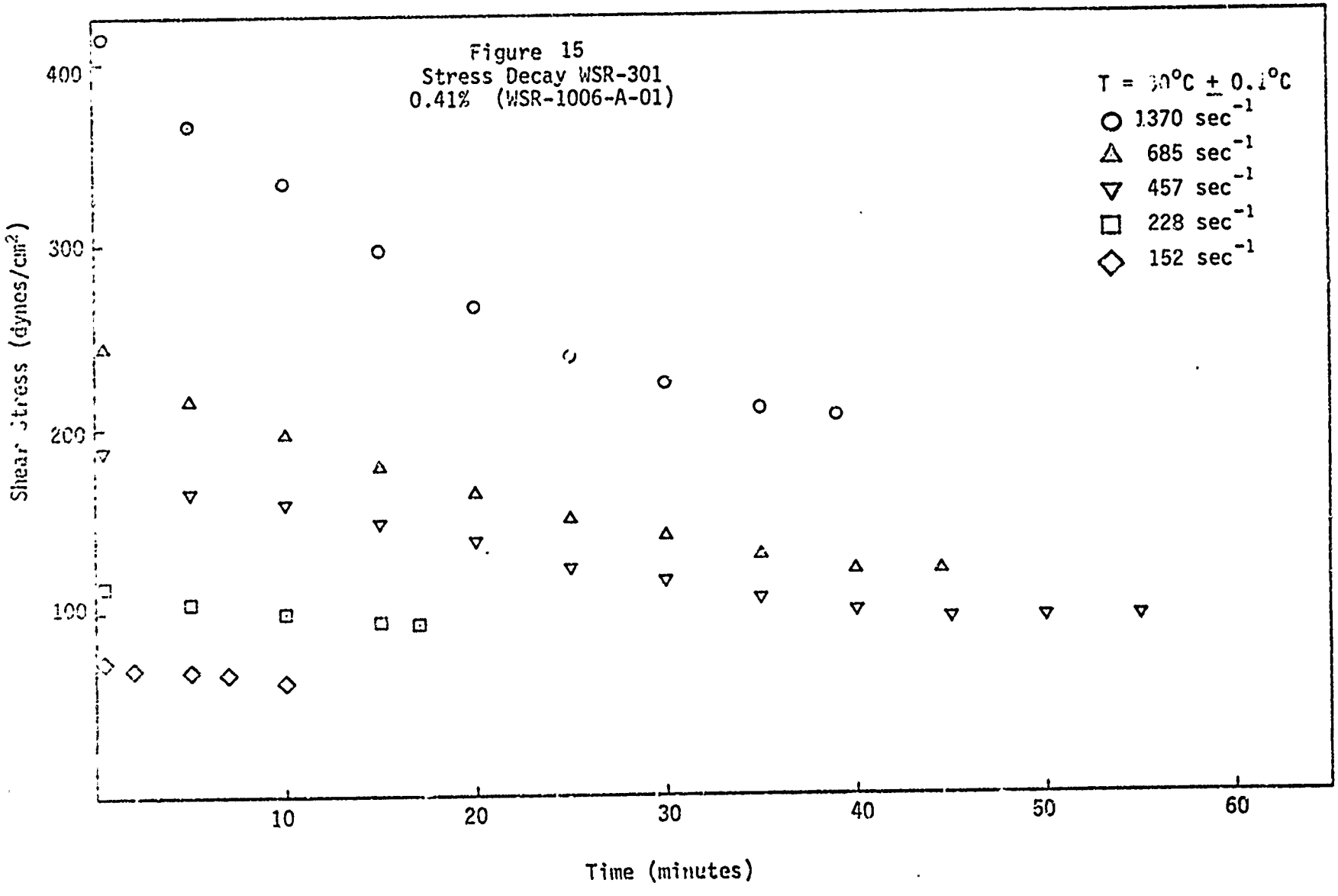
Figure 15
Stress Decay WSR-301
0.41% (WSR-1006-A-01)
T = 30°C ± 0.1°C
1370 sec^{-1}
685 sec^{-1}
457 sec^{-1}
228 sec^{-1}
152 sec^{-1}
Shear Stress (dynes/cm^2)
400
300
200
100
10
20
30
40
50
60
Time (minutes)

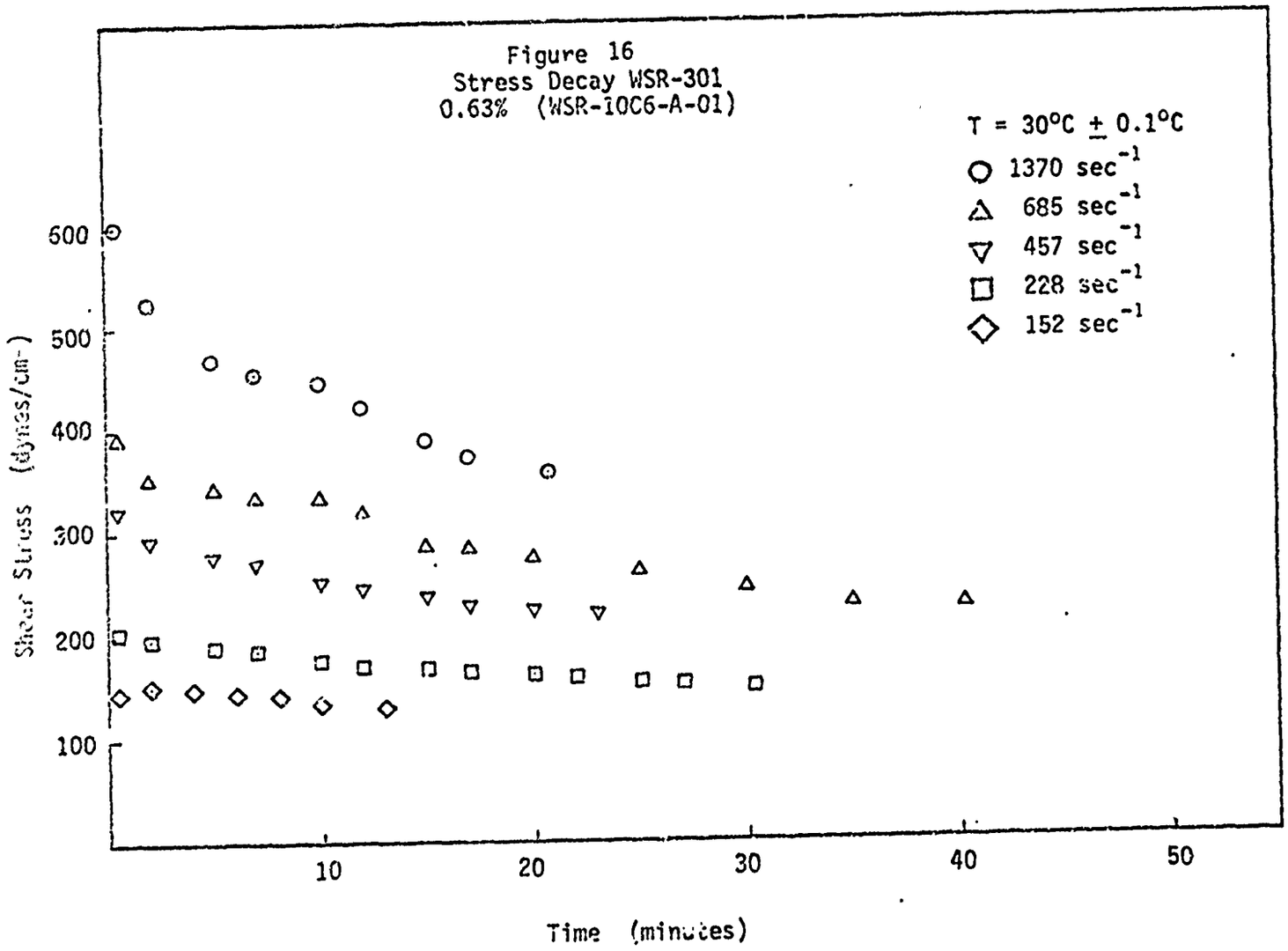

Figure 16
Stress Decay WSR-301
0.63% (WSR-10C6-A-01)

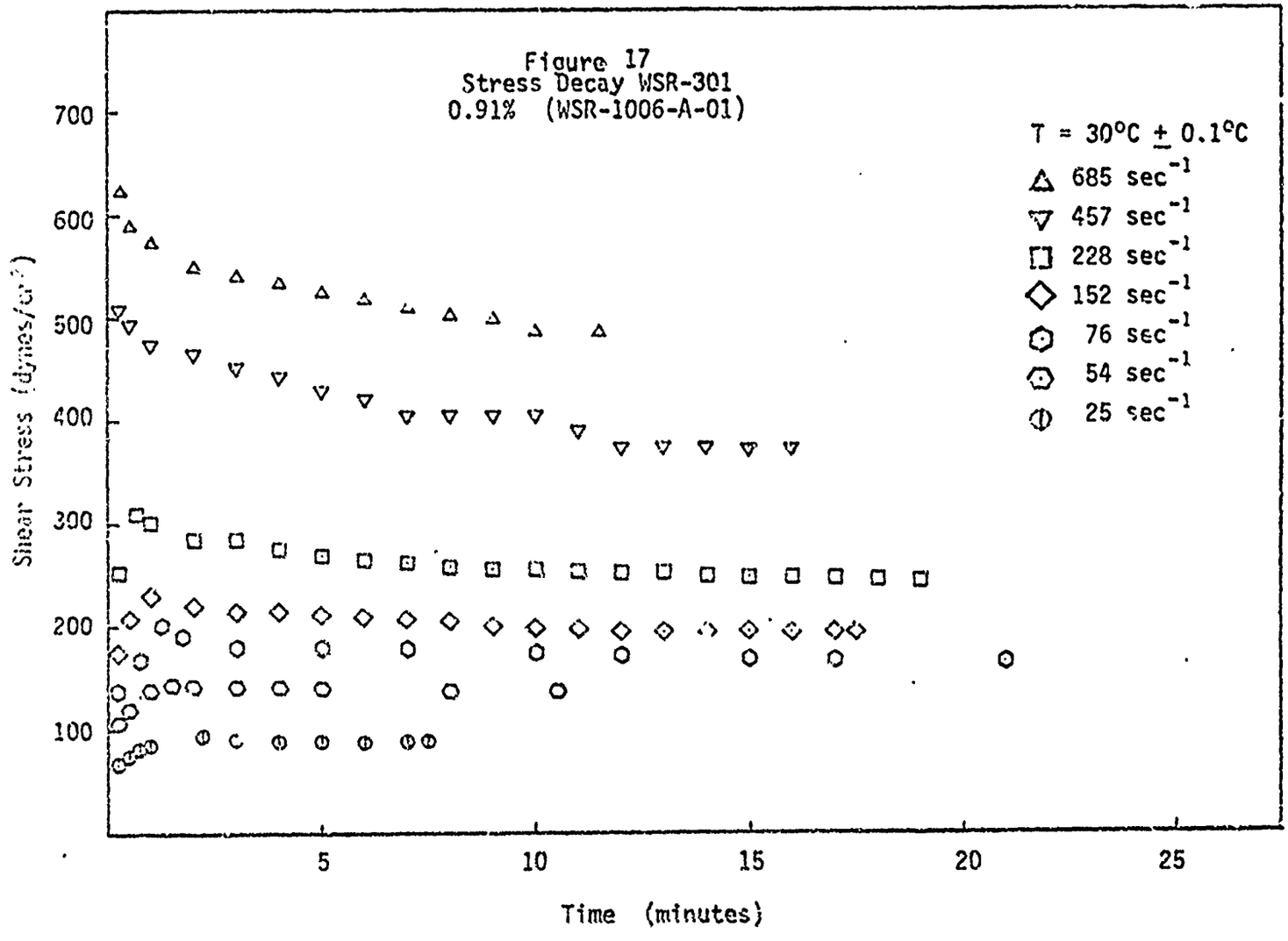
Figure 17
Stress Decay WSR-301
0.91% (WSR-1006-A-01)
T = 30°C ± 0.1°C
685 sec^{-1}
457 sec^{-1}
228 sec^{-1}
152 sec^{-1}
76 sec^{-1}
54 sec^{-1}
25 sec^{-1}
Shear Stress (dynes/cm^2)
700
600
500
400
300
200
100
5
10
15
20
25
Time (minutes)

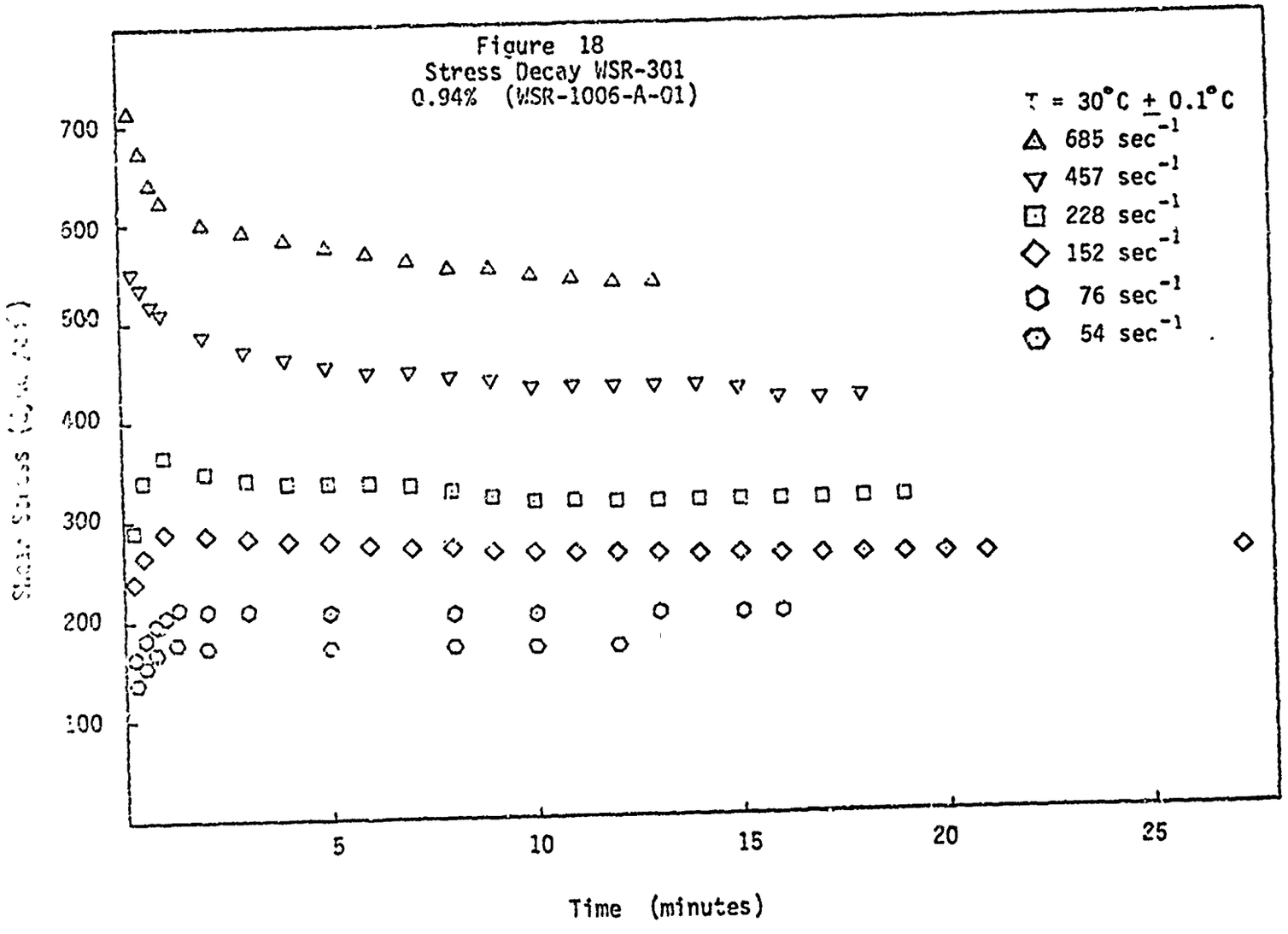
Figure 18
Stress Decay WSR-301
0.94% (WSR-1006-A-01)
T = 30°C ± 0.1°C
685 sec⁻¹
457 sec⁻¹
228 sec⁻¹
152 sec⁻¹
76 sec⁻¹
54 sec⁻¹
700
600
500
400
300
200
100
5
10
15
20
25
Time (minutes)

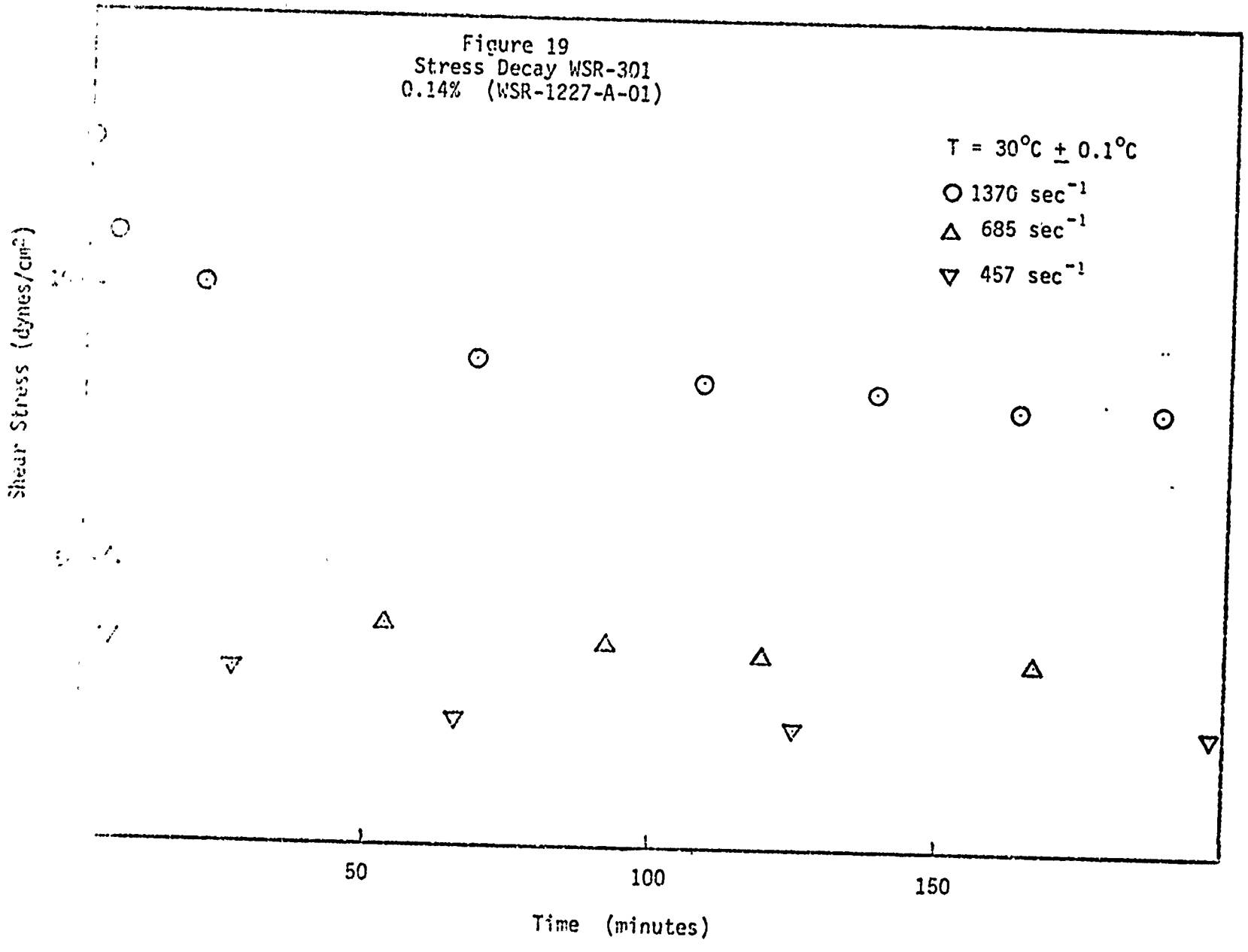

Figure 19
Stress Decay WSR-301
0.14% (WSR-1227-A-01)

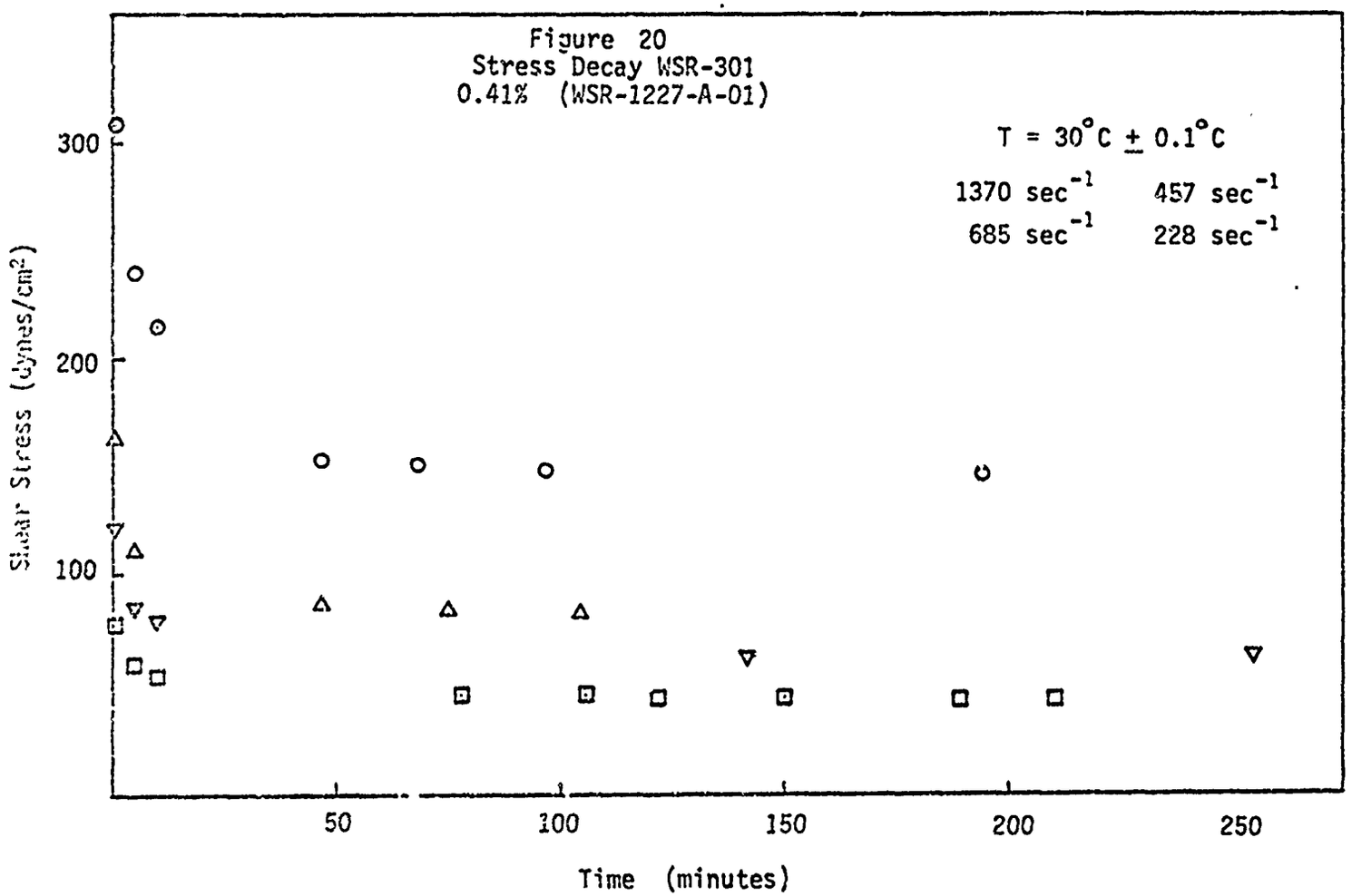

Figure 20
Stress Decay WSR-301
0.41% (WSR-1227-A-01)

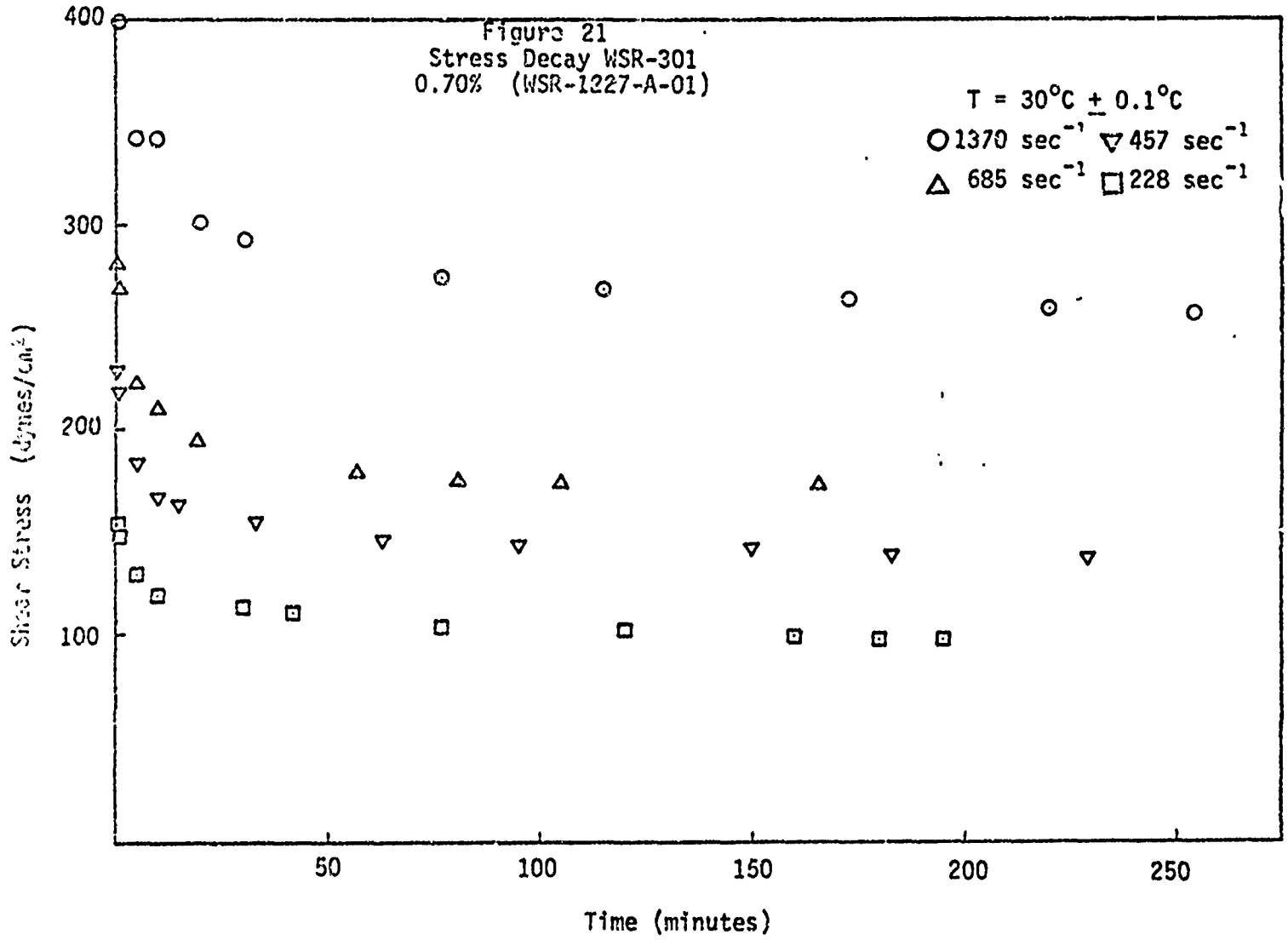
Figure 21
Stress Decay WSR-301
0.70% (WSR-1227-A-01)
T = 30°C ± 0.1°C
1370 sec⁻¹
457 sec⁻¹
685 sec⁻¹
228 sec⁻¹
400
300
200
100
Shear Stress (dynes/cm²)
50
100
150
200
250
Time (minutes)

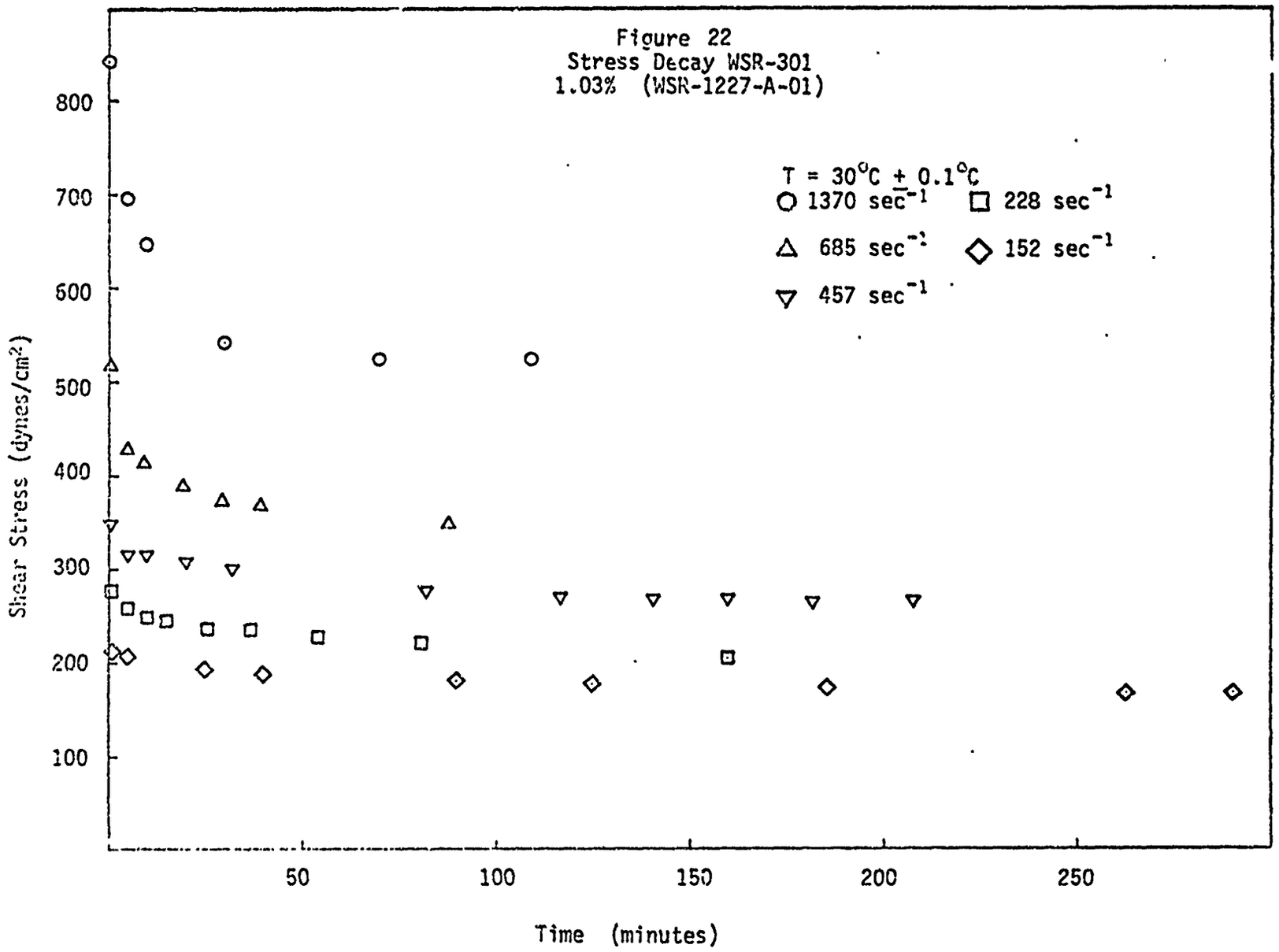
Figure 22
Stress Decay WSR-301
1.03% (WSR-1227-A-01)
T = 30°C ± 0.1°C
1370 sec⁻¹
228 sec⁻¹
685 sec⁻¹
152 sec⁻¹
457 sec⁻¹
Shear Stress (dynes/cm²)
800
700
600
500
400
300
200
100
50
100
150
200
250
Time (minutes)

Figure 23
Viscoelastic Phenomena in Rotational Shearing Flows

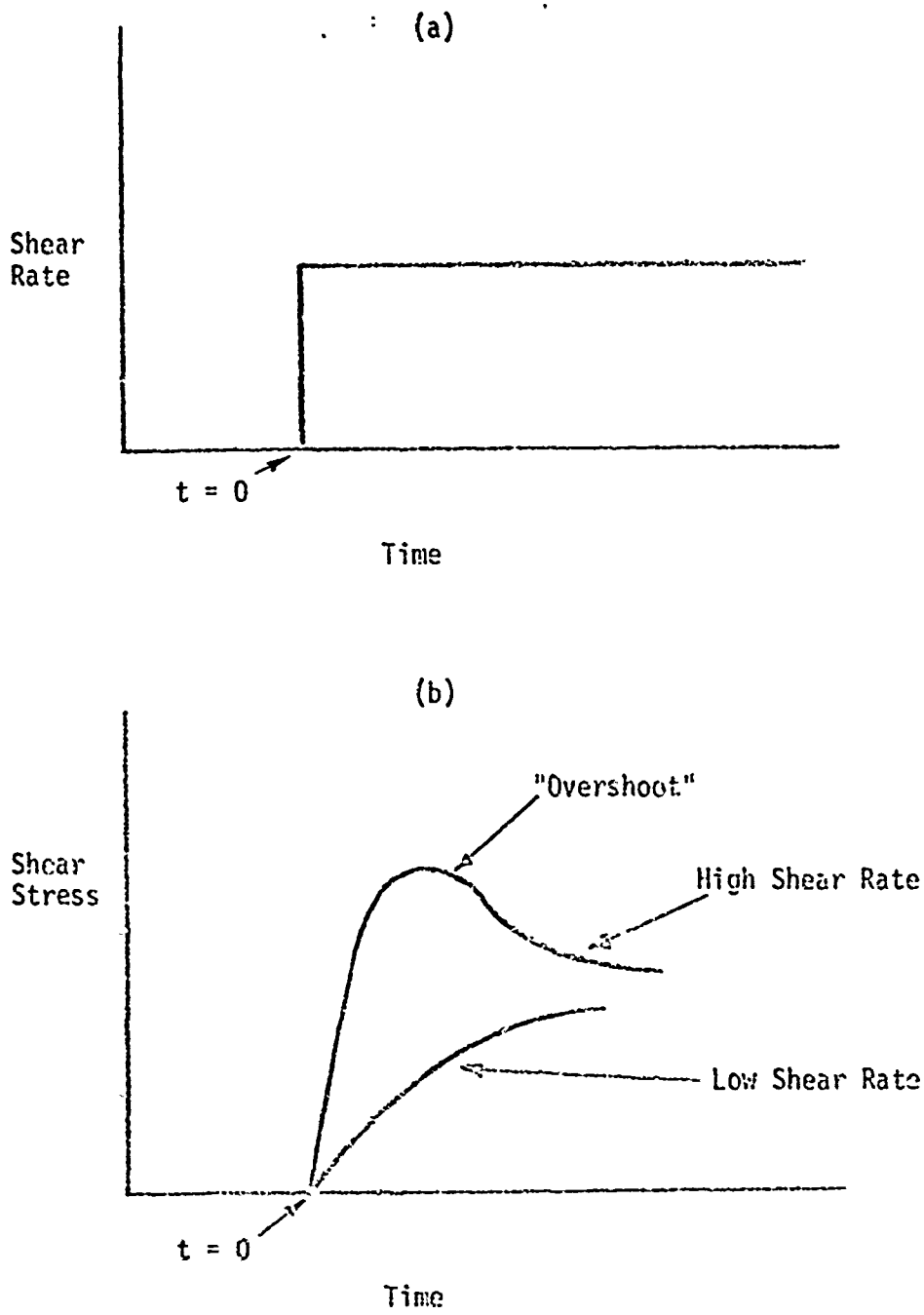

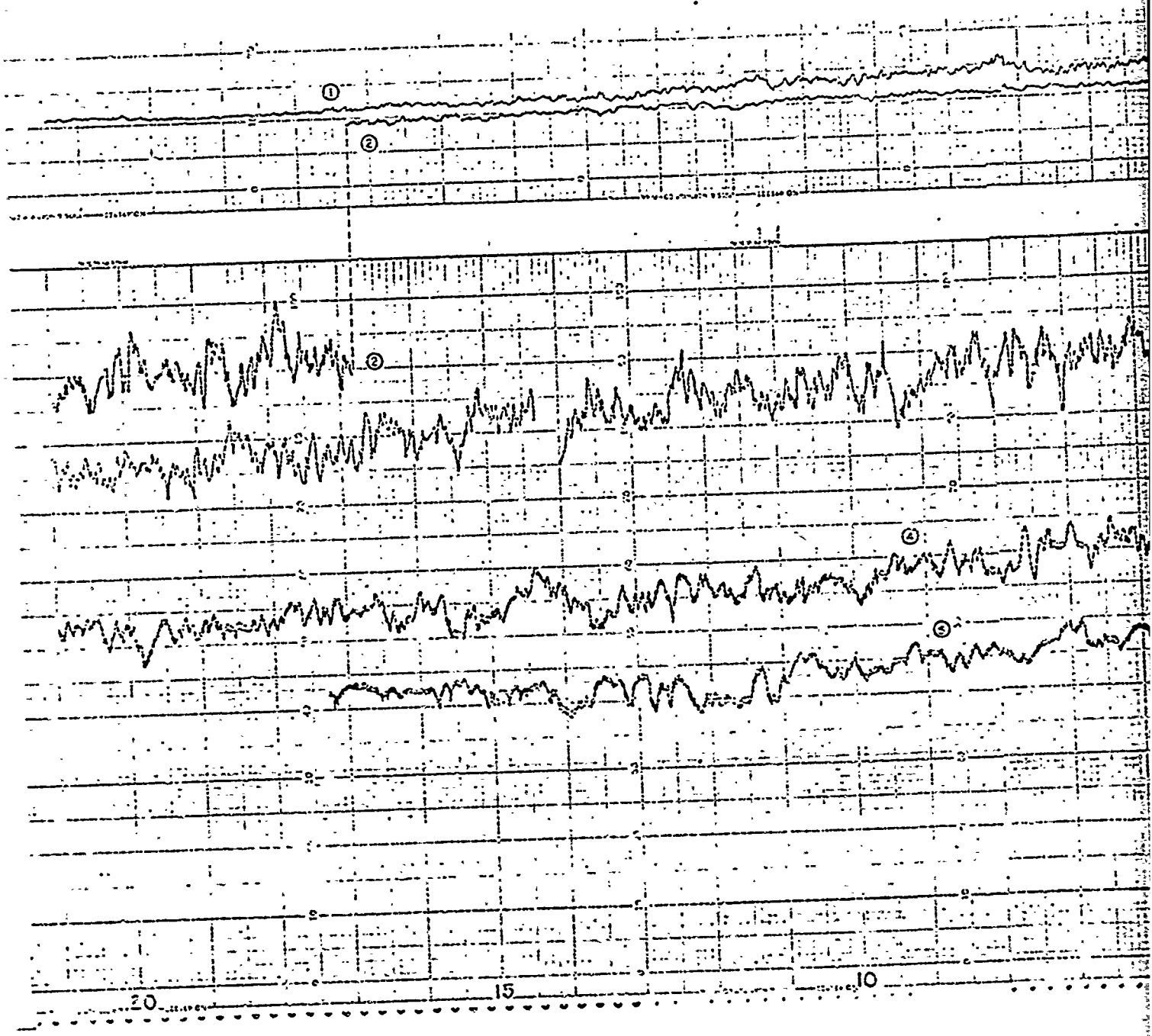
①
②
②
④
⑤
20
15
10

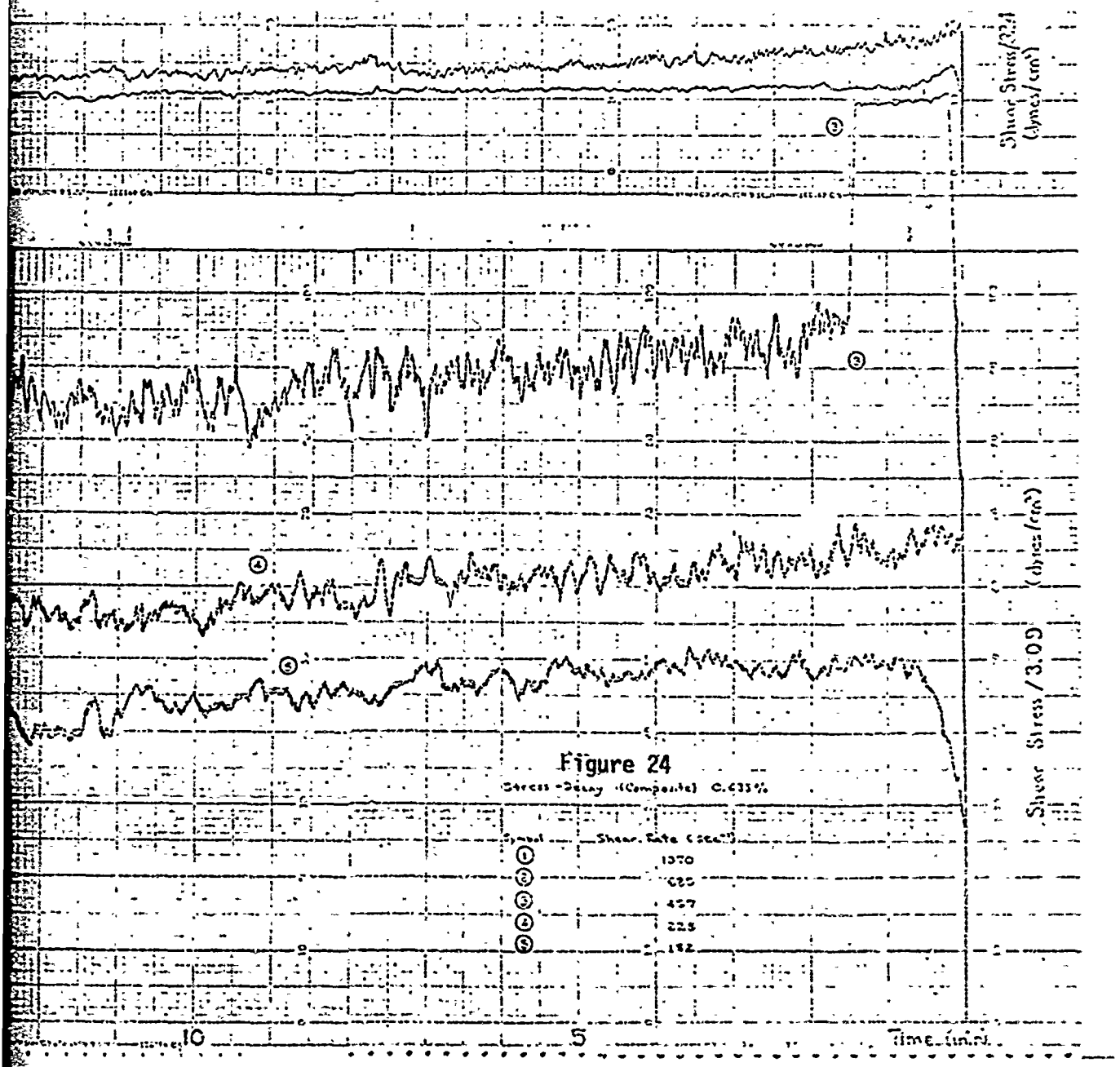

Figure 24

Stress-Decay (Composite) 0.633%

Speed	Shear Rate (sec⁻¹)
①	1370
②	625
③	457
④	225
⑤	152

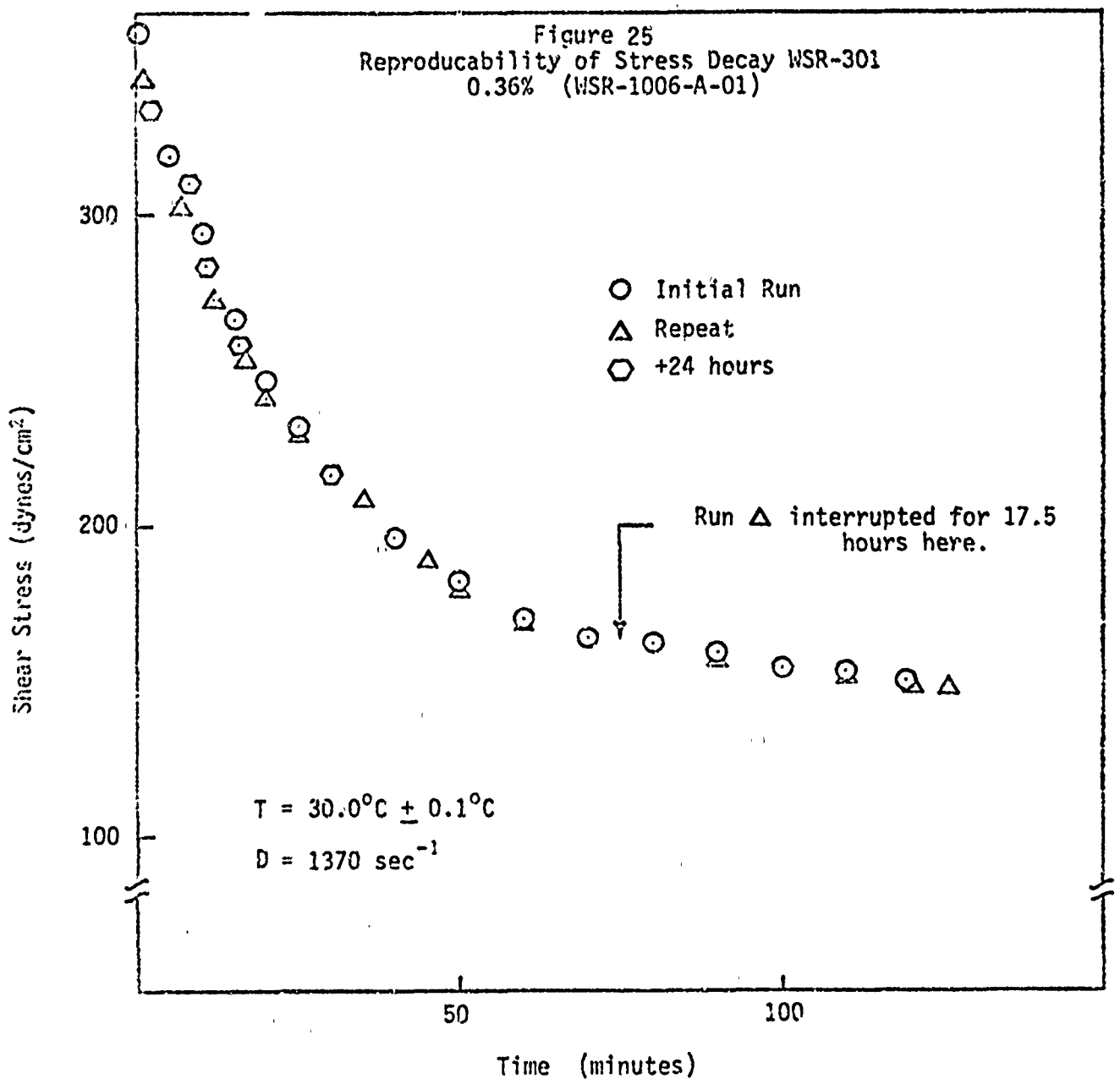

Figure 25
Reproducability of Stress Decay WSR-301
0.36% (WSR-1006-A-01)

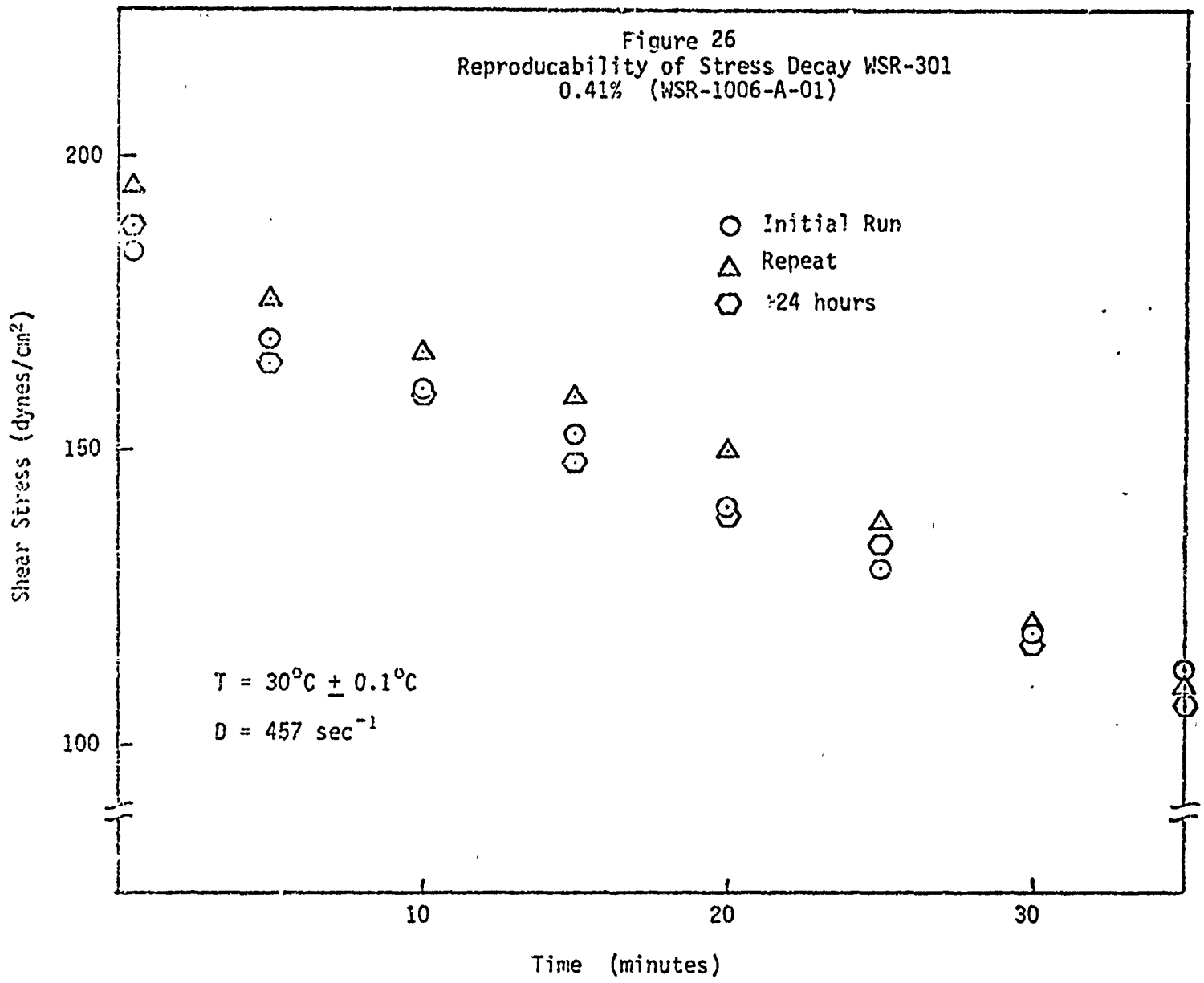
Figure 26
Reproducability of Stress Decay WSR-301
0.41% (WSR-1006-A-01)
Initial Run
Repeat
+24 hours
T = 30°C ± 0.1°C
D = 457 sec⁻¹
Shear Stress (dynes/cm²)
200
150
100
10
20
30
Time (minutes)

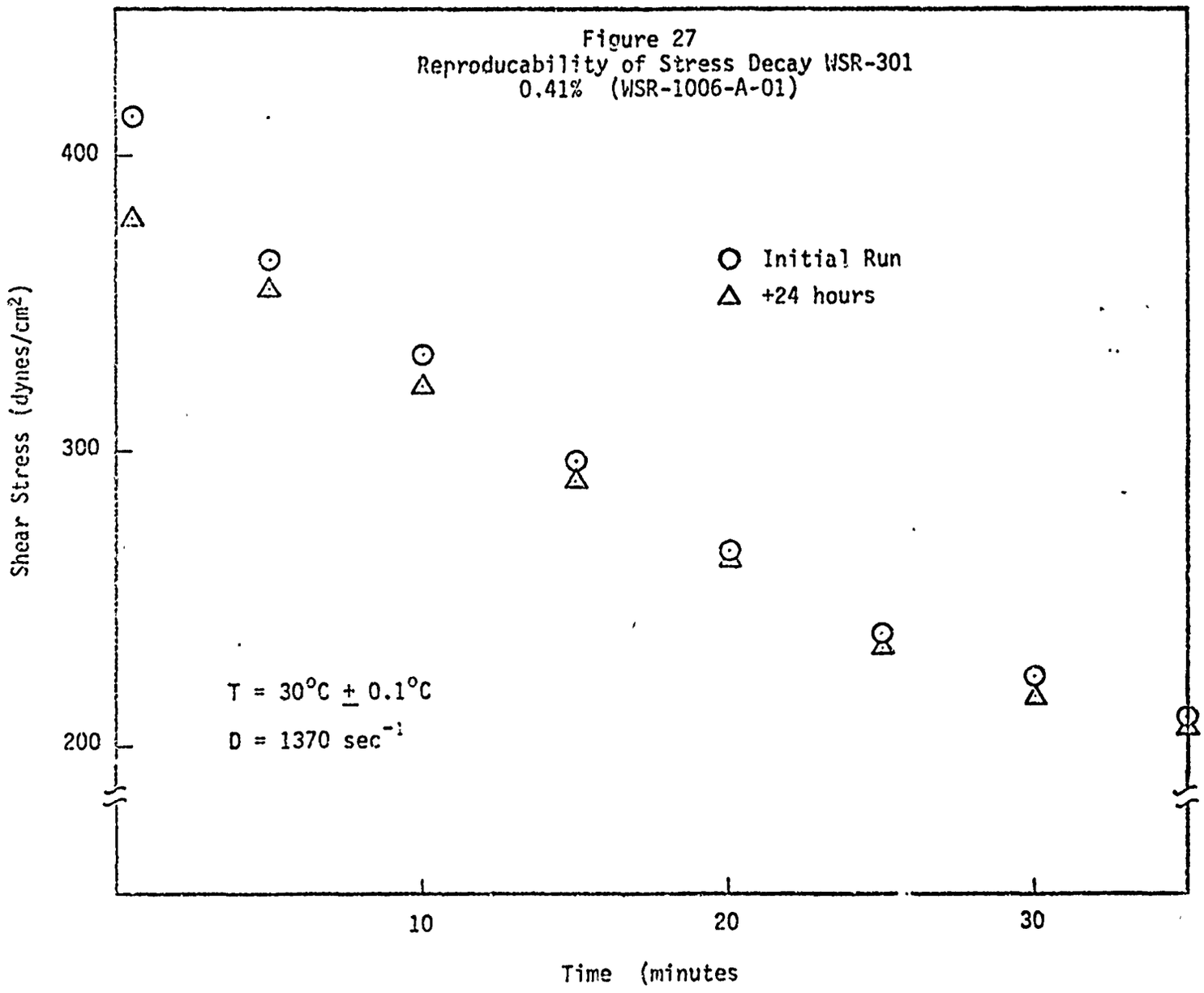

Figure 27
Reproducability of Stress Decay WSR-301
0.41% (WSR-1006-A-01)

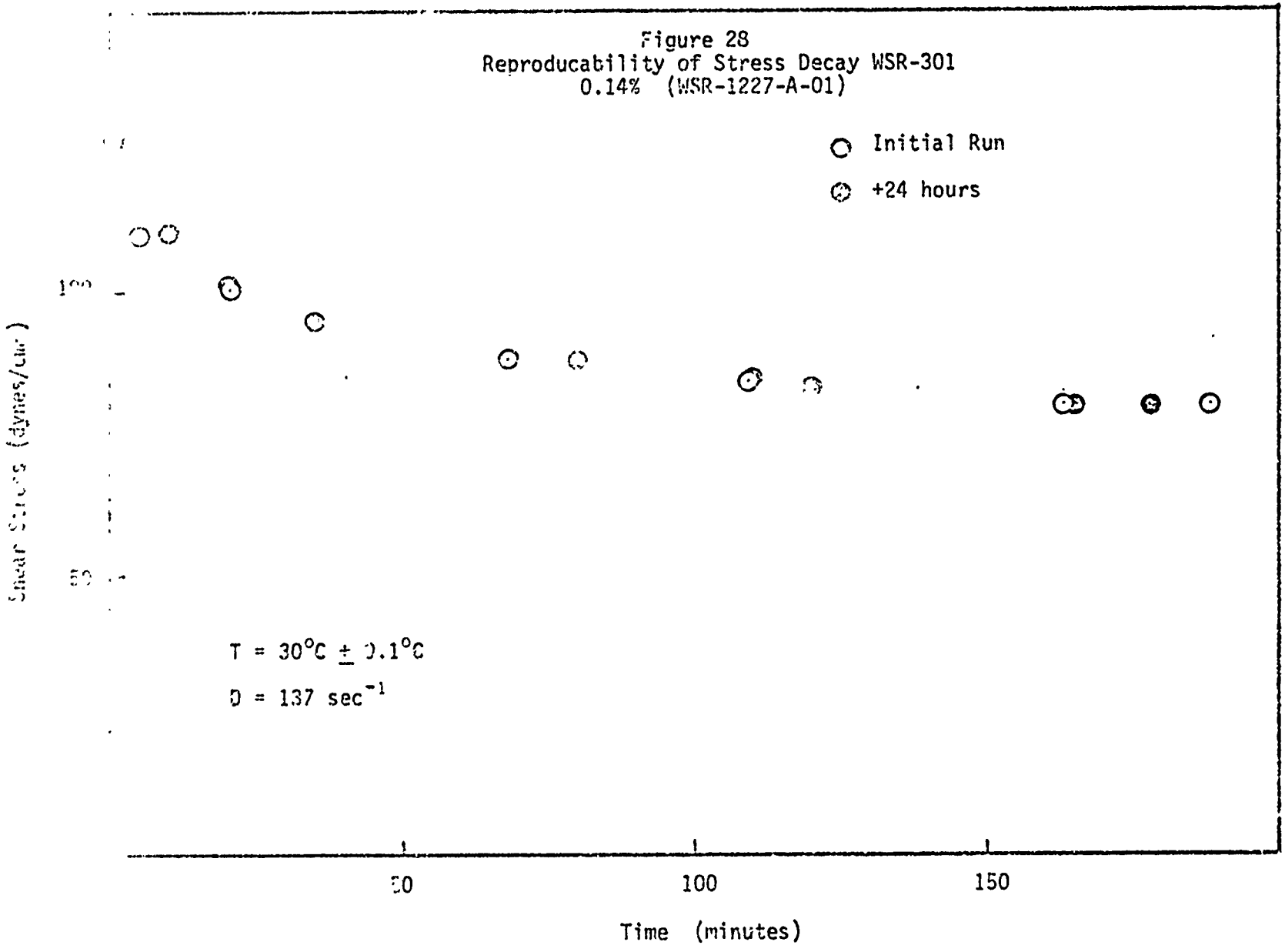

Figure 28
Reproducability of Stress Decay WSR-301
0.14% (WSR-1227-A-01)

Figure 29
Reproducability of Stress Decay WSR-301
0.7%, 0.41% (WSR-1227-A-01)

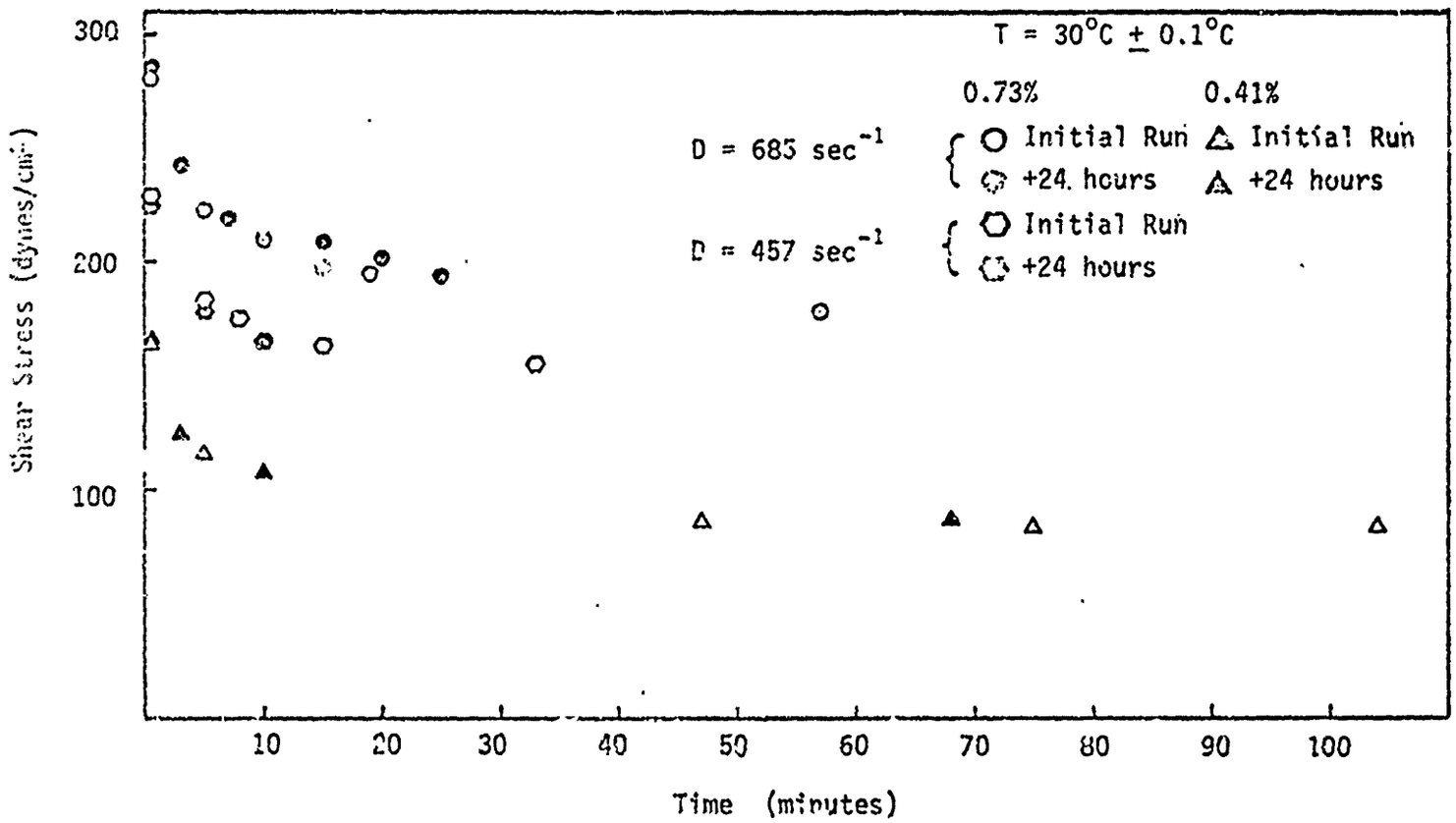

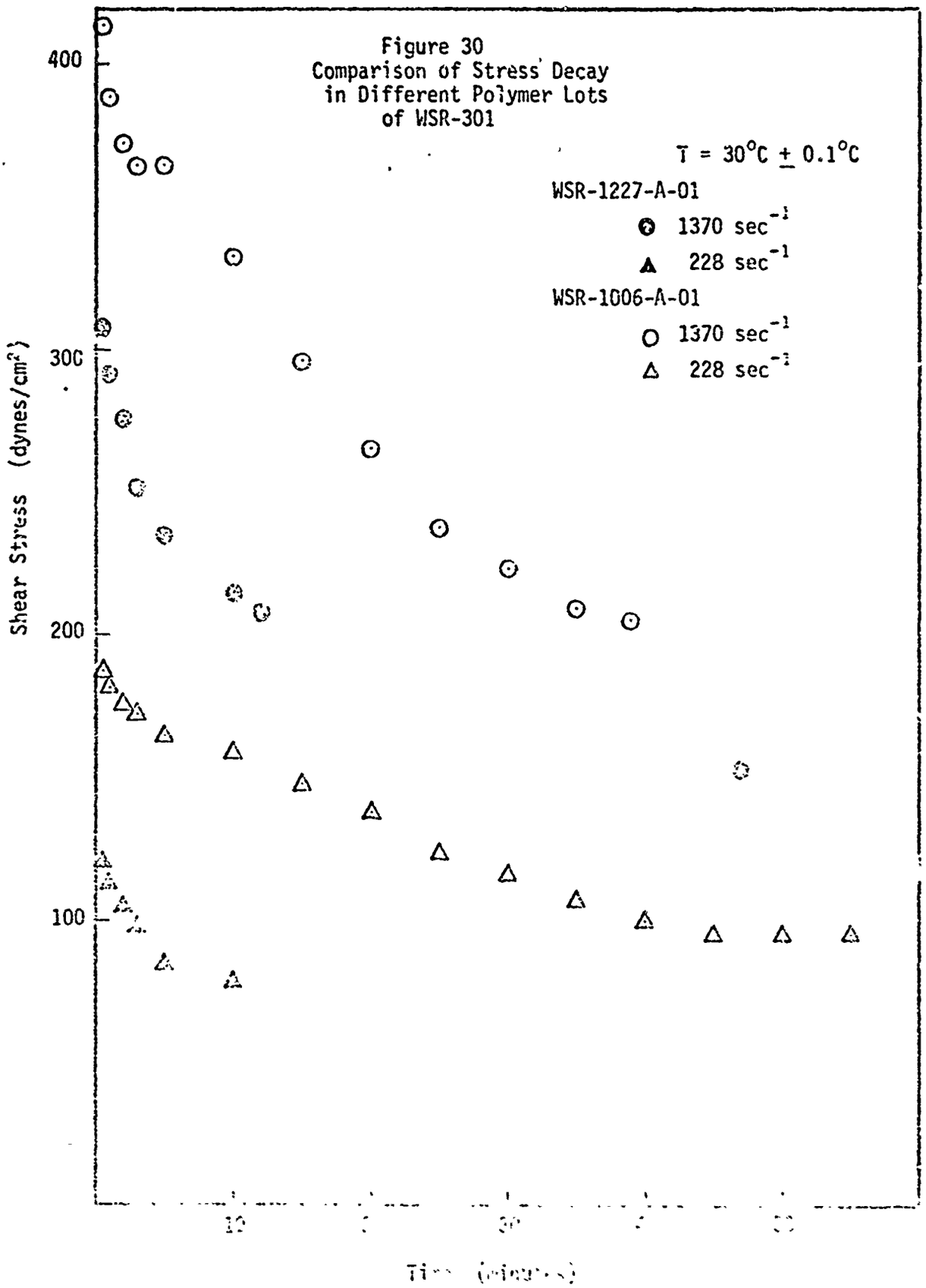
Figure 30
Comparison of Stress Decay
in Different Polymer Lots
of WSR-301
T = 30°C ± 0.1°C
WSR-1227-A-01
1370 sec⁻¹
228 sec⁻¹
WSR-1006-A-01
1370 sec⁻¹
228 sec⁻¹
Shear Stress (dynes/cm²)
400
300
200
100
10
30

Figure 31
Effect of Polymer Powder Age
on Concentrated Solution Viscosity

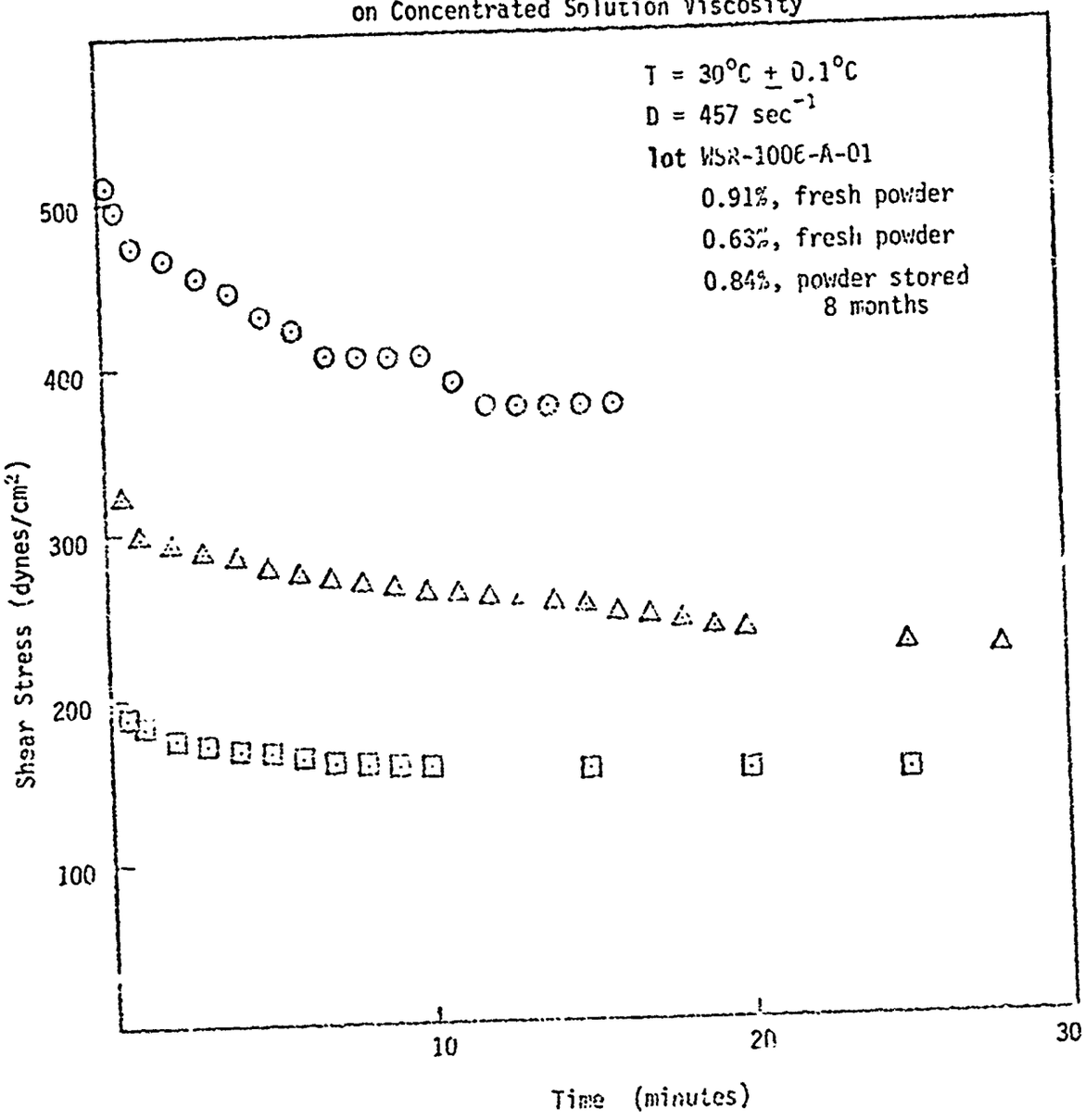

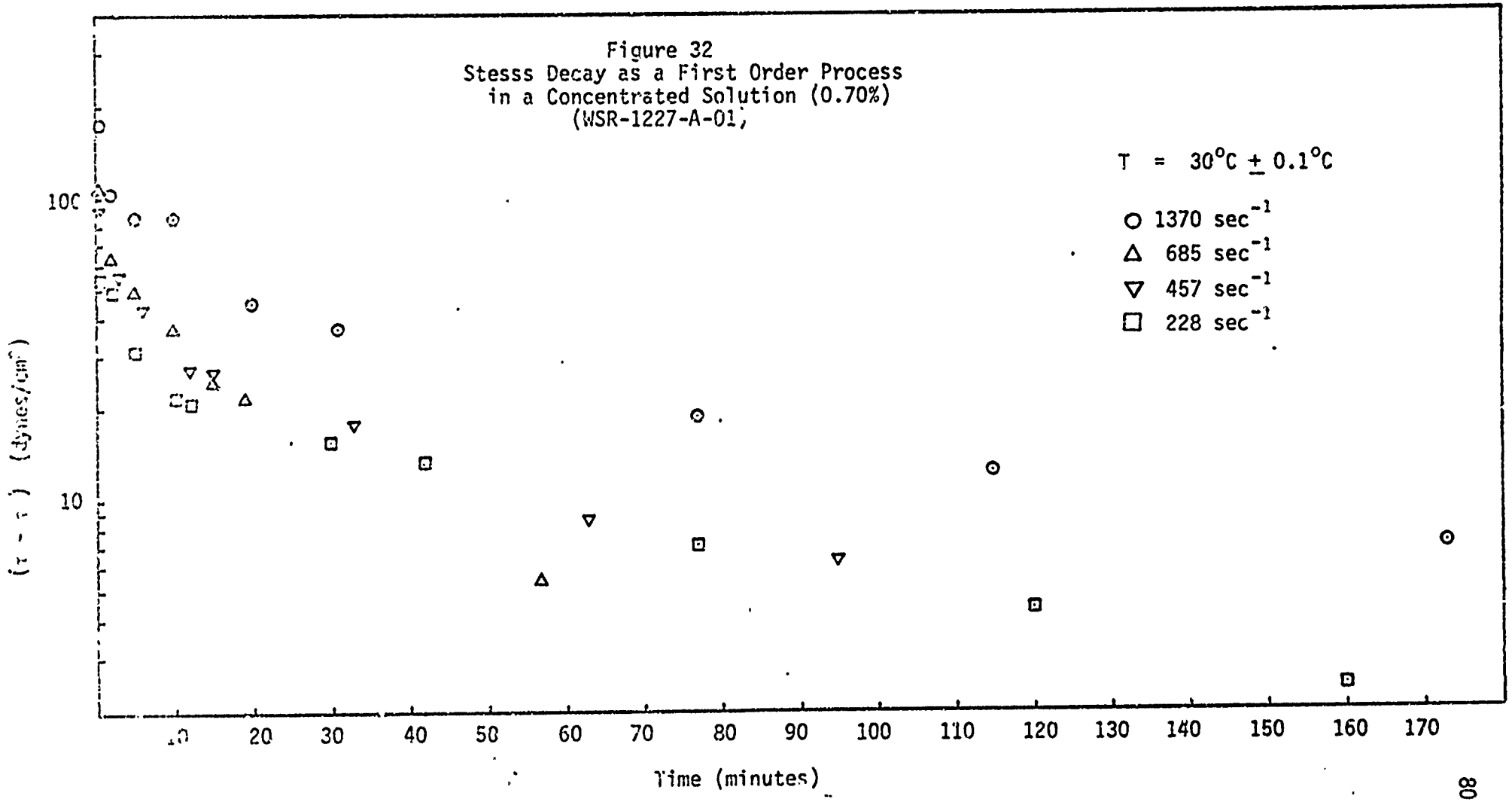

Figure 32
Stesss Decay as a First Order Process
in a Concentrated Solution (0.70%)
(WSR-1227-A-01)

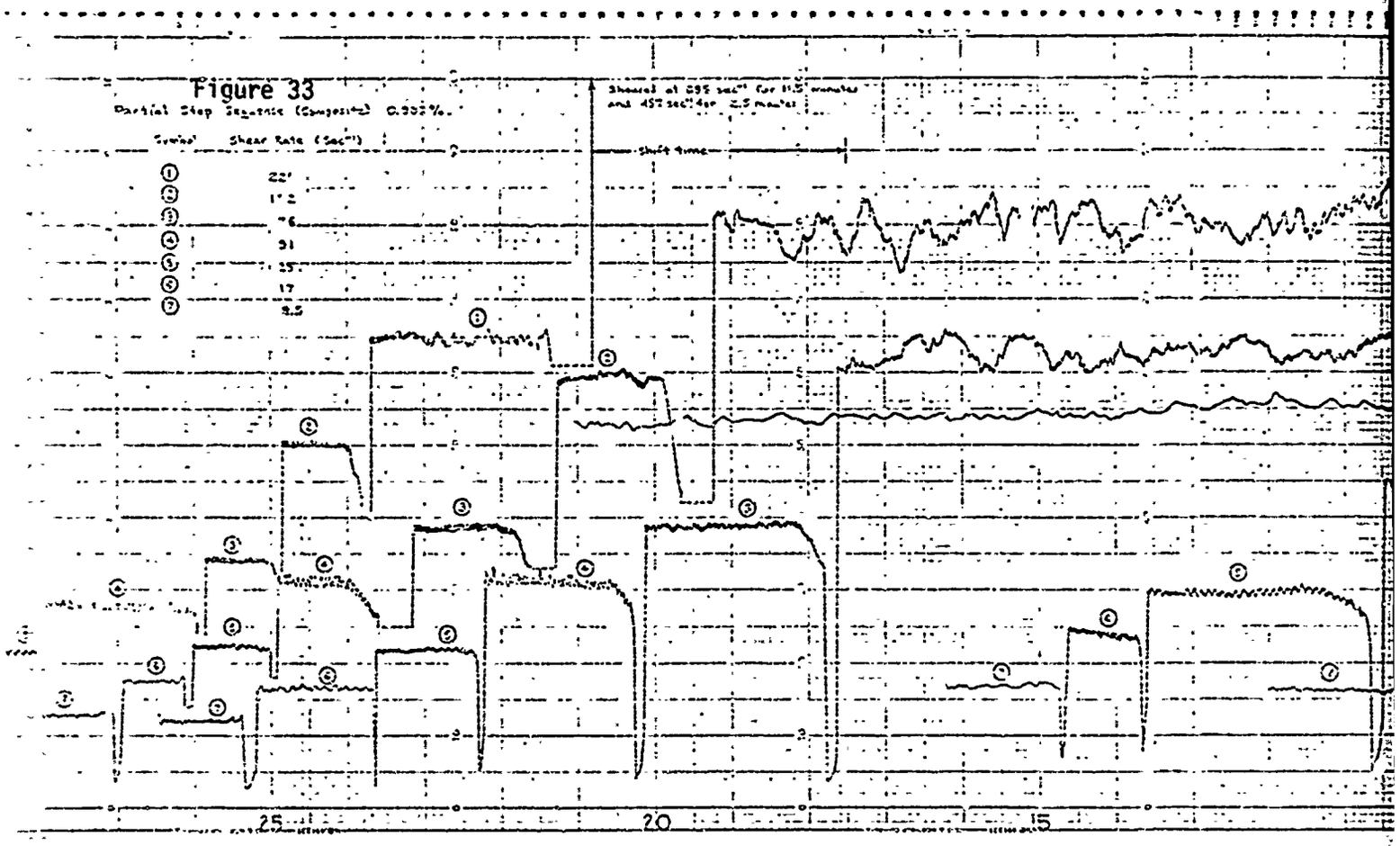
Figure 33
Partial Step Rheotric (Composite) 0.905%
Symbol
Shear Rate (Sec⁻¹)
Shift Time
25
20
15

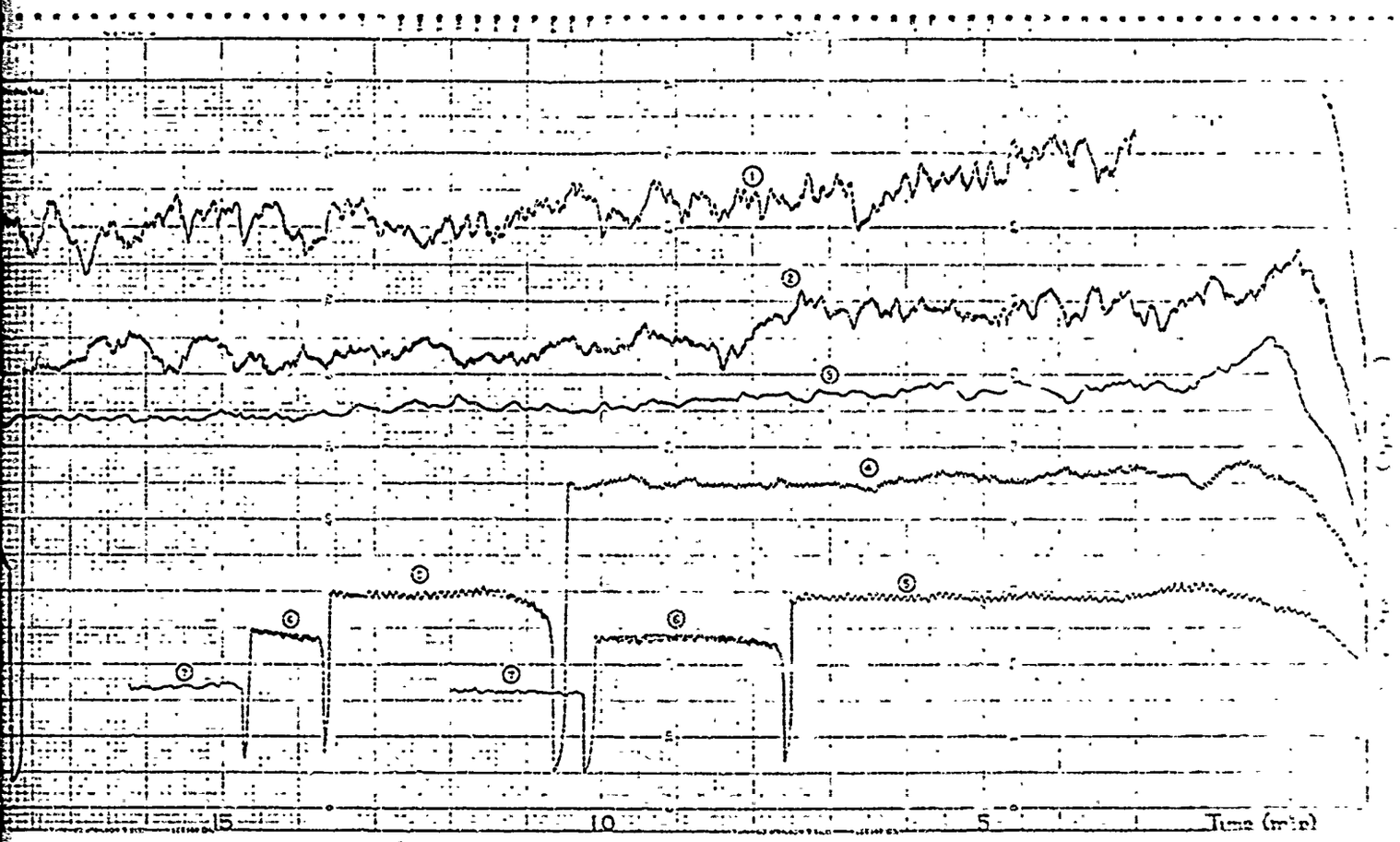
1
2
3
4
5
6
7
8
15
10
5
Time (min)

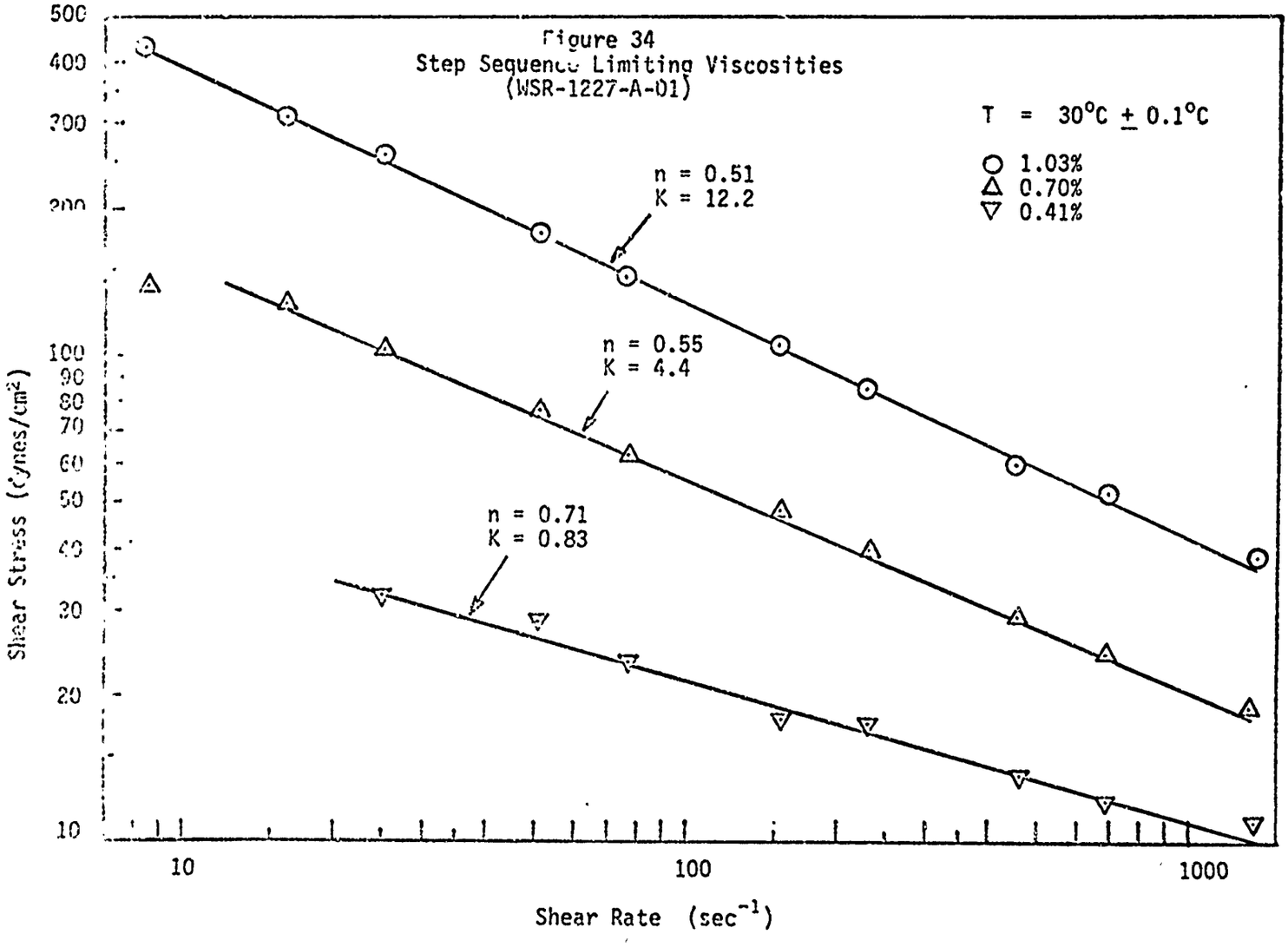
Figure 34
Step Sequence Limiting Viscosities
(WSR-1227-A-01)
T = 30°C ± 0.1°C
1.03%
0.70%
0.41%
n = 0.51
K = 12.2
n = 0.55
K = 4.4
n = 0.71
K = 0.83
Shear Stress (dynes/cm²)
Shear Rate (sec⁻¹)
500
400
300
200
100
90
80
70
60
50
40
30
20
10
10
100
1000

5.0 Frictional Drag Reduction in Dilute PEO Solutions

5.1 Introduction

5.1.1 Preliminary Remarks

For the past seven or eight years, the field of Fluid Mechanics of dilute solutions of long chain polymers has received much attention. This interest was primarily motivated by a phenomenon generally known as the Toms effect, which is manifested by the reduction of wall friction in turbulent flow when very small amounts of high molecular-weight polymers are present in the flowing solvent. Toms (25) in 1948, in what has become a landmark paper, showed for the first time the beneficial effects of long-chain polymers added to turbulent fluid flows. It is because of his work that the term "Toms phenomenon" has been applied to this drag reduction effect.

The additives which exhibit the Toms effect have 10^5 or more monomer units. They are highly flexible, linear molecular chains. Of all the additives that change the characteristics of turbulent flow in a solvent, random-coiling polymers are the most impressive as judged by the magnitude of the changes

produced per unit weight of additive. The dissolved polymer molecules are said to be "randomly coiled", because the molecular chain has a random walk configuration. Polymer molecules in dilute solution assume expanded ball-like shapes containing mostly entrained solvent. Solutions are considered to be "dilute" when the spatial separation of polymer molecules does not permit direct physical interaction.

5.1.2 Theories of Drag Reduction

A subject of great academic interest has been the search for an explanation of the drag reduction phenomenon. A number of theoretical explanations have been offered for the effect. Two comprehensive reviews of the theories were made by Fabula (7) and Hoyt (13). Here only a summary based on their works is presented.

The first research was directed towards the field of non-Newtonian shear-thinning fluids. Up to that time the efforts of most researchers were directed towards comparatively high polymer concentrations---in the range of 2000 to 6000 weight parts per million (wppm.). In this range of concentrations, the polymer solutions do show deviations from the Newtonian model

and behave as power-law fluids. A power-law fluid is one in which the stress-shear rate relation can be represented by the equation:

$$\tau = K_1 \left(\frac{du}{dy}\right)^n \tag{1}$$

where K_1 and n are constants. Merrill and Shaver (22) made an attempt to relate friction factor-Reynolds number data by means of the above constants K_1 and n. However at very low concentrations of 10 to 100 wppm., the constants K_1 and n were found to be basically the same as for water, while the drag reduction phenomenon persisted. Thus the hypothesis basing the drag reduction on non-Newtonian pseudo-plasticity failed to explain the Toms phenomenon.

According to another theory, viscoelastic properties of polymers modify the turbulent flow characteristics. These dilute polymer solutions curtail frictional drag by hindering the onset of turbulence and by damping turbulence when it does occur. While viscoelastic properties are quite evident in thick solutions, dilute solutions often seem to show no measureable viscoelastic effect. Brennen and Gadd (5) showed that fresh solutions of polyethylene oxide (PEO) did possess normal stress differences, but this

vanished with time, while the drag reduction remained unchanged. Thus the relation between Viscoelasticity and drag reduction is doubtful.

According to a different theory, it was postulated that polymer molecules adsorb on to the flow system boundaries. This adsorbed layer was thought to lower the viscosity near the wall and suppress turbulence pulsations (6). However this concept is in conflict with the observed concentration-drag reduction effects noted with polymer solutions. Also it cannot explain the observed phenomenon of drag reduction by particles and fibres.

Shin (23) discussed the mechanism of "anisotropic viscosity" to explain drag reduction. He stated that polymer molecules in a turbulent flow field will be elongated in the direction of shear. It was postulated that the viscosity perpendicular to the axis of elongation would be very large, while the viscosity in the direction of elongation would be essentially the same as that of flowing solvent. This locally anisotropic viscosity, it was suggested, would tend to dampen the turbulent fluctuations.

In another recent extensive wo Virk (27)

found that the phenomenon of friction reduction was associated with a "threshold" or critical wall shear stress or wall shear rate, below which the drag reduction would not occur.

Evidence also has been presented to indicate that perhaps the friction reduction phenomenon may be caused by more than one mechanism. Gadd (9) noted that all polymers might not reduce friction in the same manner. Thus agreement as to the mechanism responsible for the Toms phenomenon has yet to be achieved.

5.1.3 Polymer Degradation

Degradation of dilute polymer solutions, or the breaking of polymer linkages to form lower molecular weight components, is a problem which invariably occurs in flow of polymer solutions at high shear stresses. PEO is perhaps the most susceptible of all the drag reducing polymers to degradation. In addition to mechanical degradation (molecular scission) caused by shear field, PEO, in both aqueous and organic solution, has a tendency to degrade on long-term aging; i.e. the solution viscosity decreases. Brennen and Gadd (5) found that aged PEO lost viscosity slightly, but the drag reduction seemed unchanged. McGary (15) found that

PEO was very susceptible to oxidizing agents, apparently forming hydroperoxides which subsequently decompose with consequent chain scission. In the presence of oxidizing substances, solutions of PEO rapidly decrease in viscosity. McGary also found tap water, due to its chlorine and metallic salts gave lower initial viscosities and poorer long-term stabilities than distilled water stored in glass containers. Shin (23) found that PEO was subjected to bacteriological degradation which could be eliminated by a small amount of formaldehyde. Ultraviolet light also causes marked degradation in terms of viscosity loss, but this can be partially eliminated by the addition of certain alcohols.

It seems certain that chemical, biological and photo-sensitivity problems of long-te storage of solutions of friction reducing polymers such as PEO can be solved with reasonable attention to the dilute solution chemistry involved. However the major mechanical degradation effect resulting in polymer-chain scission, can be attacked only by specifying the maximum permissable shear stress in a particular flow geometry.

Another recent field of investigation (which represents an important part of this program) is concerned with the effect of shearing concentrated PEO

solutions on the drag reduction effectiveness of subsequently diluted forms. Thick PEO solutions show time-dependent rheological behavior. The apparent viscosity of fresh, initially unstirred solutions decreases with time of shearing at constant shear rate. Asbeck and Baxter (3) state that degradation of the polymer to one of lower molecular weight occurs under these conditions. This is because viscosity provides a means of measuring molecular weight. However, Gawler (10) notes that the mechanical shearing of thick solutions does produce appreciable change in solution viscosity but does not result in significant molecular scission (provided constancy of drag reduction is taken to signify preservation of molecular weight).

5.1.4 Enclosed Disk Flow

The external flow of fluids on rotating disks becomes turbulent at Reynolds numbers greater than 3×10^5. The Reynolds number for disk flow is defined as

$$Re = \frac{\omega R^2}{\nu} \tag{2}$$

where

ω = angular velocity of disk

R = disk radius

ν = Kinematic viscosity of fluid

Von Karman (20) showed theoretically that the turbulent flow resisting moment on both sides of a rotating disk in a Newtonian fluid can be represented by

(3) $$M = (\tfrac{1}{2})\, Cm\, \omega^2 R^5 \rho$$

where

Cm = Dimensionless moment coefficient

ρ = Fluid density

He also found that $Cm = 0.146\ (Re)^{-0.2}$ (turbulent)

Giles (12), in his analytical work on the rotating disk in a drag reducing non-Newtonian fluid, gave the following relation for the Moment coefficient:

(4) $$Cm = 0.684/(Re)^{0.362}$$

where Cm indicates the torque on both sides of the rotating disk. He used empirical velocity profiles deduced from pipe flow pressure drop data. His expression has been effective in predicting disk friction in drag reducing fluids to within about 8% of the available experimental data. This small discrepancy could possibly be due to end losses in the test disk arrangement. This work is particularly interesting in that it shows that disk and pipe flows are mutually compatible through transformations based on empirically defined friction

relationships.

Most of the experimental work on the turbulent disk flow of drag-reducing fluids was done by Hoyt and Fabula (14) and Gilbert and Ripken (11). Whereas the former study was concerned with drag reducing effectiveness of various polymers, the latter involved the study of boundary layer near the edge of the disk.

Measurement of driving torque provides a sensitive means of evaluating the frictional drag reduction relative to water. This is so because most of the torque is developed near the outer disk edge and torque reduction is essentially equivalent to friction reduction. The percent drag reduction in the present study is defined as

(5) $$\% f_R = 100 \left(\frac{To-T}{To}\right)$$

where

To = Torque at the surface of the disk with solvent (distilled water)

T = Torque with dilute PEO solution

5.1.5 Objectives of the Present Investigation

As already indicated, PEO is highly susceptible to mechanical degradation. The main objective of the

research herein described was to study the dependence of mechanical degradation of dilute aqueous PEO solutions on the solution concentration, polymer molecular weight and the solution temperature. In addition an effort was made to investigate the effect of shearing thick PEO solutions on the drag reduction effectiveness and subsequent mechanical degradation of the subsequently diluted forms.

5.2 Effect of Shearing Thick Solutions on Drag Reduction Effectiveness and Mechanical Degradation

Because of their high viscosity and visco-elasticity, handling of thick polymer solutions causes problems in piping, pumps, and flow meters. Thick polymer solutions also exhibit the so called Weissenberg effect, which seriously affects the performance of centrifugal pumps. Handling and transfer of thick polymer solutions becomes much easier with viscosity reduction.

The objective of this series of tests was to determine if the viscosities of thick polymer solutions could be appreciably reduced without affecting the friction reducing ability of dilute solutions made from them.

Figures 35 through 42 depict the results of

experiments performed to study the effect of shearing concentrated solutions (0.44% - 1%) of PEO in laminar flow, on the drag reduction and subsequent mechanical degradation of very dilute solutions (12-50 wppm.) made from those samples of concentrated solutions. The Polyox samples tested were WSR-301, Coagulant, and WSR-205. The thick solutions were sheared in the "Rotovisco" previously described. Figure represents the viscosity degradation of six concentrated solutions. The "apparent" shear rate for all viscosity degradation tests was 1370(Sec.)$^{-1}$. The range of shear stress was 150-1360 dynes/cm.^{2}. The temperature was not controlled. However, the temperature range for all tests was 22.5°C to 24°C, depending upon room temperature.

Figures 36 through 41 show two different sets of data representing initial drag reduction and mechanical degradation of dilute solutions prepared from sheared and unsheared master solutions. In these graphs percent drag reduction is plotted against time. It is evident from these figures that the degradation characteristics are essentially identical for these two runs. It can be seen from Figure 42, which represents the relationship between percent friction reduction and concentration of WSR-301, at time t=o, for sheared and unsheared master

solutions, that the two sets of points fall on the same curve, right down to very low concentrations.

These results indicate that the shearing of concentrated solutions does not cause any measurable change in drag reduction effectiveness and subsequent mechanical degradation in PEO solutions. This implies that there is no degradation of molecular weight of the polymer. However, the viscosity is reduced considerably by shearing the concentrated solutions, as shown in Figure . This implies that the viscosity reduction is largely due to a microscopic disentanglement and ordering of polymer chains and the rupture of relatively weak inter-chain hydrogen bonds, rather than actual molecular scission (provided constancy of initial drag reduction and similar degradation characteristics are taken to signify preservation of molecular weight). These results also suggest that PEO molecules are not fragile and are not readily broken in the range of shear rates, shear stresses and concentrations involved in the present study.

The above mentioned conclusions are in conflict with a proposal by Asbeck and Baxter (3), who contend that a decrease in solution viscosity represents a degradation of polymer molecular weight. However, these

results are in agreement with the results obtained by Gawler (10). He showed that a reduction in viscosity (caused, in his case, by pumping the concentrated solutions using a positive displacement rotary pump) was not necessarily accompanied by a decrease in drag reduction effectiveness in turbulent pipe flow.

5.3 Mechanical Degradation of Dilute Solutions of PEO in a Turbulent Field

5.3.1 Theoretical Background

It has been known for sometime that long-chain molecules can be broken mechanically, both in solution and in the bulk phase. The details of the mechanism by which degradation or molecular scission of long-chain polymers occurs are unknown. Solutions of PEO can be degraded by the addition of certain substances to the solution, by heating, and by subjecting the solution to high shear fields. A qualitative model of degradation can be obtained by attributing to the main chain bonds a certain activation energy which, if exceeded, results in primary valence bond rupture. The addition of certain substances can lower this activation energy and heating can increase the Brownian motion energy of the solvent. Both of these effects contribute to the degradation. In a similar manner, hydrodynamic shear

fields produce molecular stresses in the main chain which strain the bond. The bond will rupture in a sufficiently strong shear field.

Under these conditions, not only is a quantitative treatment of the hydrodynamic problem difficult, but additional complications may enter, such as local intense adiabatic heating due to cavitation. Such effects create the possibility of chain scission by a thermal mechanism. Apart from difficulties of this nature, a quantitative discussion of the problem is primarily limited by the absence of an adequate theory of non-Newtonian flow under conditions of high shear and, frequently, as well, by uncertainties in the rheology of the apparatus used. Consequently, in spite of the relatively abundant literature on hydrodynamic shear degradation, the process is not well understood.

An attempt was made by Paterson (16) to qualitatively treat the turbulent shear degradation of PEO solutions. He assumed that the degradation proceeds according to the first order irreversible reaction:

$$A \rightarrow B + C$$

Where A is the initial molecular weight and species B and C are the two products of the molecular scission. He further assumed that the rupture into two equally

sized parts would be the most probable scission and that the probability would decrease as the two parts become less equal in size. Another drastic simplification was made by stating that the simplest model of degradation is a "two-group" model, where the distribution of molecular weight at time, t=o, is assumed to consist of two molecular weight species, one with half the molecular weight of the other. He further assumed (which seems to be verified by his experimental results) that degradation preferentially attacks the highest molecular weight species present in the spectrum and the lower molecular species do not degrade.

According to this model one would expect the rate of degradation to increase with increased shear rate, molecule size, and solvent viscosity, but be independent of concentration (for very dilute solutions interparticle effects should be negligible). The above model is expected to approximate the actual situation for very short times when the molecular weight change is dominated by the destruction of the high molecular weight species. For later times the second species (with lower molecular weight) would dominate since the higher component would have been destroyed. A state of "stable plateau of residual benefits" is reached under these conditions and

the low molecular weight species left in the system are highly resistant to the existing shear field.

Paterson's model is verified, at least qualitatively, in the present study (described in the next section) in that the rate of degradation (in terms of reduced viscosity) is very fast in the first few minutes, then drops down to a low rate, and finally approaches zero. No further attempt was made to compare theory and experiment in a more quantitative manner since the theory is so simplified compared to the actual experimental conditions.

5.3.2 Experimental Results

The results of turbulent shear degradation tests appear in Figures 43 through 52. As mentioned previously, the tests were conducted with a 5" diameter disk at a constant speed setting of 1800 rpm. and 30°C (correspond- Reynolds number = 9.6×10^5).

Figures 43 through 45 show the effect of concentration on initial drag reduction for three grades of polymers. Figure 46 is the combined representation of the above three figures. The flat shape of the curve for each of the three different molecular weight polymers agrees with the results of Hoyt and Fabula (14), who worked with a rotating disk in an open housing containing

TABLE I

REDUCED VISCOSITY (R.V.)-DRAG REDUCTION (D.R.)
CORRELATION FOR 200 WPPM., WSR-205

Time of shear min.	Efflux time tp, Sec.	R.V.	% D.R.	% change in R.V.	% change in D.R.	% change in R.V. between successive intervals	% change in D.R. between successive intervals
1	213.020	4.67	36.33	-	-	-	-
60	212.912	4.64	28.94	.64	20.34	.64	20.34
180	212.110	4.44	22.51	4.93	38.04	4.50	22.22
240	212.030	4.42	19.29	5.35	46.90	.45	14.30

TABLE II

REDUCED VISCOSITY (R.V.)-DRAG REDUCTION (D.R.)
CORRELATION FOR 100 WPPM., COAGULANT

Time of shear min.	Efflux time tp, Sec.	R.V.	% D.R.	% change in R.V.	% change in D.R.	% change in R.V. between successive intervals	% change in D.R. between successive intervals
2	223.77	13.92	36.75	-	-	-	-
15	216.70	10.32	36.14	25.86	1.66	25.86	1.66
60	212.88	8.37	30.72	39.85	16.41	18.87	15.00
120	212.99	8.43	24.70	39.45	32.79	-.669	19.6
180	212.75	8.31	22.29	40.32	39.35	1.45	9.76
240	212.40	8.13	21.69	41.60	40.98	2.14	2.70
300	212.09	7.97	20.48	42.74	44.27	1.93	5.58

TABLE II

REDUCED VISCOSITY (R.V.)-DRAG REDUCTION (D.R.)
CORRELATION FOR 100 WPPM., COAGULANT

Time of shear min.	Efflux time tp, Sec.	R.V.	% D.R.	% change in R.V.	% change in D.R.	% change in R.V. between successive intervals	% change in D.R. between successive intervals
2	223.77	13.92	36.75	-	-	-	-
15	216.70	10.32	36.14	25.86	1.66	25.86	1.66
60	212.88	8.37	30.72	39.85	16.41	18.87	15.00
120	212.99	8.43	24.70	39.45	32.79	-.669	19.6
180	212.75	8.31	22.29	40.32	39.35	1.45	9.76
240	212.40	8.13	21.69	41.60	40.98	2.14	2.70
300	212.09	7.97	20.48	42.74	44.27	1.93	5.58

TABLE III

REDUCED VISCOSITY (R.V.)-DRAG REDUCTION (D.R.)
CORRELATION FOR 200 WPPM., COAGULANT

Time of shear min.	Efflux time tp, Sec.	R.V.	% D.R.	% change in R.V.	% change in D.R.	% change in R.V. between successive intervals	% change in D.R. between successive intervals
2	260.36	16.776	34.46	-	-	-	-
60	236.63	10.566	32.93	37.01	4.65	37.01	4.65
120	228.48	8.383	30.77	50.10	10.71	20.72	6.56
240	228.10	8.383	27.08	50.10	21.42	0.00	12.00
360	228.00	8.360	24.68	50.18	28.38	0.24	8.86

PEO solutions. However, the similarity of the three flat curves, except for very low concentrations, as seen in Figure 46, indicates that the extent of initial drag reduction is essentially independent of the molecular weight of the polymer, for a certain Reynolds number and for this particular flow geometry. This behavior for disk flow does not agree with pipe flow or circular Couette flow. In those cases drag reduction increases with polymer molecular weight, other conditions being equal.

Figure 47 demonstrates the relative resistance to shear degradation of 2, 50, 100 and 200 wppm. solutions of WSR-301. Figures 48 and 49 show the similar concentration effects on the magnitude of shear degradation for WSR-205 and Coagulant. The 2 wppm. case for all three polymers indicates an immediate and rapid degradation effect. As the concentration is increased, the degradation rate is lowered. This can be explained on the basis that a 100 wppm. solution has more polymer than does a 50 wppm. solution. These tests indicate that the drag increases gradually and would reach an asymptote of residual benefits after a sufficiently long time. This can also be seen from Tables I, II and III.

These tests also indicate a possibly valuable

aspect of PEO solutions in that many degraded molecules can produce a drag reduction which is comparable to drag reduction obtainable from lower concentrations lesser degraded molecules. For instance, in Table III, the 200 wppm. solution after six hours of shearing still has the drag reducing capability of a 100 wppm. solution which has been sheared for two hours under similar conditions.

Figures 50 through 52 show the effect of molecular weight on the mechanical degradation of PEO solutions for three different concentrations. The curves in these figures indicate that WSR-205, which has a much lower molecular weight than WSR-301 or Coagulant, degrades faster than the other two when comparison is made in terms of percent drag reduction. This is also true for 50 and 100 wppm. solutions of WSR-301, which degrade faster (in terms of drag reduction) than corresponding solutions of Coagulant. WSR-205, WSR-301 and Coagulant samples had approximate molecular weights of 9×10^5, 3.2×10^6 and 3.5×10^6, respectively. These molecular weights are based on the corrected reduced viscosities of 200 wppm. solutions of the above grades and Shin's relation between intrinsic viscosity and molecular weight (described in Section 3.0).

Paterson (16) demonstrated that intrinsic viscosity failed to correlate the extent of drag reduction for fixed concentrations in pipe flow. He reported that:

> The solutions which have been degraded show a disproportionately large decrease in drag reduction effectiveness for the small decrease in the intrinsic viscosity. There is, of course, no a priori reason that drag reduction should depend on the same moment of molecular weight distribution as the intrinsic viscosity. Since degradation should preferentially attack the highest molecular weight species present in the spectrum, the disproportionate decrease in drag reduction suggests that the drag reduction depends primarily on the high molecular weight components of the distribution. Since these components are present in relatively small concentrations their disappearance would cause only a small effect on the weight average molecular weight. A more appropriate average to correlate the drag reduction would then be one which weighs the high end of the distribution to a greater extent.

Some interesting conclusions can be drawn from these tables. The reduced viscosity of 200 wppm. solutions of WSR-205 (Table I) degrades by 5.35% after four hours of continuous turbulent shearing. The corresponding reduction in drag reduction is about 47%. The change in reduced viscosity in this case must be viewed with caution since this corresponds to a change in efflux time of only one second in the capillary viscometer. This very little change could possibly be attributed to the limit of accuracy of the Autoviscometer

and may mean that the change in reduced viscosity is practically zero for the duration of the experiment.

Tables II and III display the typical features of high molecular weight Coagulant. A 100 wppm. Coagulant solution shows a drastic reduction of about 26% in reduced viscosity in 13 minutes of shear, whereas the change in drag reduction was only 1.66%. The corresponding values for the 200 wppm. solution of Coagulant are 37% and 4.65% for 58 minutes of shear. This phenomenon, though not tabulated, was also observed for a 200 wppm. solution of WSR-301. In addition, it can be seen from these tables that reduced viscosity remains essentially constant after a few hours of shearing. However, there is a continuous gradual decrease in drag reduction.

At first glance, the results for WSR-205 and Coagulant seem to be in conflict with Paterson's model described in the preceding section. For the 200 wppm. solution of WSR-205, the reduced viscosity and drag reduction (Table I) changed by 0.64% and 20.34% in the first hour of shearing. The corresponding values for the 200 wppm. Coagulant solution are 37% and 4.65%. Thus the initial rate of degradation in terms of reduced viscosity is very fast for Coagulant (which supports Paterson's model), but the accompanying change in drag reduction is

disproportionately very small. This could be explained on the basis that Coagulant has a greater proportion of high molecular weight molecules in its distribution, providing many more high molecular weight molecules than are required for optimum drag reduction. The breaking of these high molecular weight molecules could result in a sharp reduction of reduced viscosity. However, the drag reduction is expected to change by a small amount because an appreciable number of high molecular weight molecules is still present in the system. For the 200 wppm. solution of WSR-205, the reduced viscosity remains essentially constant for first hour of shearing, but drag reduction decreases by 20%. Initial drag reduction is practically the same as for Coagulant. This indicates that WSR-205 initially has enough high molecular weight molecules to provide a drag reduction comparable to Coagulant, but their number must be much smaller than that present in Coagulant. This means that for WSR-205, only the narrow tail end of the distribution lies in the drag reduction and degradation range. Breaking of these molecules, therefore, would result in a small change of reduced viscosity. It would, however, reduce the drag reduction considerably because drag reduction depends upon high molecular components of the distribution.

The failure of reduced viscosity (which is a measure of intrinsic viscosity) to correlate drag reduction and degradation for disk flow is indicated from these tables. The disproportionate decrease in drag reduction after a few hours of shearing (while the reduced viscosity remains essentially constant) suggests that drag reduction depends primarily on the high molecular weight components of the distribution.

5.4 The Effect of Temperature on Drag Reduction and Mechanical Degradation

The purpose of this series of experiments was to determine the effect of temperature on the initial drag reduction and mechanical degradation of dilute PEO solutions. Polyox WSR-301 was tested at three concentrations (2, 50, 100 wppm.) at three temperatures (30, 45, and 60°C). As already noted, a 6" diameter, brass disk rotating at 1700 rpm. was used for temperature studies.

Severs (21) states that a solution of polymer in a good solvent will decrease in viscosity as the temperature is raised. This decrease is caused by the decrease in solvent viscosity with temperature. The relative viscosity, η_r , will be essentially constant since the division by the solution viscosity will correct for

temperature effects. However, the relative viscosity of a polymer in a poor solvent will rise with the temperature as the polymer molecules unfold.

Temperature plays an important part in the solubility of polymers. Although PEO is completely soluble in water at room temperature, it precipitates from water solution at or near the boiling point. For example, in a 100 wppm. solution of PEO in water, the polymer would precipitate from solution at 100.5°C (17). Alfrey, et. al. (1) demonstrated not only that a polymer chain uncurls as the temperature of a poor solvent is raised, but that there is a tendency for a polymer chain to curl somewhat in a good solvent as the temperature is raised. They also showed that the nearer the polymer (in a good solvent) is to precipitation, the smaller is the intrinsic viscosity. Pruitt et al. (19) also found a decrease in reduced viscosity with increasing temperature for PEO solutions. They observed that, except for the low concentrations of PEO, there is little change in drag reduction in pipe flow from 2°C to 40°C, but a substantial loss in drag reduction from 40°C to 60°C.

Increased degradation due to increased temperature is commonly referred to as thermal degradation. Increased

temperature accelerates the chemical degradation and increases the Brownian motion of polymer molecules.

The data shown in Figure 53 illustrates the drag reduction and shear degradation at different temperatures for a 2 wppm. solution of WSR-301. Figures 54 and 55 show the effects of temperature for 50 and 100 wppm. solutions. Figure 56 indicates the effect of temperature on initial drag reduction at time, t=o, for three concentrations of WSR-301.

For the 2 wppm. (Figures 53 and 56) solution, the initial drag reduction remains practically unaffected (about 44.5%) when the temperature is changed from 30°C to 45°C. However at 60°C, initial drag reduction is about 36%--a 19% "reduction" in drag reduction. For high concentrations of 50 and 100 wppm. solutions (Figures 54 and 55), the initial drag reduction increases as the temperature increases from 30°C to 60°C. The initial drag reduction, for both of these tests, increases by about 10% when the temperature is changed from 30°C to 60°C. The shear degradation rate for all concentrations is highly accelerated as solution temperature is increased. It is noteworthy that a substantial increase in degradation rate occurs as the temperature is increased from 30°C to 45°C, whereas the degradation curves follow the

same pattern when the temperature is changed by an equal amount from 45°C to 60°C.

These results do not agree with Pruitt, et al. (19), who found, for pipe flow, a substantial loss in initial drag reduction from 40°C to 60°C for concentrations varying from 2 to 250 wppm. of Coagulant. Two possible reasons for this variation could be dissimilar flow geometries and the quality of solvent (distilled water instead to tap water which was used in their study).

5.5 Effect of Static Storage of Master Solutions on Drag Reduction

Four master solutions of WSR-301 were tested in this series: (1) 8 months old, 0.8% solution prepared by the Vortex Mixer method with 0.5% isopropyl alcohol, (2) 9 months old, 1% solution prepared by the Boiling Water method, (3) a freshly prepared 0.8% solution prepared by the Vortex Mixer method with 0.5% isopropyl alcohol, (4) 8 months old, 0.8% solution prepared by the Vortex Mixer method, but no isopropyl alcohol added. The master solutions were stored in polyethylene bottles under normal room conditions.

These master solutions were diluted to 50 wppm. concentration to check their drag reduction ability. The results of these tests are depicted in Figure 57. The similarity of initial drag reduction and shear degradation characteristics for the first three master solutions shows that the chemical degradation during static storage can be practically stopped by adding isopropyl alcohol and by using distilled water. However, it is noteworthy that the master solution in the

fourth case (where no isopropyl alcohol was added) lost its drag reduction effectiveness completely after eight months of static storage.

5.6 Static Viscosity Degradation of Dilute Solutions

McGary (15) found that polymer solutions in distilled water gave good long-term stabilities. To test the effectiveness of isopropyl alcohol and distilled water to stabilize the dilute polymer solutions during static storage, a 200 wppm. solution of WSR-301 was made. This dilute solution was made from a 1% master solution prepared by the Vortex Mixer method (0.5% isopropyl alcohol added).

Figure 58 shows the static viscosity degradation of the dilute solution stored in a polyethylene vessel under normal room conditions. Over a period of 29 days, the relative viscosity changed from 1.264 to 1.252 i.e., a decrease of only .94%. This behavior indicates that the chemical degradation of dilute polymer solutions during static storage can be mitigated by adding isopropyl alcohol to master solutions and using distilled water.

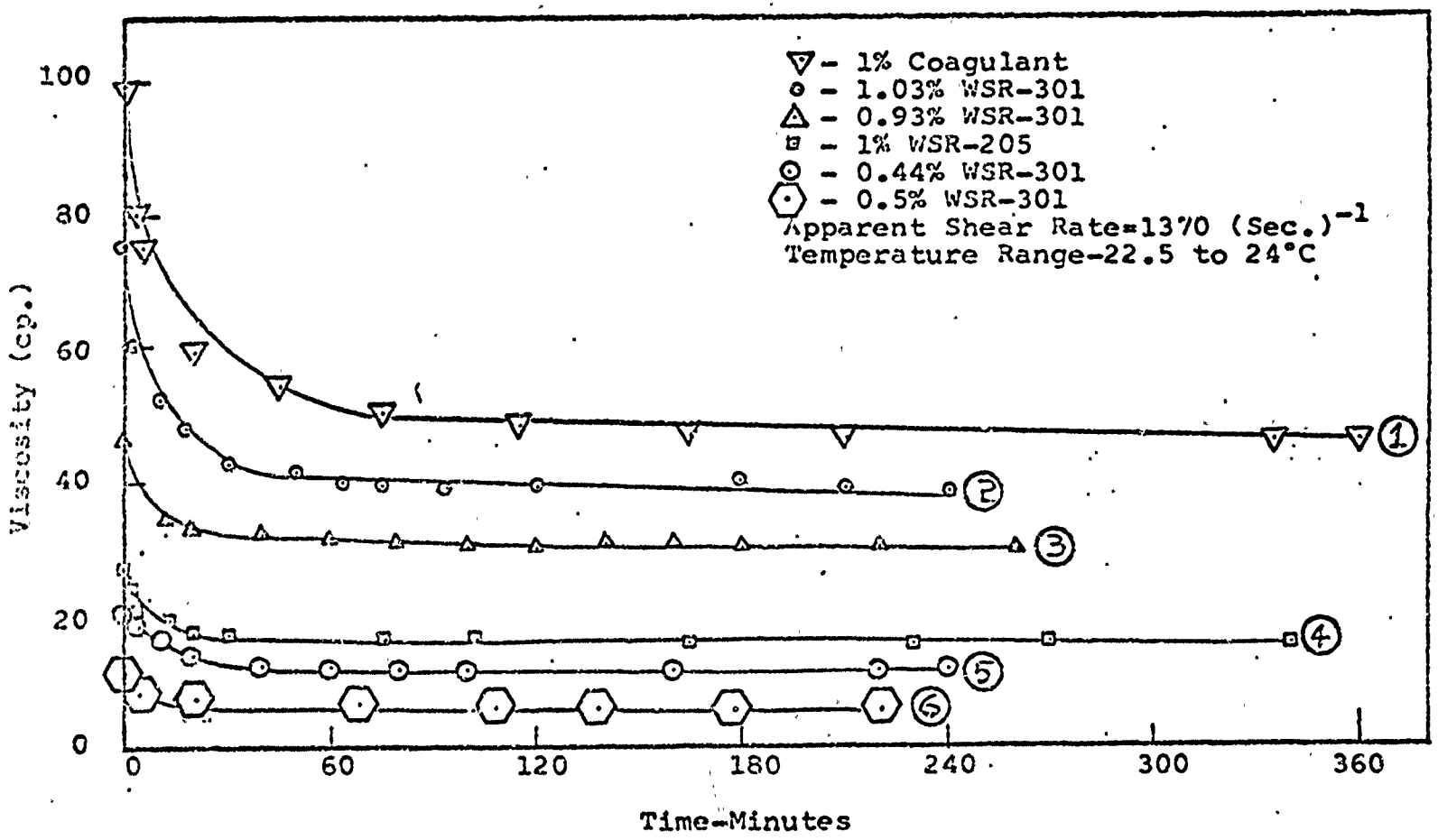

FIGURE 35
VISCOSITY DEGRADATION OF MASTER SOLUTIONS

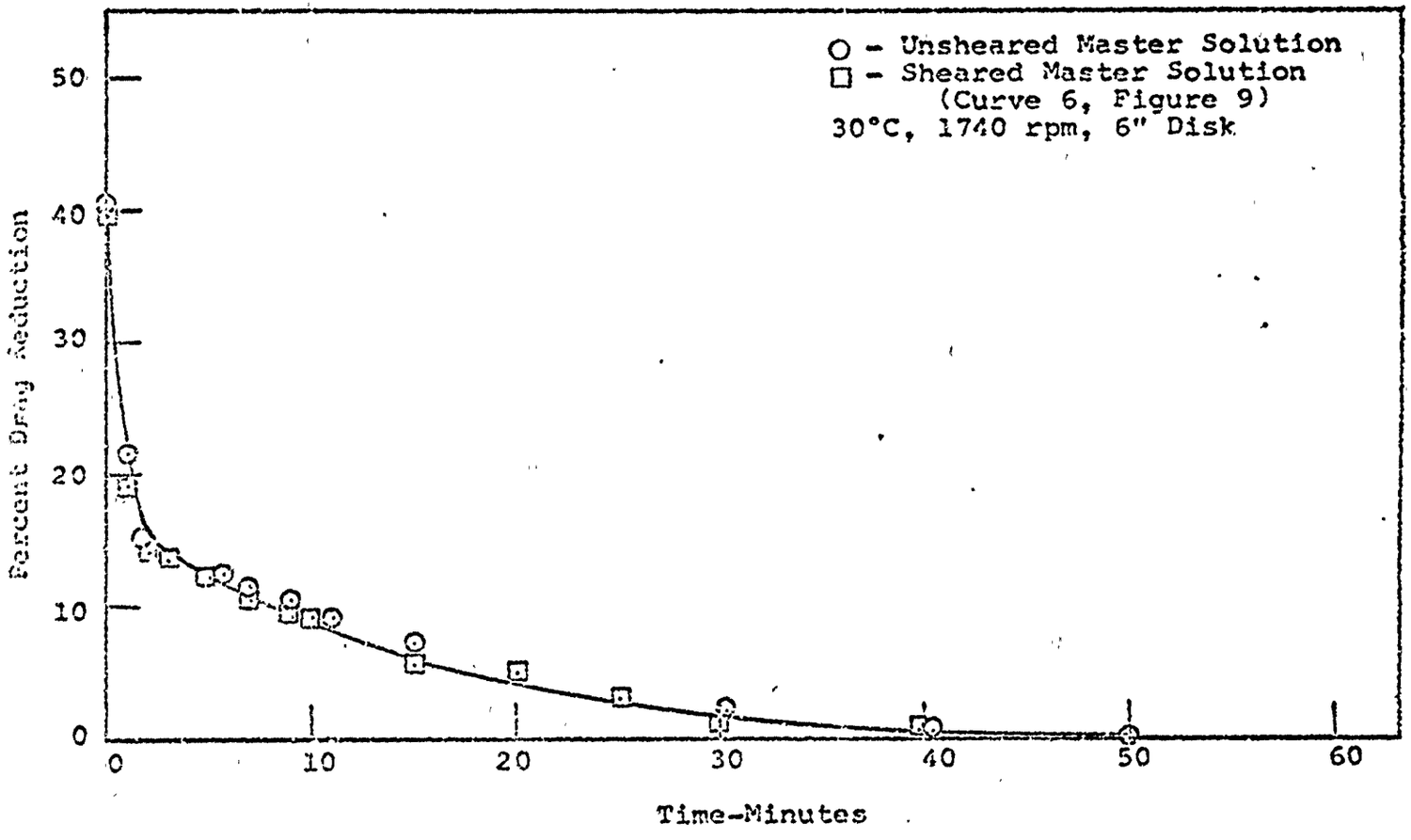

FIGURE 36

INITIAL DRAG REDUCTION AND MECHANICAL DEGRADATION OF 2 WPPM., WSR-301

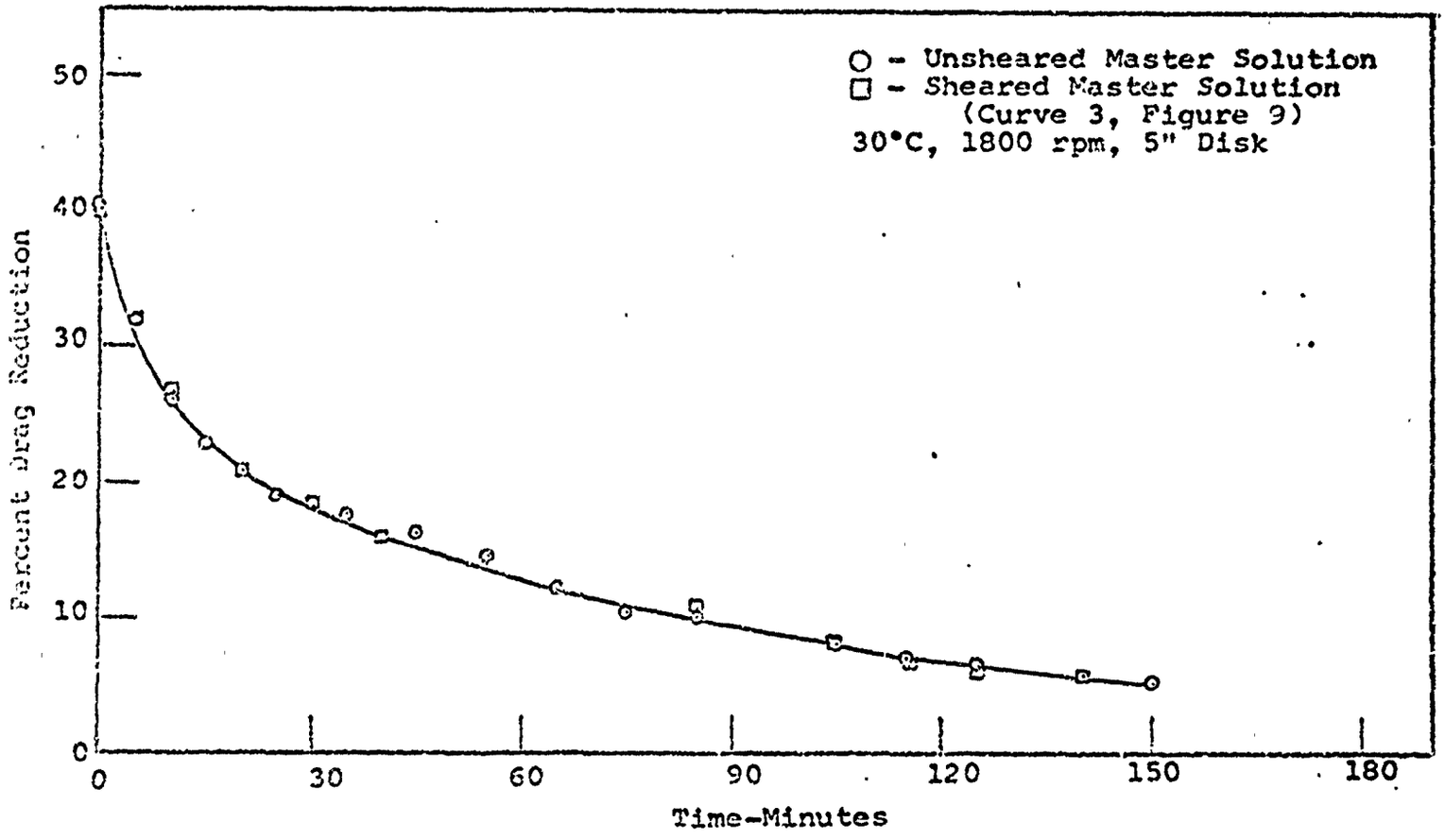

FIGURE 37

INITIAL DRAG REDUCTION AND MECHANICAL DEGRADATION OF 12 WPPM., WSR-301

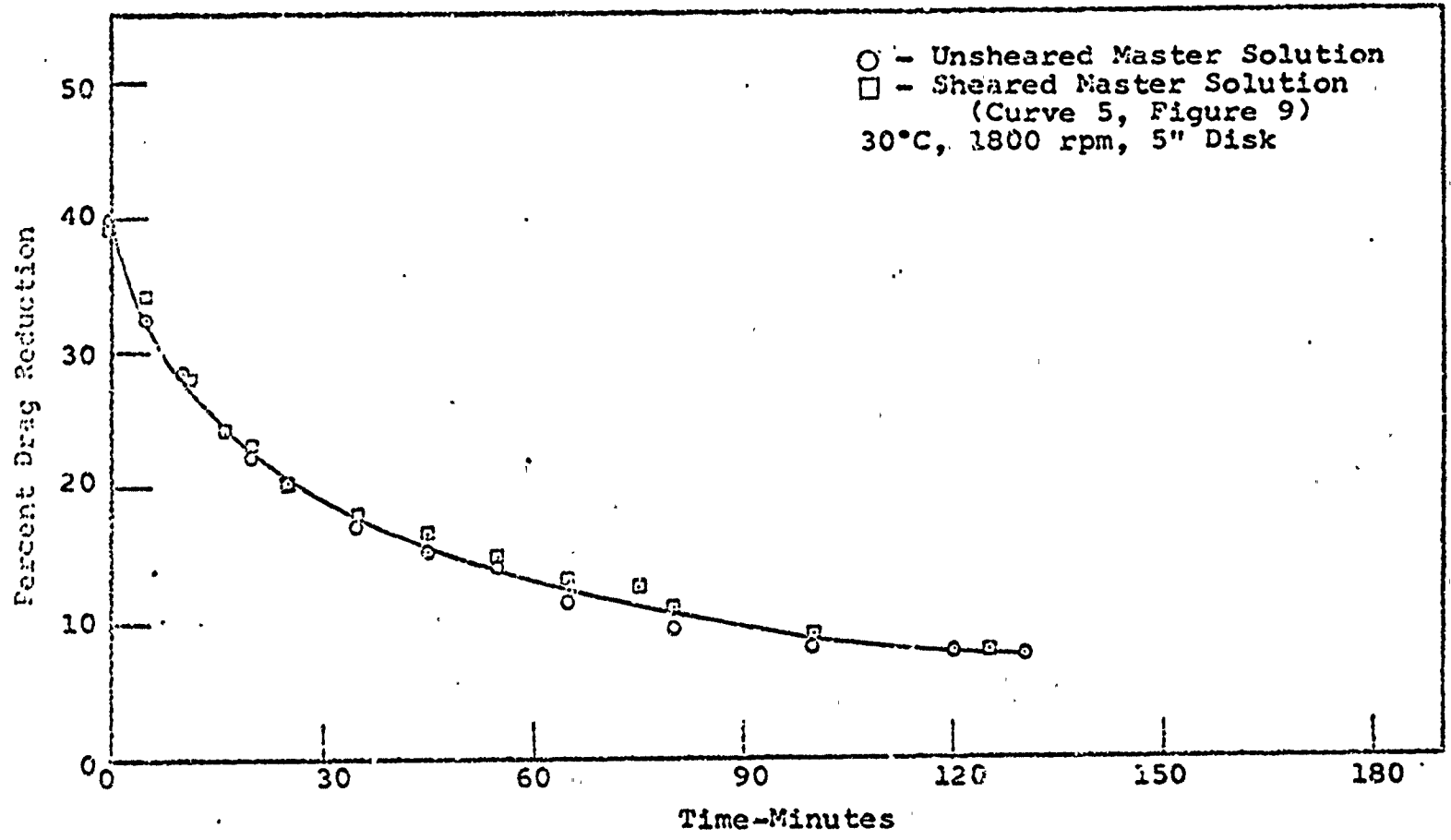

FIGURE 38

INITIAL DRAG REDUCTION AND MECHANICAL DEGRADATION OF 14 WPPM., WSR-301

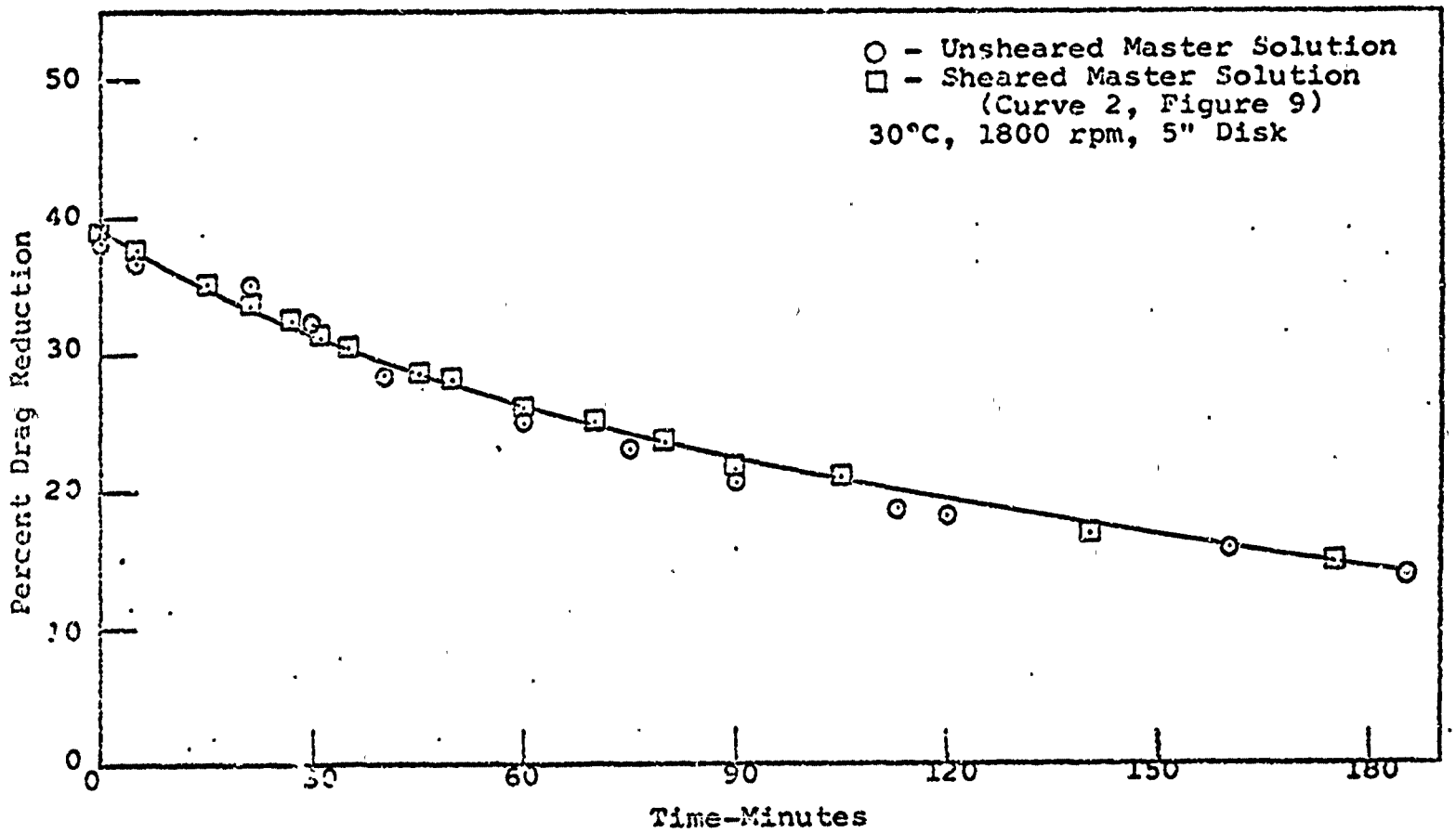

FIGURE 39

INITIAL DRAG REDUCTION AND MECHANICAL DEGRADATION OF 50 WPPM., WSR-301

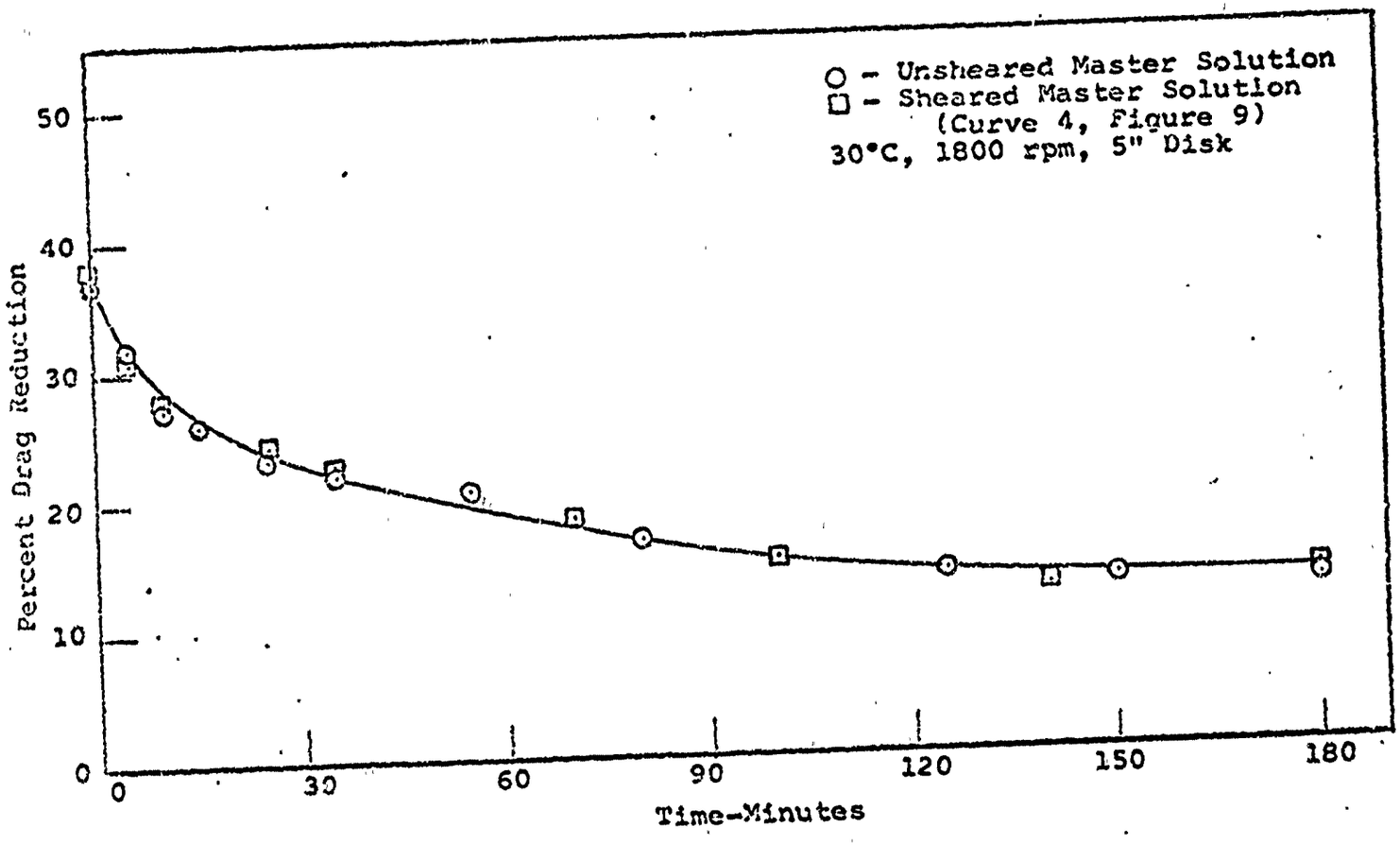

FIGURE 40

INITIAL DRAG REDUCTION AND MECHANICAL DEGRADATION OF 50 WPPM., WSR-205

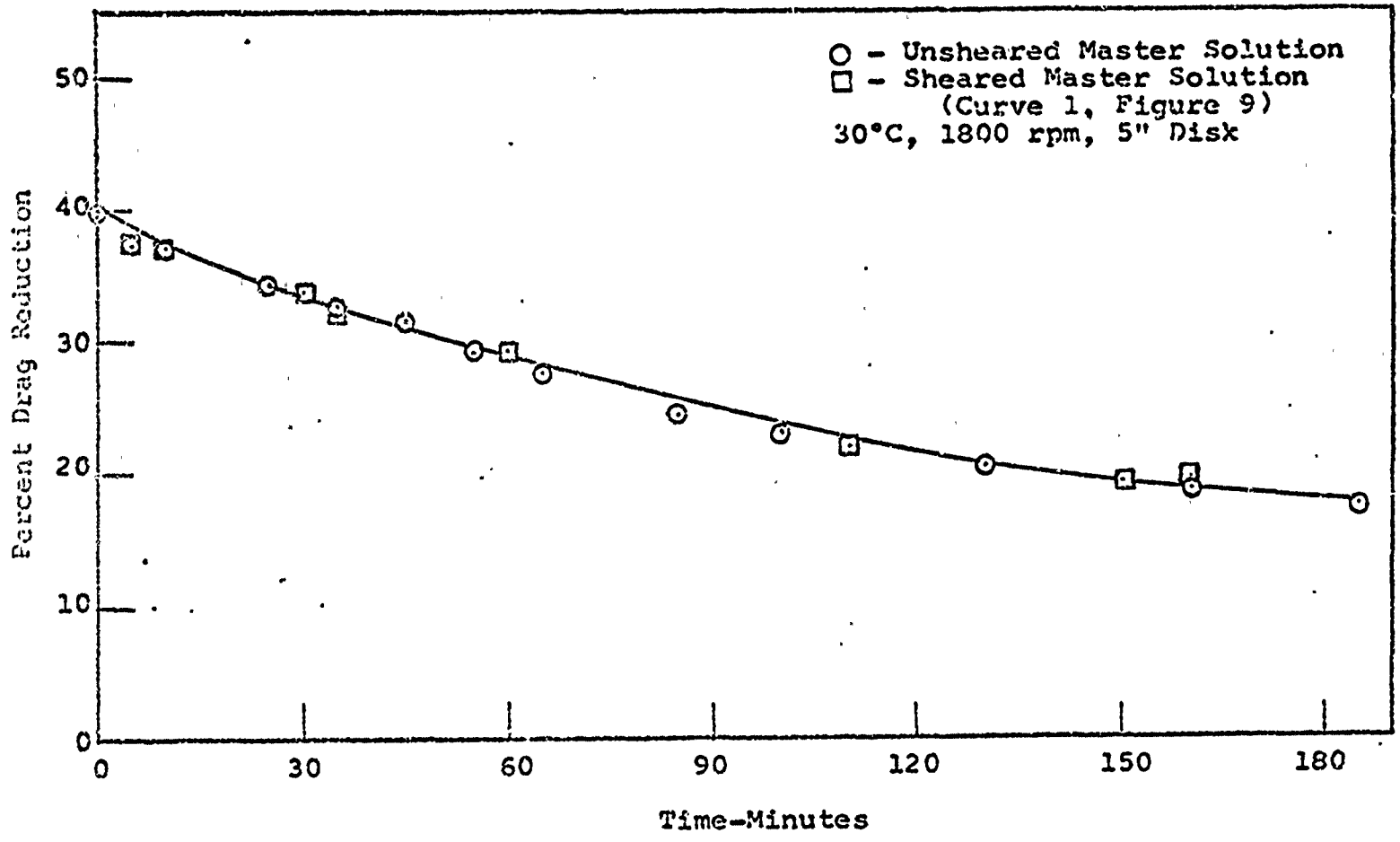

FIGURE 41

INITIAL DRAG REDUCTION AND MECHANICAL DEGRADATION OF 50 WPPM., COAGULANT

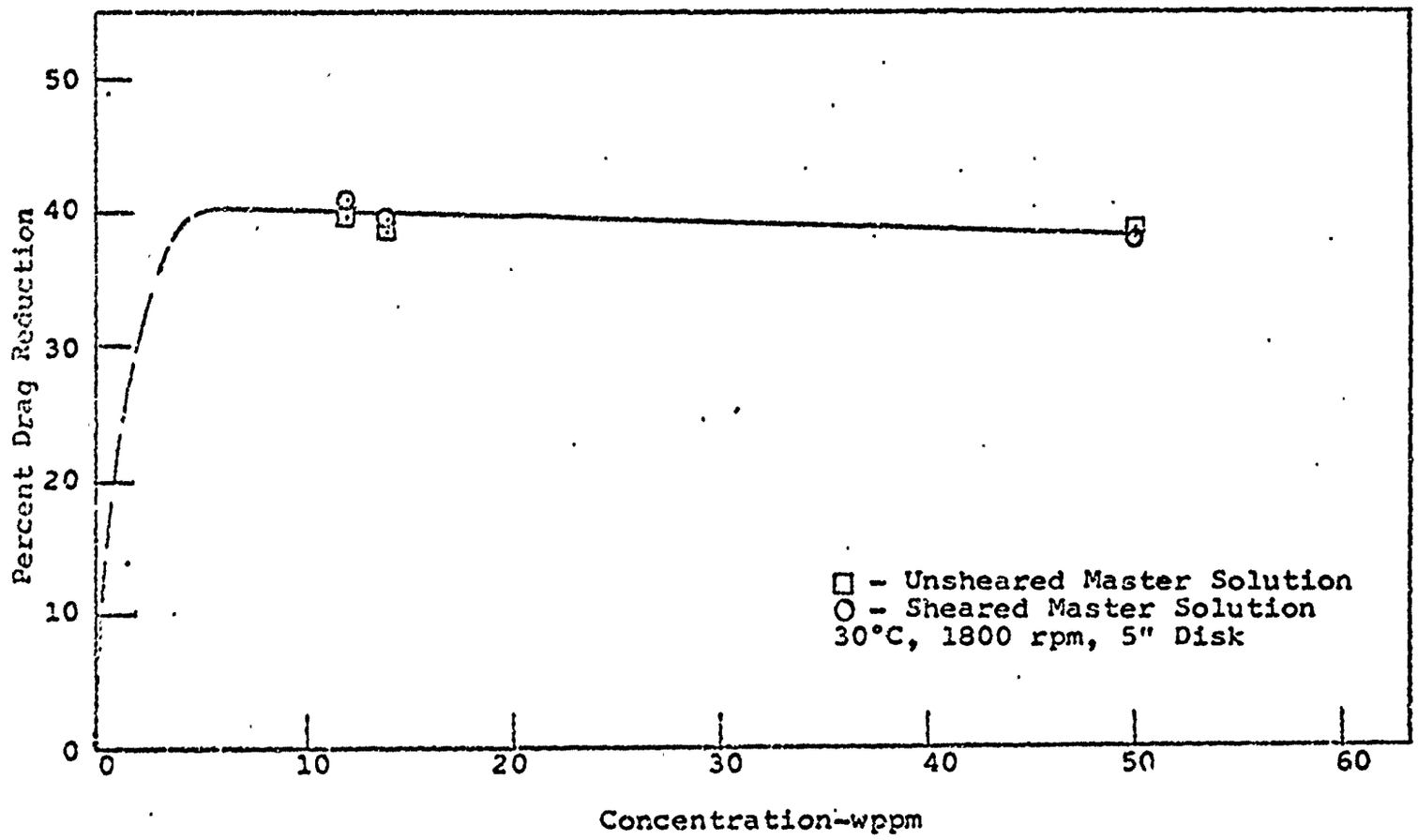

FIGURE 42

EFFECT OF SHEARING MASTER SOLUTIONS ON INITIAL DRAG REDUCTION FOR WSR-301

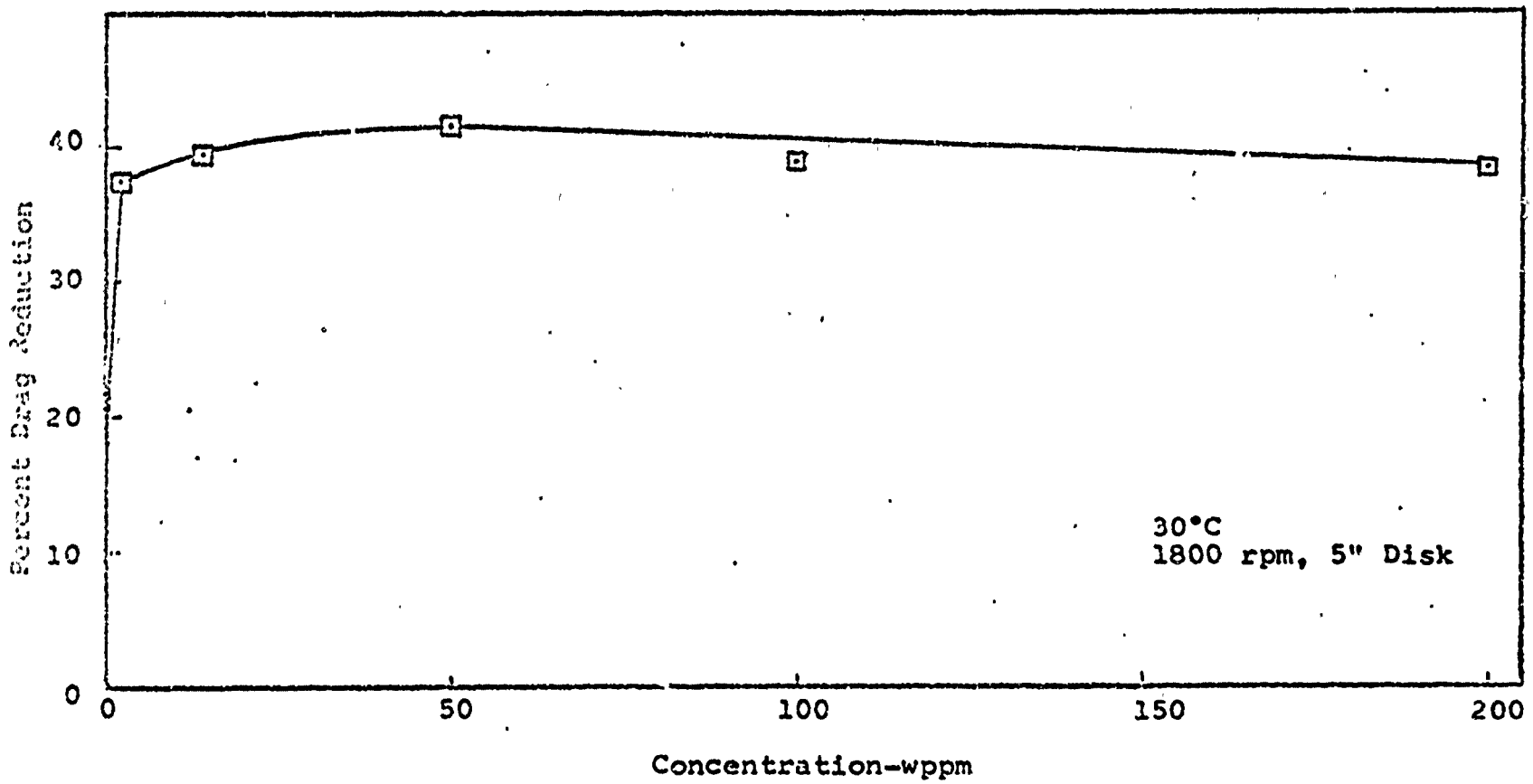

FIGURE 43

CONCENTRATION VERSUS INITIAL DRAG REDUCTION FOR WSR-301

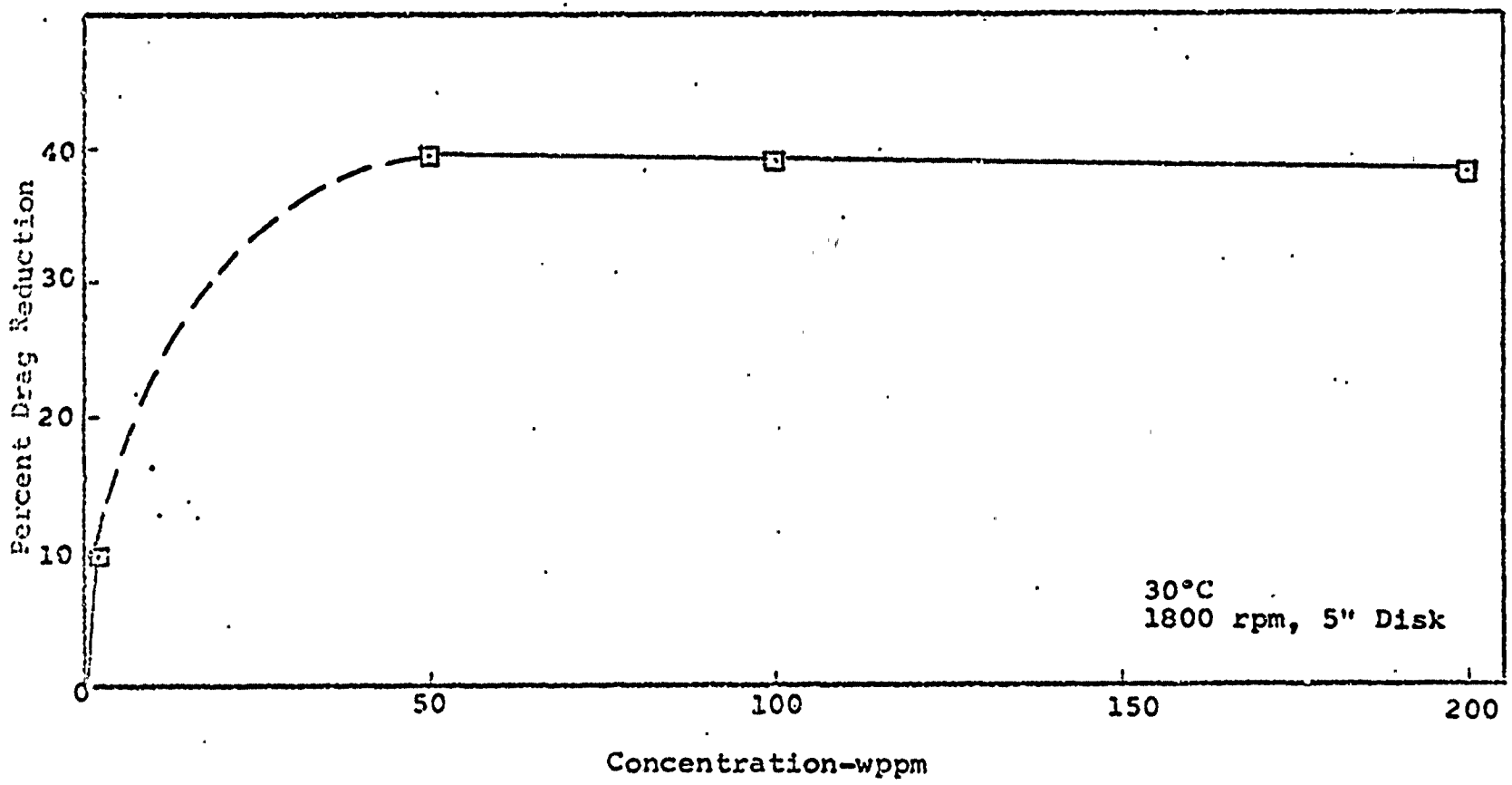

FIGURE 44
CONCENTRATION VERSUS INITIAL DRAG REDUCTION FOR WSR-205

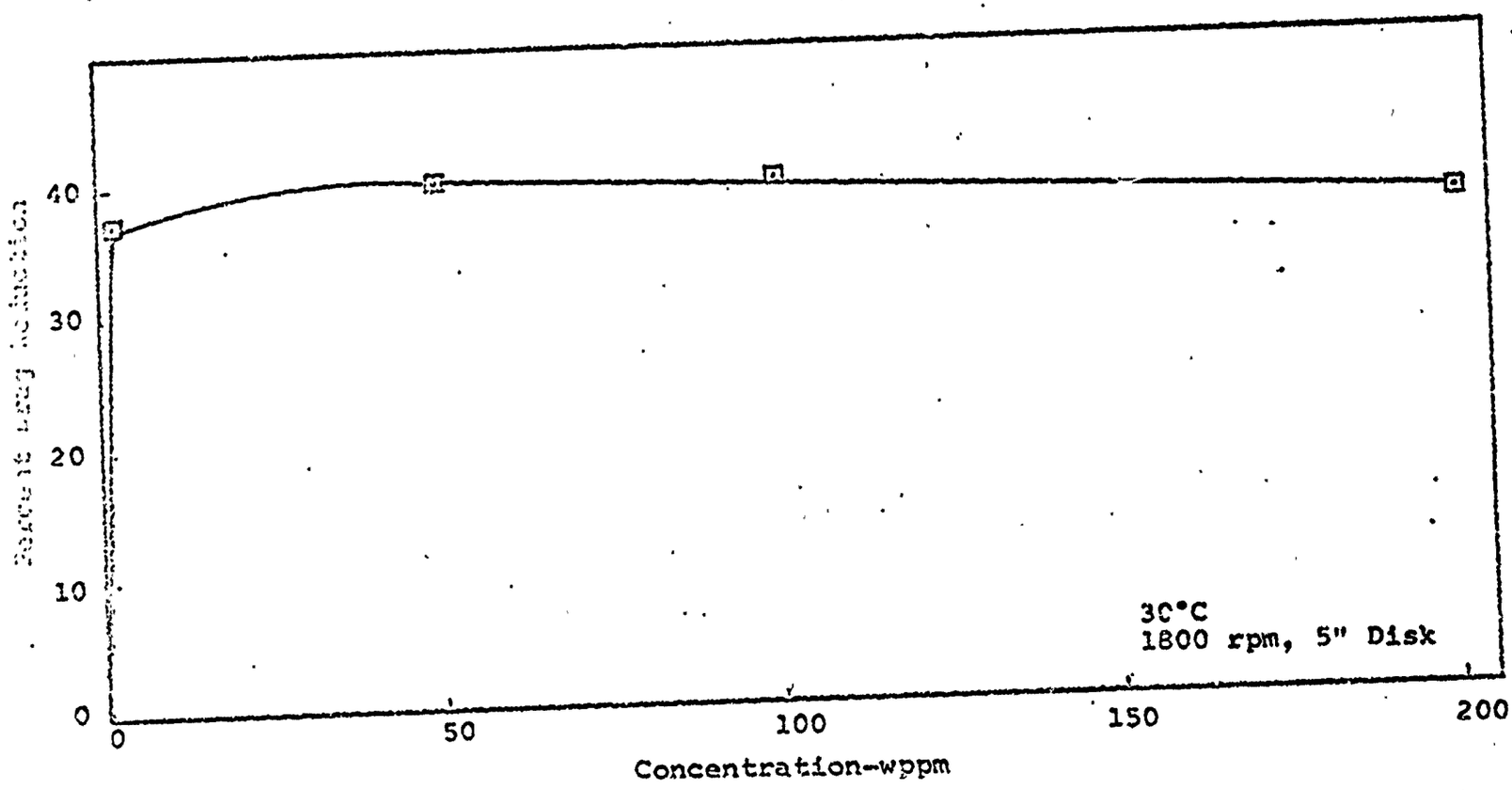

FIGURE 45

CONCENTRATION VERSUS INITIAL DRAG REDUCTION FOR COAGULANT

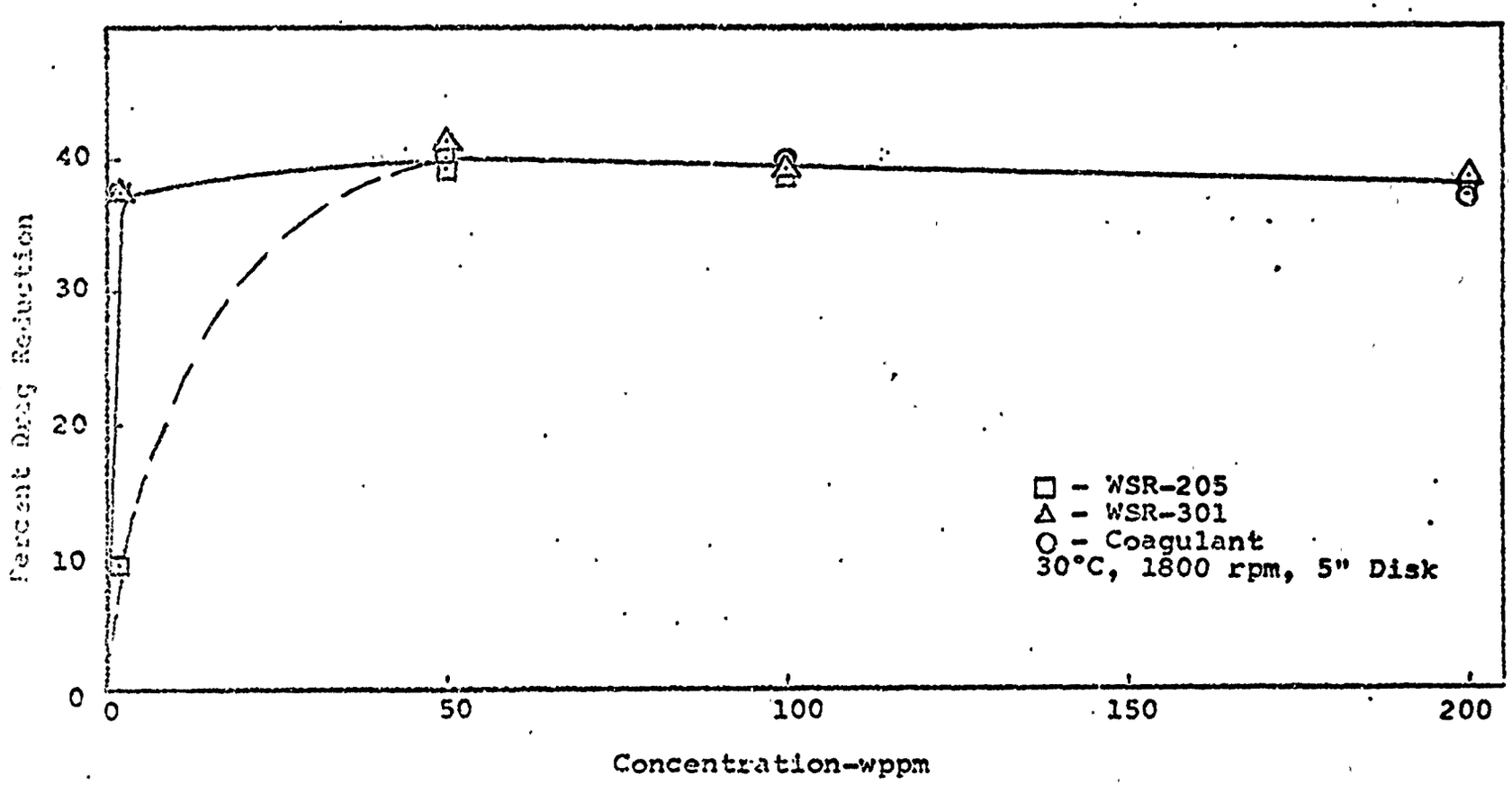

FIGURE 46
CONCENTRATION VERSUS INITIAL DRAG REDUCTION
FOR WSR-205, WSR-301, AND COAGULANT

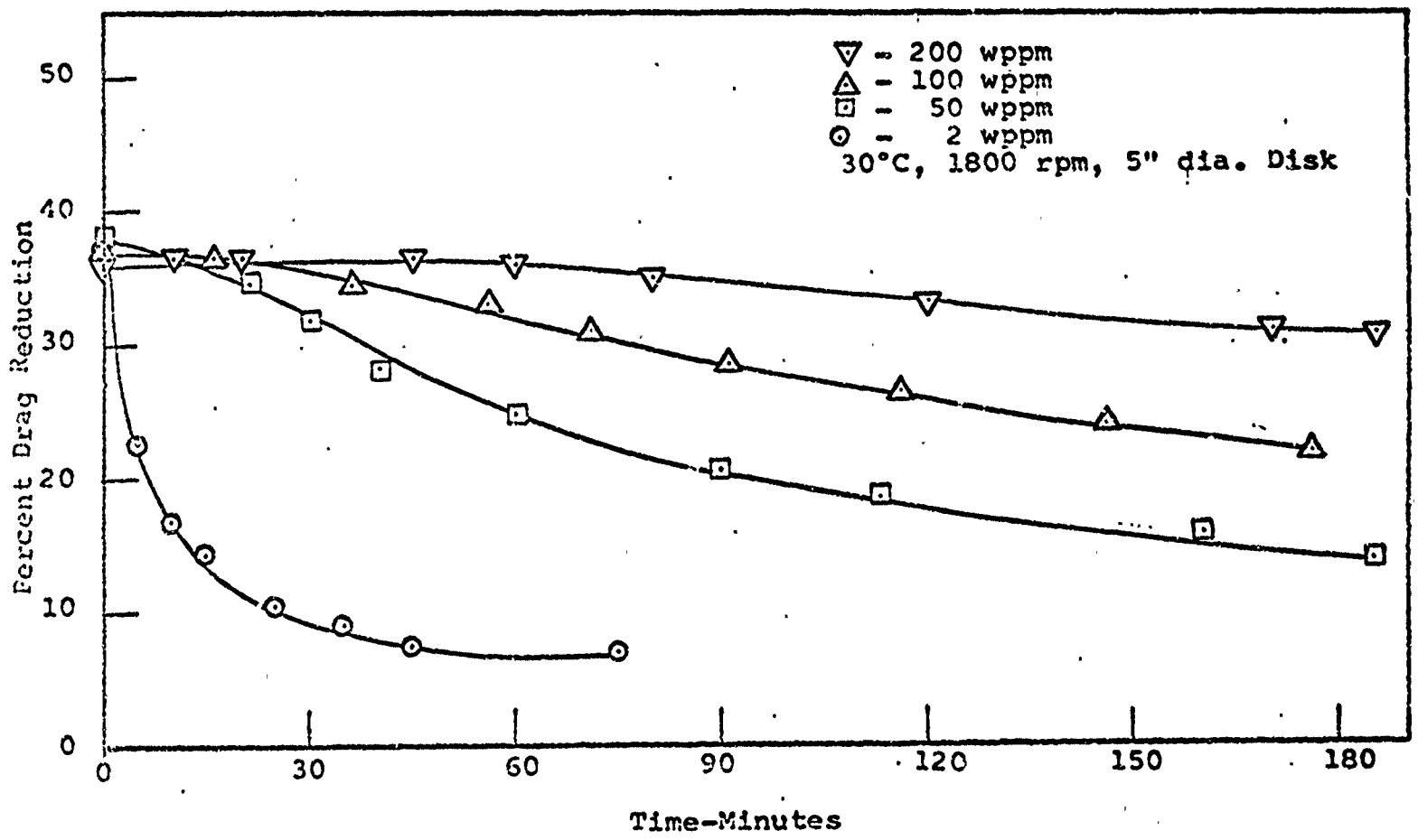

FIGURE 47
RELATIVE RESISTANCE TO MECHANICAL DEGRADATION
OF VARIOUS SOLUTION CONCENTRATIONS OF WSR-301

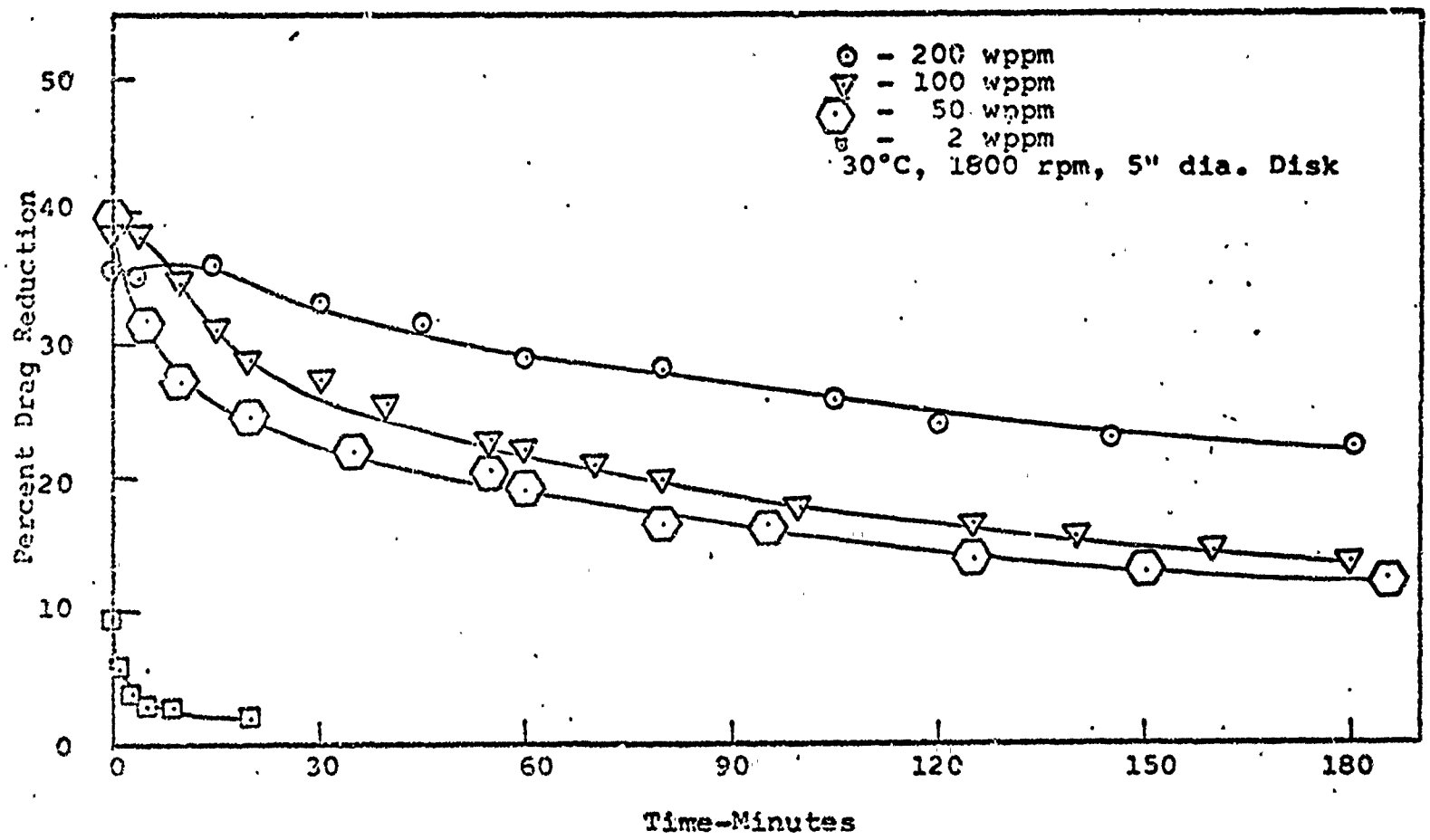

FIGURE 48
RELATIVE RESISTANCE TO MECHANICAL DEGRADATION
OF VARIOUS SOLUTION CONCENTRATIONS OF WSR-205

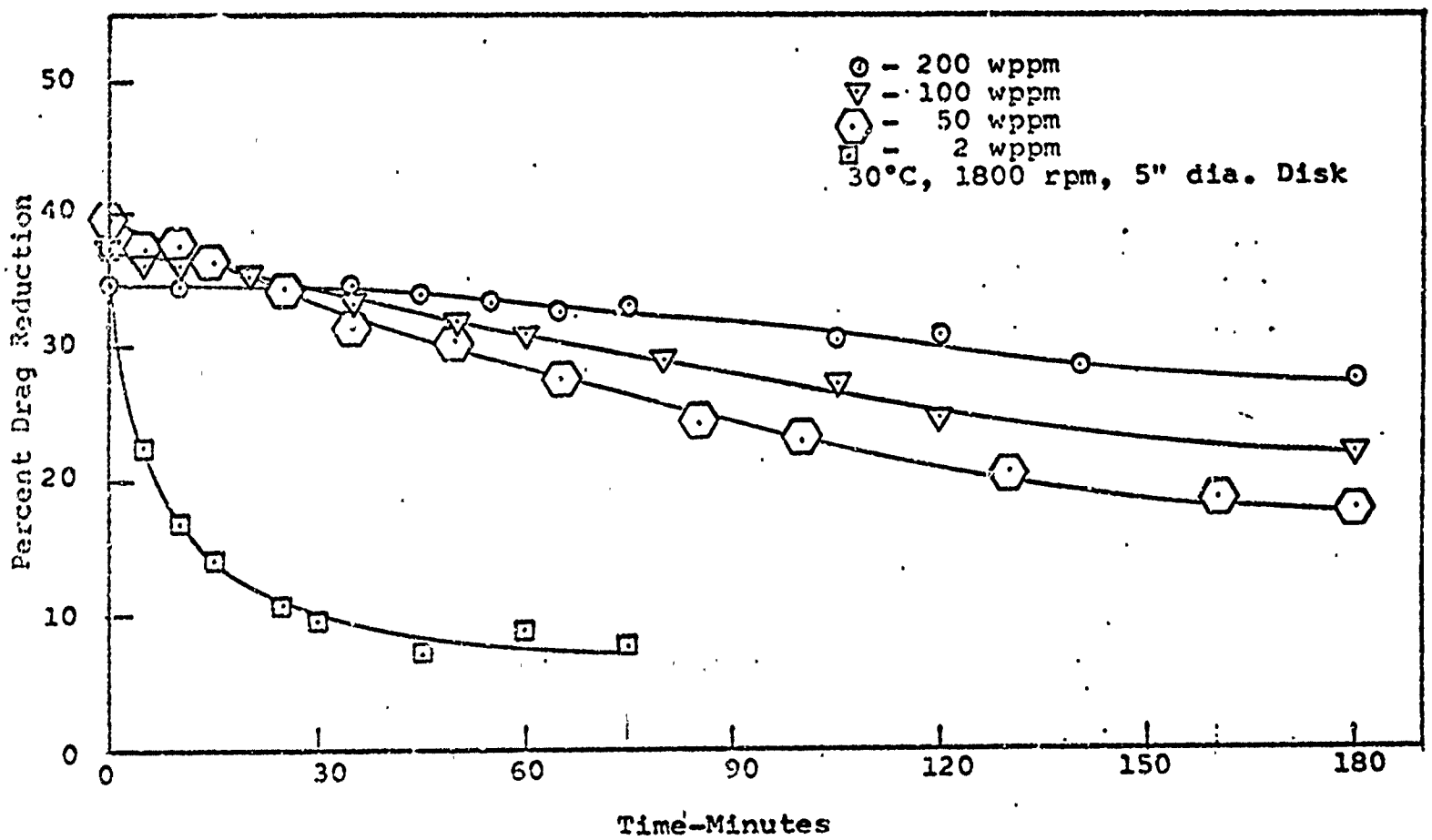

FIGURE 49
RELATIVE RESISTANCE TO MECHANICAL DEGRADATION OF
VARIOUS SOLUTION CONCENTRATIONS OF COAGULANT

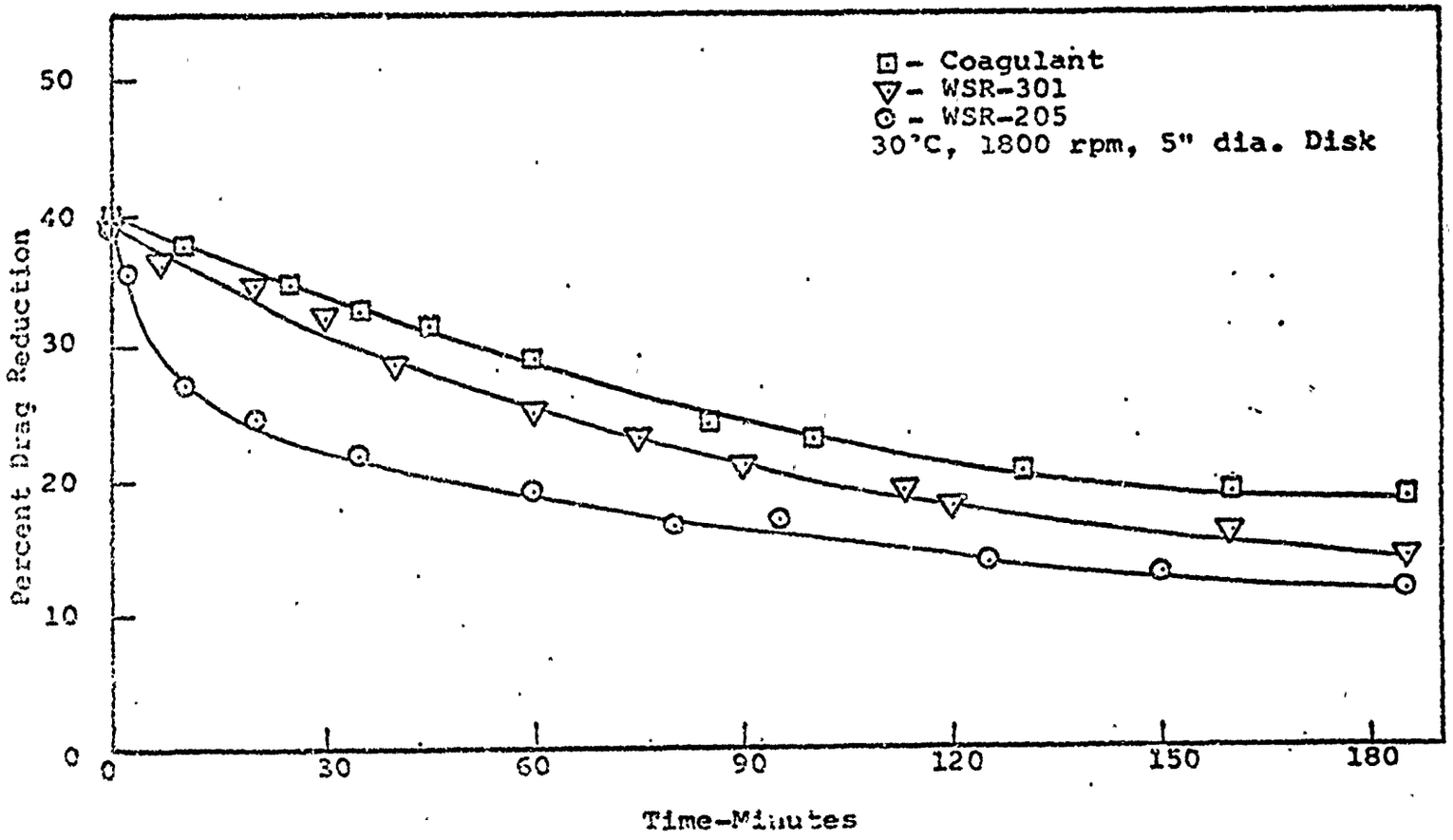

FIGURE 50
EFFECTS OF POLYMER MOLECULAR WEIGHT
ON MECHANICAL DEGRADATION FOR 50 WPPM. SOLUTIONS

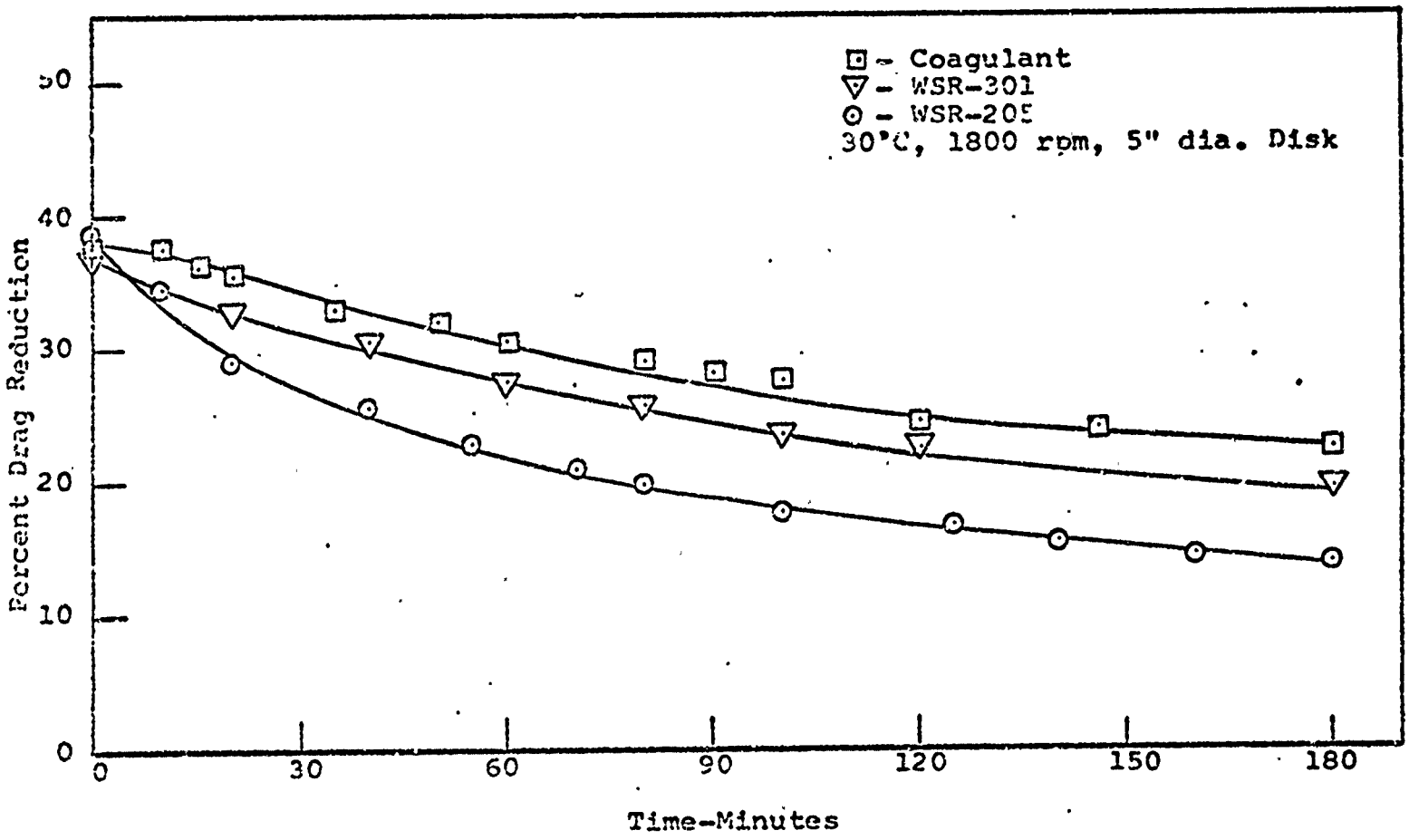

FIGURE 51
EFFECTS OF POLYMER MOLECULAR WEIGHT
ON MECHANICAL DEGRADATION FOR 100 WPPM. SOLUTIONS

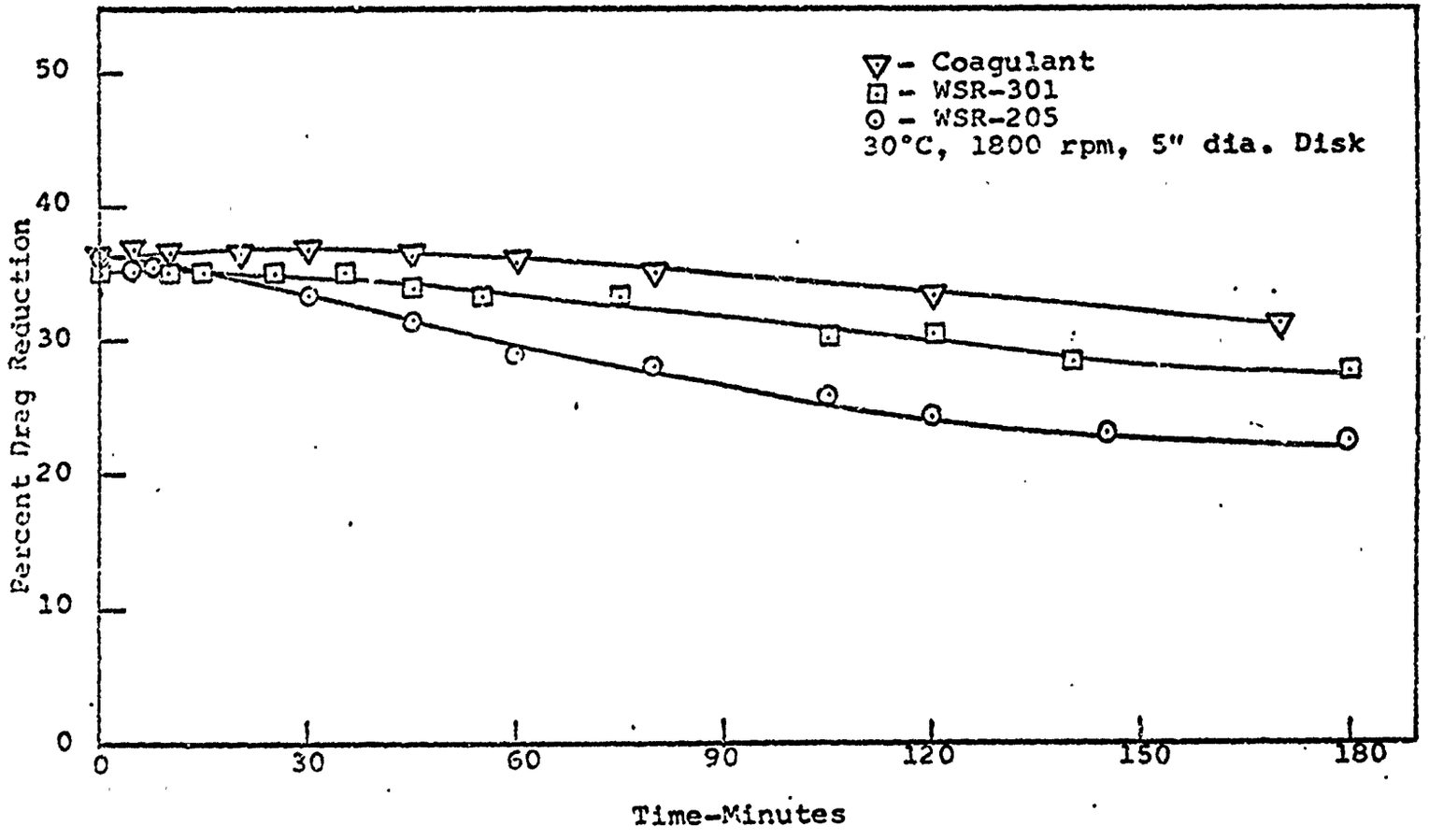

FIGURE 52
EFFECTS OF POLYMER MOLECULAR WEIGHT
ON MECHANICAL DEGRADATION FOR 200 WPPM. SOLUTIONS

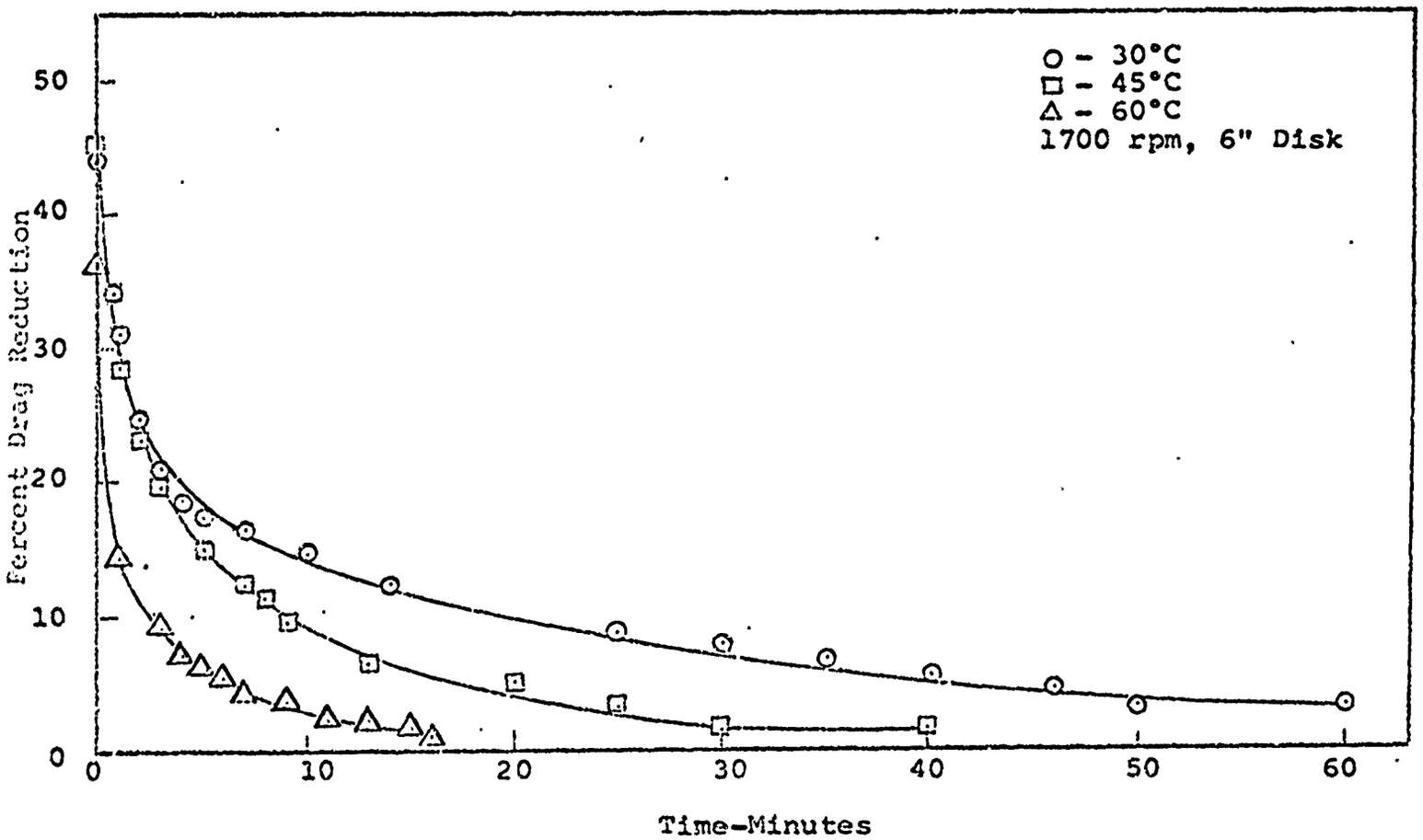

FIGURE 53
EFFECTS OF TEMPERATURE ON DRAG REDUCTION AND MECHANICAL DEGRADATION OF 2 WPPM., WSR-301

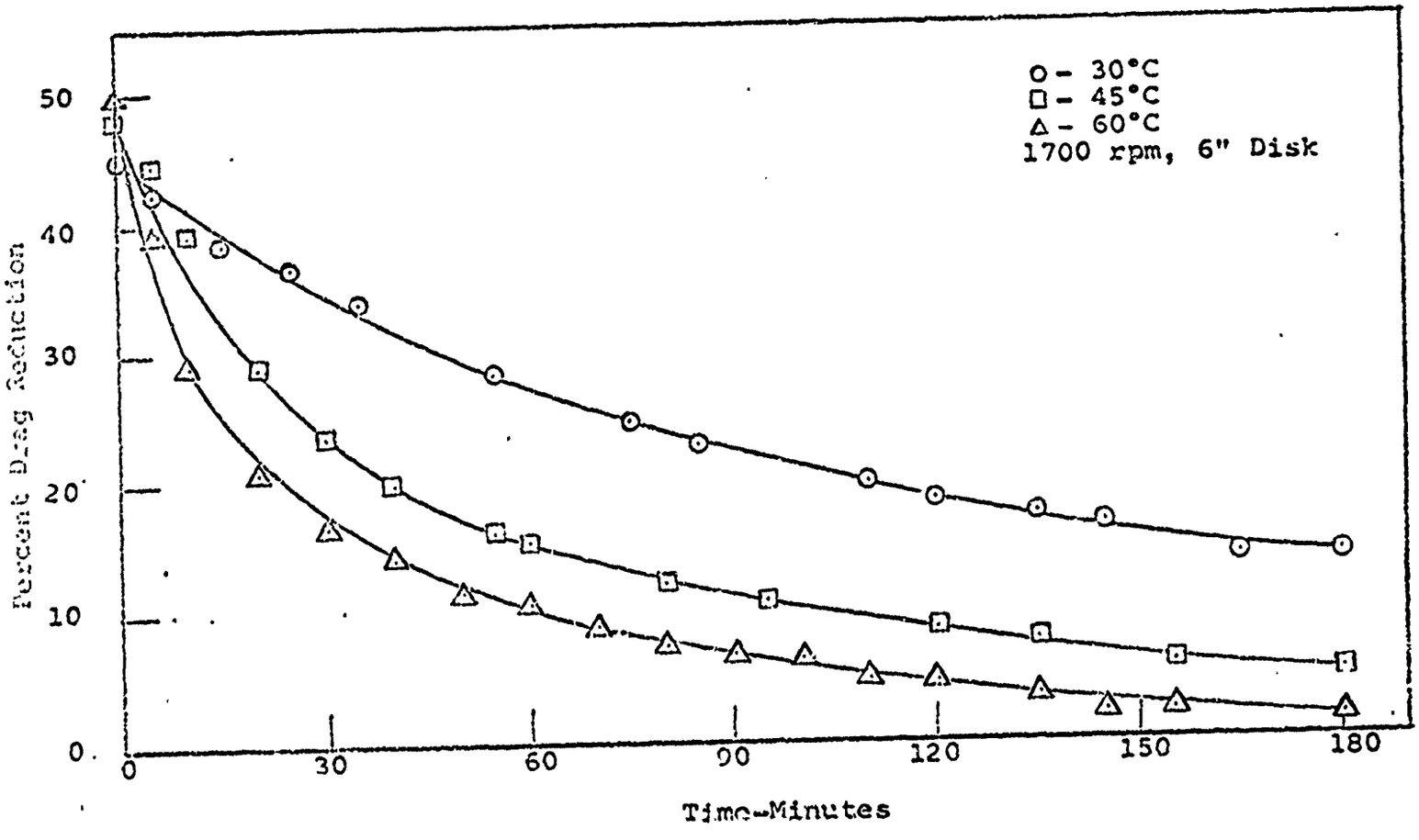

FIGURE 54
EFFECTS OF TEMPERATURE ON DRAG REDUCTION AND MECHANICAL DEGRADATION OF 50 WPPM., WSR-301

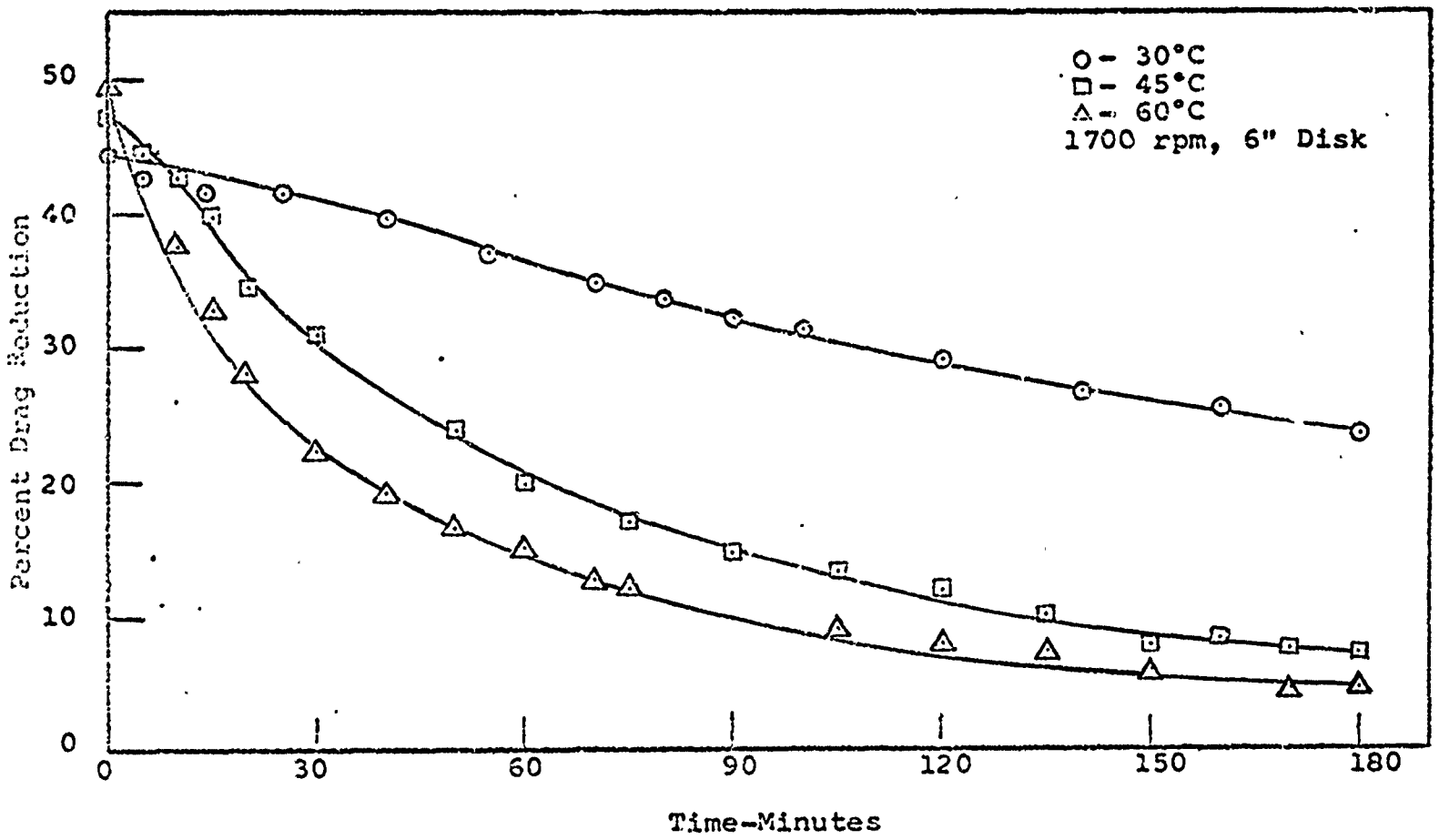

FIGURE 55
EFFECTS OF TEMPERATURE ON DRAG REDUCTION AND MECHANICAL DEGRADATION OF 100 WPPM., WSR-301

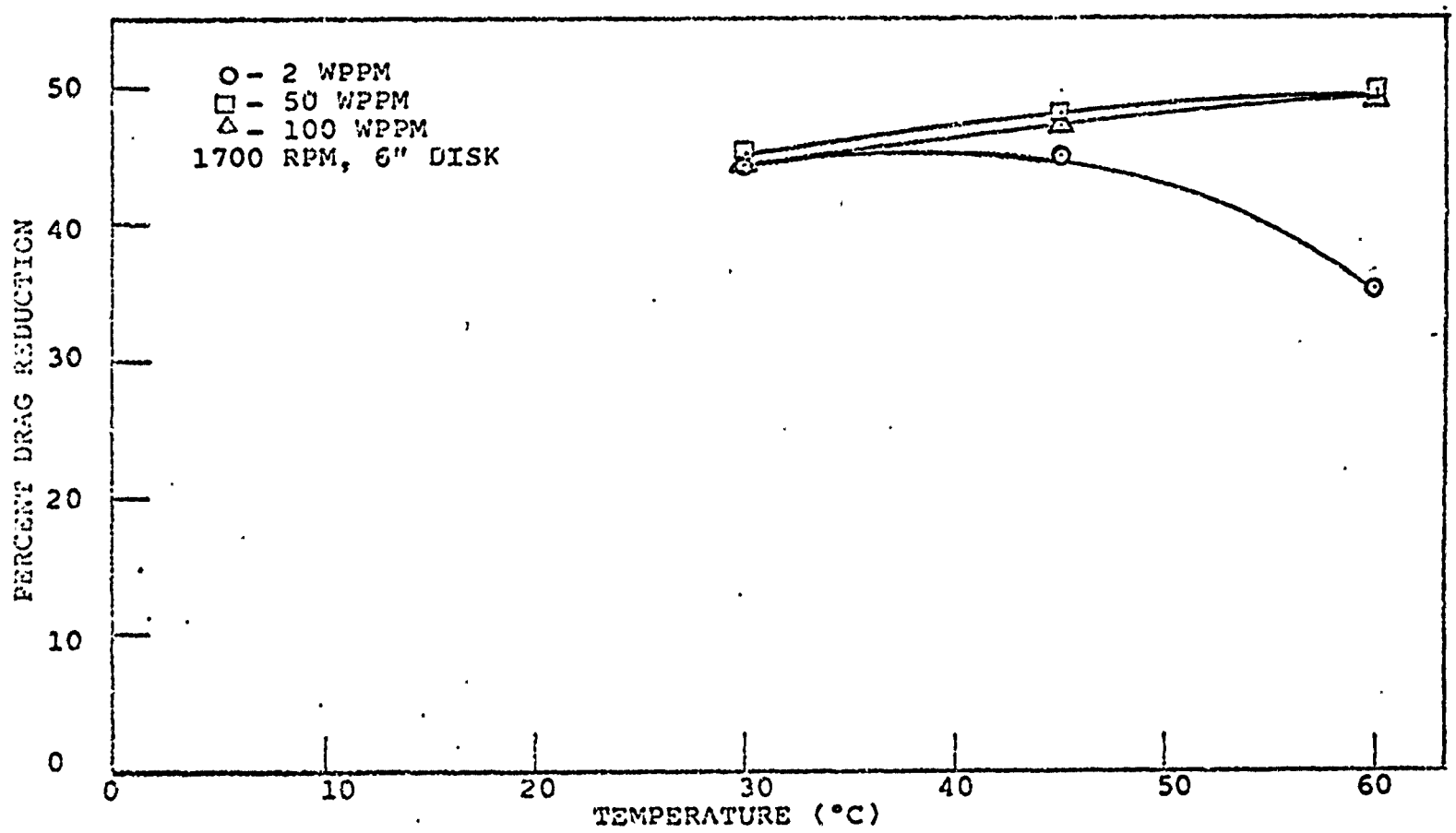

FIGURE 56
EFFECTS OF TEMPERATURE ON INITIAL DRAG
REDUCTION AT TIME t=o FOR WSR-301

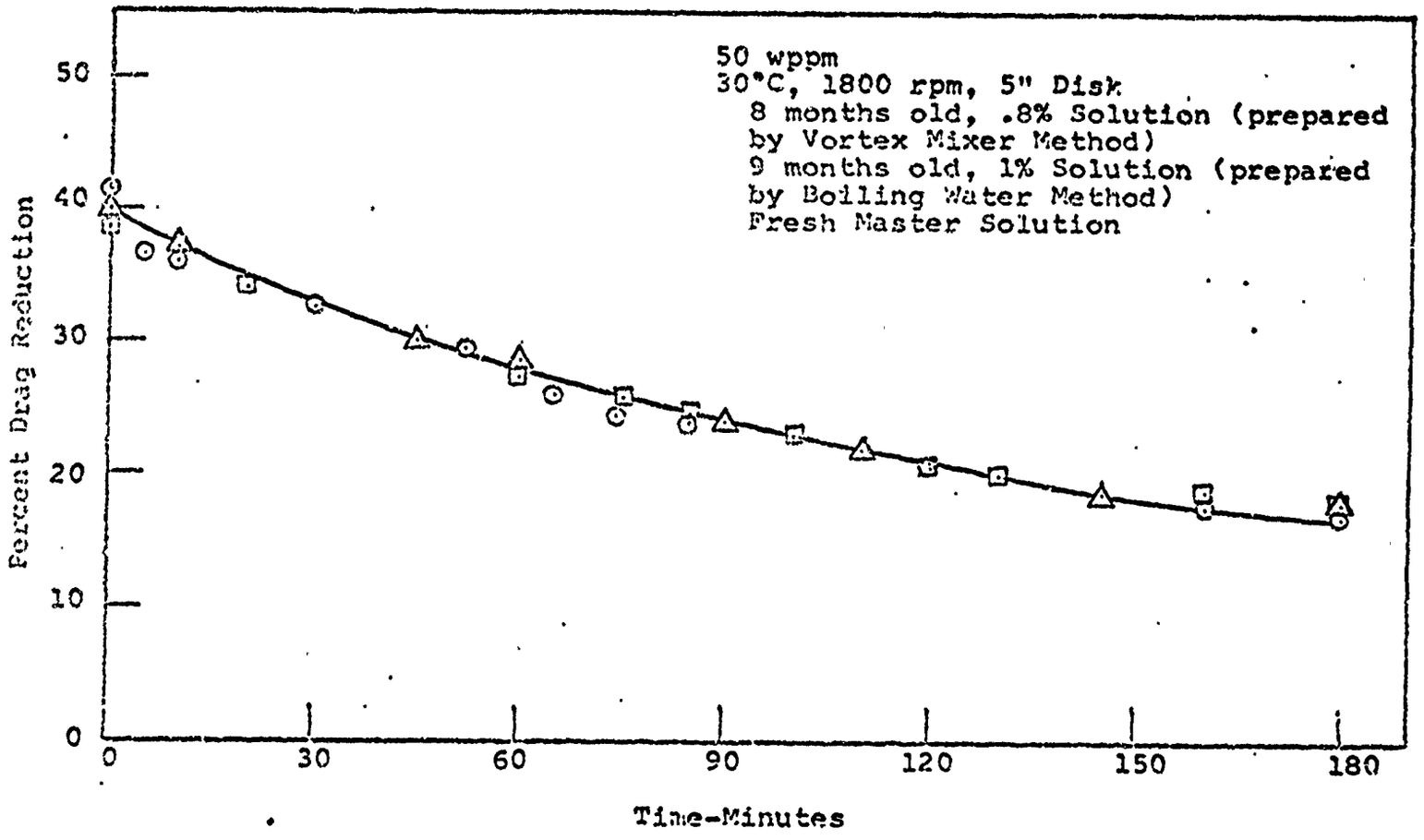

FIGURE 57
EFFECTS OF STATIC STORAGE OF MASTER SOLUTIONS OF WSR-301 ON DRAG REDUCTION AND MECHANICAL DEGRADATION OF DILUTE SOLUTIONS

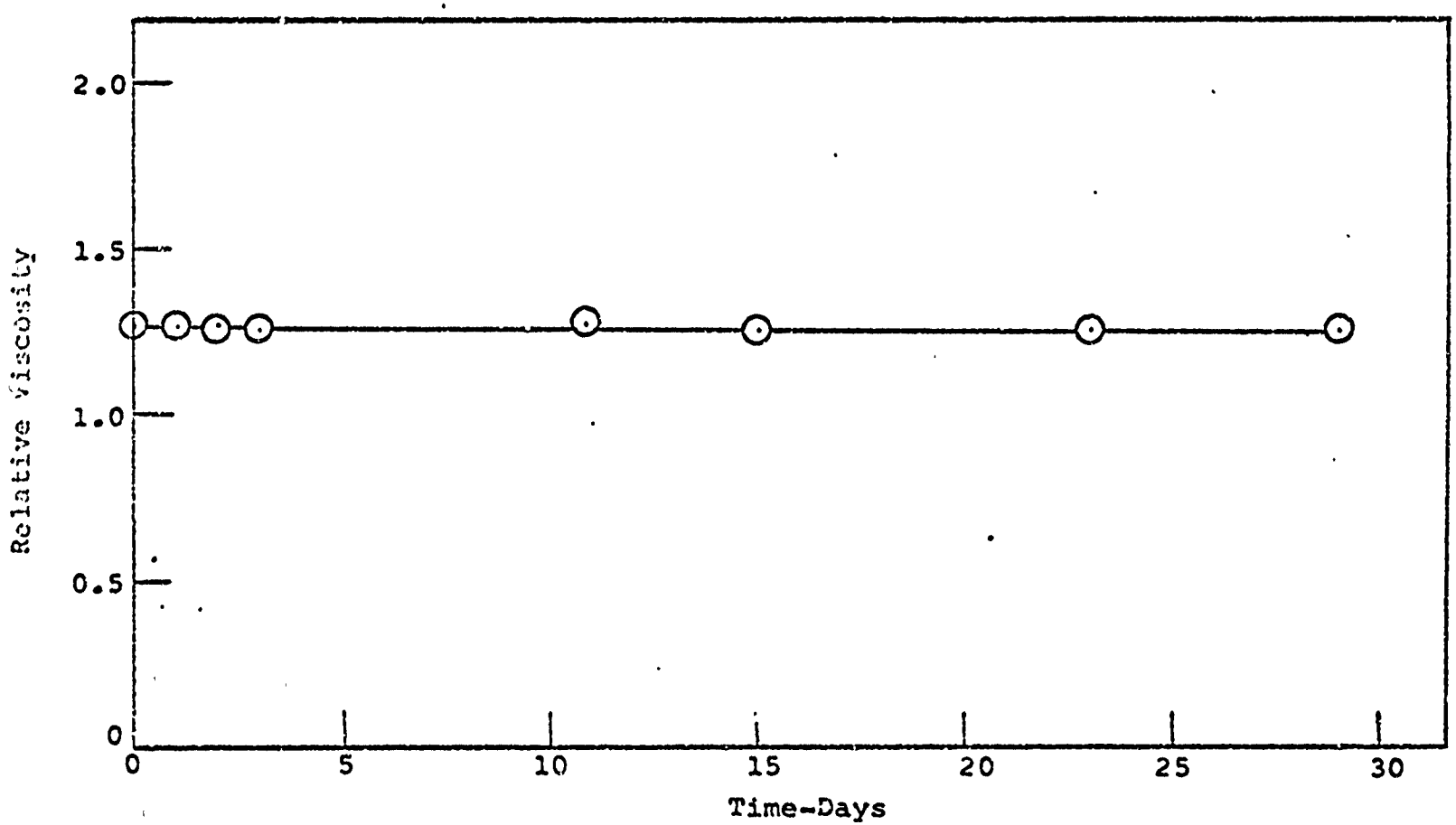

FIGURE 58

STATIC VISCOSITY DEGRADATION OF DILUTE PEO SOLUTIONS

6.0 Conclusions and Recommendations.

This research has endeavored to contribute to the understanding of degradation phenomena observed in PEO solutions. In concentrated solutions this is manifested by a decrease in the apparent viscosity resulting from mechanical agitation. In dilute solutions which exhibit friction reduction degradation, it takes the form of a decrease in the friction reducing capability. The expressed purpose of this research effort has been to observe both of these phenomena with a view towards the development of an understanding of the fundamental processes involved.

It is clear that the degradation of dilute solutions which are subjected to intense turbulent flow fields results from molecular scission. The same mechanism has been postulated to explain the decrease of apparent viscosity in concentrated solutions subjected to intense shear fields. The results of this program cast some doubt on the identification of scission as the principal contributor to the observed viscosity decay.

A number of concentrated solutions in the approximate range 0.1 - 1.0% (by weight) of polymer were subjected to laminar shear flows with shear rates ranging up to 1370 sec^{-1} and as low as 25 sec^{-1}. Although the resulting stress decay curves could not be correlated in terms of any simple model of viscoelasticity, net reductions in apparent viscosity of up to 50% were noted. On the other hand, when these "sheared" concentrated solutions were diluted and their corresponding friction reducing characteristics measured, they were found to be identical to the friction reducing characteristics of diluted forms of "unsheared" concentrated solution. This implies that the observed viscosity reduction is largely due to

microscopic disentanglement and ordering of polymer chains and the rupture of relatively weak inter-chain hydrogen bonds, rather than actual molecular scission.

In addition to the stress decay characteristics of concentrated solutions, measurements were made of the limiting, or steady-state, viscosities of these solutions. From a quantitative point of view, these limiting viscosities were found to obey a power law relationship over the entire range of shear rates at which limiting viscosities were determined (a matter of almost 4 decades of shear rate). In addition, it was found that the limiting viscosities were virtually independent of the "solution history" - at least within the shear rate range considered. That is, the magnitude of the limiting viscosity at any shear rate was found to be independent of any prior shear history, the only effect being that the limiting value is achieved in a much shorter time if the solution is sheared at a higher rate.

Turning to a consideration of the results of the study of drag reduction is dilute solutions, it was found that the extent of initial drag reduction, except for very low concentrations, was essentially independent of the polymer molecular weight and solution concentration for the case of disk flow. It is suggested that since there is a concentration plateau, there could well be a molecular weight plateau depending on the flow geometry.

The lower molecular weight samples of PEO degrade more slowly than higher molecular weight polymers if comparison is made in terms of degradation of reduced viscosity. However, the opposite is true if comparison is made in terms of degradation of drag reduction. This suggests that the

phenomenon of drag reduction depends primarily on the high molecular weight components and the process of mechanical degradation preferentially attacks the highest molecular weight species present in the spectrum of the molecular weight distribution. It is further concluded that Coagulant has a greater proportion of high molecular weight molecules in its distribution, providing many more high molecular weight molecules than are required for optimum drag reduction. The breaking of these high molecular weight molecules could result in a sharp reduction of reduced viscosity. However, the drag reduction would change by a small amount because an appreciable number of high molecular weight molecules is still present in the system. In the case of low molecular weight WSR-205, the reduced viscosity remains essentially constant during the shearing period, but drag reduction decreases by a disproportionately large value. The initial drag reduction comparable to Coagulant suggests that WSR-205 initially has enough high molecular weight molecules to provide significant drag reduction, but their number must be much smaller than that present in Coagulant. Only the narrow tail end of the distribution must lie in the drag reduction and degradation range in the case of WSR-205. Breaking of these molecules results in a small change of reduced viscosity. However, the drag reduction would decrease considerably because drag reduction depends upon the high molecular components of the distribution.

Initial drag reduction, except for very low concentrations, increases as the temperature is raised from 30°C to 60°C. The rate of degradation of drag reduction is very severe at higher temperatures because of the accelerated chemical degradation and increased Brownian motion of polymer molecules.

The static storage of concentrated solutions in distilled water containing a minute amount of isopropyl alcohol for as long as nine months does not affect their drag reducing effectiveness.

6.1 Recommendations for Future Efforts.

Continuing efforts in the field should be focused upon the development of a quantitative description of the stress decay characteristics of concentrated solutions and degradation of friction reducing capability in dilu e solutions in terms of the molecular processes involved. These efforts should emphasize a number of those factors, identified in the current research, which hinder such a development.

For example, the interpretation of the influence of polymer molecular weight (chain length) on frictional drag characteristics is made difficult by uncertainties in the molecular weight distributions of the PEO samples used. An effort should be made to develop separation techniques for the preparation of more sharply defined distributions. Alternatively, it would be useful to consider different polymer systems with inherently sharper distributions.

The shear field which the polymer molecule experiences in the case of disk flow varies in magnitude, being maximum at the surface of the disk at its outside radius. It is difficult to assign an appropriate value to the average shear stress which the polymer experiences. In a statistical sense, however, the intense turbulent mixing causes the average polymer molecules to experience the same "average" shear field. It is recommended that the phenomenon of mechanical degradation of dilute polymer solutions be studied using monodisperse solutions and preferably in a rotating

Couette apparatus. In Couette flow, it is possible to accurately estimate the mangitude of the shearing stresses. The use of monodisperse samples would eliminate the effects of the broad distribution on mechanical degradation.

The process of mechanical degradation is also dependent upon the shape of the polymer coil in solution. These configurational effects can be studied by utilizing different solvents. The proper choice of solvent can cause the polymer molecule to assume extended or compacted configurations.

In terms of the study of stress decay in concentrated solutions, efforts to develop a quantitative description of this phenomenon should continue. This activity should emphasize improvements in the techniques for the measurement of transient shear stresses.

Although it has not been mentioned explicity, the decay of viscous characteristics of PEO solutions is always observed to be accompanied by a corresponding decay of viscoelastic characteristics such as the rod-climbing or Weissenberg effect. It is suggested that research be directed towards the quantitative investigation of these phenomena.

7.0 Bibliography

1. Alfrey, T., Bartovics, A., and Mark, H., "Comparative Osmatic and Viscosity Measurements With Polystyrene Fractions," Journal of American Chemical Society, Vol. 65, No. 12, Dec. 1943, pp. 2319-2323.

2. American Society for Testing and Materials, ASTM Standards, Part 17, 1968, pp. 180-186.

3. Asbeck, W. K., and Baxter, M. K., "Coatings: Physical Studies, Shear Degradation of Aqueous Poly(ethylene oxide) Solutions," Project Report No. 18630, Feb. 1959, Union Carbide Chemicals Company, South Charleston, W. Virginia.

4. Bailey, F. E., Kucera, J. L., and Imhot, L. G., "Molecular Weight Relations of Poly(ethylene oxide)," Journal of Polymer Science, Vol. 32, 1958, pp. 517-518.

5. Brennen, C., and Gadd, G. E., "Aging and Degradation in Dilute Polymer Solutions," Nature, Vol. 215, No. 5108, September 23, 1967, pp. 1368-1370.

6. El'perin, I. T., Smol'skii, B. M., and Leventhal, L. I., "Decreasing the Hydrodynamic Resistance of Pipeline," International Chemical Engineering, Vol. 7, 1967, p. 276.

7. Fabula, A. G., "An Experimental Study of Grid Turbulence in Dilute High Polymer Solutions," Ph.D. Thesis, June 1966, The Pennsylvania State University, University Park, Pennsylvania.

8. Flory, P. J., "Determination of Molecular Weights," Principles of Polymer Chemistry, Cornell University Press, New York, 1953, pp. 308-314.

9. Gadd, G. E., "Differences in Normal Stress in Aqueous Solutions of Turbulent Drag Reducing Additives," Nature, Vol. 212, No. 5068, Dec. 17, 1966, pp. 1348-1350.

10. Gawler, D. R. R., "Preliminary Design Tests for a Shipborne Fluid Additive Ejection System," A.U.L.E.

Technical Note 245/67, July 1967, (Available from Naval Undersea Research and Development Center, Pasadena, Calif.).

11. Gilbert, C. G., and Ripken, J. F., "Drag Reduction on a Rotating Disk Using a Polymer Additive," Viscous Drag Reduction, Wells, C. S., ed., Plenum Press, New York, 1969, pp. 251-263.

12. Giles, W. B., "Similarity Laws of Friction-Reduced Flows," Journal of Hydronautics, Vol. 2, 1968, p. 34.

13. Hoyt, J. W., Hydrodynamics of Dilute Polymer Solutions and Suspensions, (unpublished type script)

14. Hoyt, J. W., and Fabula, A. G., "The Effect of Additives on Fluid Friction," Proceedings of the 5th Symposium on Naval Hydrodynamics, Bergen, Norway, Sept. 1964, pp. 947-974.

15. McGary, C. W., "Degradation of Poly(ethylene oxide)," Journal of Polymer Science, Vol. 66, 1960, pp. 51-57.

16. Paterson, R. W., "Turbulent Flow Drag Reduction and Degradation with Dilute Polymer Solutions," AD-693-306, June 1969, Engineering Sciences Laboratory, Harvard University.

17. "Polyox Water-Soluble Resins," Union Carbide Corporation, New York, 1967.

18. Prandtl, L., and Tietjens, O., Applied Hydro and Aeromachines, Dover Publications, New York, 1957.

19. Pruitt, G. T., Rosen, B., and Crawford, H. R., "Effect of Polymer Coiling on Drag Reduction," Technical Report No. DTMB-2, Aug. 1966, The Western Company, Dallas, Texas.

20. Schlichting, H., "Turbulent Boundary Layers at Zero Pressure Gradient," Boundary Layer Theory, 6th ed., McGraw-Hill, New York, 1968, pp. 606-608.

21. Severs, E. T., "Solutions of Polymers," Rheology of Polymers, Reinhold Publishing Corporation, New York,

1962, pp. 91-92

22. Shaver, R. G., and Merrill, E. W., "Turbulence of Pseudoplastic Solutions in Straight Cylindrical Tubes," Journal of American Institute of Chemical Engineers, Vol. 5, No. 2, 1959, pp. 181-187.

23. Shin, H., "Reduction of Drag in Turbulence by Dilute Polymer Solutions," Sc.D. Thesis, 1965, M.I.T., Cambridge, Mass.

24. Tanford, C., "Light Scattering," Physical Chemistry of Macromolecules, Wiley, New York, 1961, pp. 281-288.

25. Toms, B. A., "Some Observations on the Flow of Linear Polymer Solutions Through Straight Tubes at Large Reynolds Numbers," Proceedings of 1st International Congress on Rheology, North Holland Publishing Co., Vol. 2, 1948, pp. 1[illegible]-141.

26. Van Wazer, J. R., et al., Viscosity and Flow Measurement, Interscience Publishers, New York, 1963, pp. 107-226.

27. Virk, P. S., "The Toms Phenomenon-Turbulent Pipe Flow of Dilute Polymer Solutions," Sc.D. Thesis, Nov. 1966, M.I.T., Cambridge, Mass.

28. Bailey, F. E., Jr., et. al., "High Molecular Weight Polymers of Ethylene Oxide," Ind. and Eng. Chem. 50, 8 (1958)

29. Swanson, E. D., "Degradation of Thick Polymer Solutions," Naval Undersea Research and Development Center, Pasadena, California (Code 2543), 19 February 1969.

30. Gold, P. I., "Mechanical Degradation of Thick Polymer Solutions," Naval Undersea Research and Development Center, Pasadena, California (Code 254), 3 September 1969.

31. Hoyt, J W., "A Turbulent-Flow Rheometer," in Symposium on Rheology, A. W. Morris and J. T. S. Wang, eds., ASME, New York, pp. 71, (1965).

32. Rodriguez, F., and L. A. Goettler, "The Flow of Moderately Concentrated Polymer Solutions in Water," Trans. Soc. Rheol., 8, 3 (1964).

33. Rodriguez, F., "Moderately Concentrated Polymer Solutions: Correlation of Flow Data by Simple Models," Trans. Soc. Rheol., 10, 169 (1966).

34. Bailey, F. E., and J. V. Koleske, "Configuration and Hydrodynamic Properties of the Polyoxyethylene Chain in Solution," in Nonionic Surfactants, Dekker, New York, 1967.

35. Carver, E. K., and J. R. Van Wazer, J. Phys. and Colloid Chem., 51, 754 (1947).

36. Green, H., "Industrial Rheology and Rheological Structures, Wiley, New York, 1949.

37. Ram, A., "High Shear Viscometry," in Rheology Vol. 4, F. Eirich, ed., Academic Press, New York, 1967.

38. Ram, A., Sc. D. Thesis, M.I.T., Cambridge, Mass., 1961.

39. Scott Blair G. W., "A Survey of General and Applied Rheology," Pittman, N. York, 1944.

40. Saville, D. A., and D. W. Thompson, "Secondary Flows Associated with the Weissenberg Effect," Nature, 223, 391-2, (1969).

8.0 Appendix I. End Corrections for Filled Cup - Newtonian Fluid

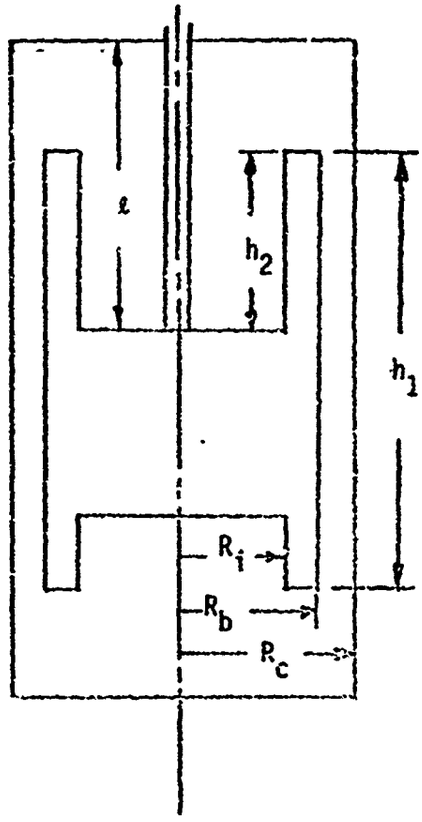

M_t = total measured torque, dyne-cm

M_1 = torque exerted due to shear stress, on annular gap, dyne-cm

M_2 = torque exerted on cylindrical surface inside bob, dyne-cm

M_3 = torque exerted on disk-shaped surface inside bob, dyne-cm

Neglected - torque exerted on annular disks on top and bottom of bob.

$$M_t = M_1 + M_2 + M_3$$

For a Newtonian fluid,

$$\eta_N = \frac{M_1}{4\pi h_1 \Omega}\left(\frac{1}{R_b^2} - \frac{1}{R_c^2}\right)$$

$$\eta_N = \frac{M_2}{4\pi h_2 \Omega}\left(\frac{1}{R_i^2}\right)$$

$$\eta_N = \frac{M_3 \ell}{\pi R_i^4 \Omega}$$

$$M_t = \frac{4\pi h_1 \Omega \eta_N}{\left(\frac{1}{R_b^2} - \frac{1}{R_c^2}\right)} + \frac{4\pi h_2 \Omega \eta_N}{\frac{1}{R_i^2}} + \frac{\pi \Omega \eta_N}{\frac{\ell}{R_i^4}} = 4\pi\Omega\eta_N\left(\frac{R_b^2 R_c^2 h_1}{R_c^2 - R_b^2} + R_i^2 h_2 + \frac{R_i^2}{4\ell}\right)$$

$$\frac{M_1}{M_t} = \frac{R_b^2 R_c^2 h_1/(R_c^2 - R_b^2)}{M_t}$$

$$\frac{M_2}{M_t} = \frac{R_i^2 h_2}{M_t}$$

$$\frac{M_3}{M_t} = \frac{R_i^2/4\ell}{M_t}$$

Data

R_b = 2.004 Cm

R_c = 2.10 Cm

h_1 = 6.0 Cm

ℓ = 5.0 Cm

h_2 = 3.52 Cm

R_i = 1.63 Cm

$$\frac{R_b^2 R_c^2 h_1}{R_c^2 - R_b^2} = \frac{(2.004)^2\ (2.10)^2\ (6.0)}{(2.10)^2 - (2.004)^2} = 269.7$$

$$R_i^2 h_2 = (1.63)^2\ (3.52) = 9.4$$

$$\frac{R_i^4}{4\ell} = \frac{(1.63)^4}{(4 \times 5)} = 0.4$$

$$M_t = 269.7 + 9.4 + 0.4 = 279.5$$

$$\frac{M_1}{M_t} = 0.965$$

It follows, therefore, that the measured scale reading is approximately 3% too high.

TABLE I

Viscosity of Glycerine Determined with RV cup (a) filled normally and (b) filled completely (T = 30° C)

U	S (Norm)		S (full)			S_{avg} (Norm)	S_{avg} (full)
162	8	8	8	8	MVI/30°C/50	8	8
81	17	17	16.5	16.5		17	16.5
54	25	25.5	25	25		25.25	25
27	52	52	51.5	51.5		52	51.5
18	79	79	79	78.5		79	78.75
9	15.0	15.4	15.2	15.3	MVI/30°C/500	15.2	15.25
6	22.5	22.7	22.5	22.5		22.6	22.5
3	44.0	44.5	44.4	44.2		44.25	44.3
2	66.3	66.5	66.2			66.4	66.2

$D\ (sec^{-1}) = \frac{1370}{U}$	η (Norm) (Cp)	η (full) (Cp)	RPM
8.45	293	293	3.6
16.9	311	302	7.2
25.4	308	305	10.8
50.8	317	314	21.6
76.2	321	320	32.4
152	322	324	64.8
228	320	320	97.2
457	313	313	194.4
685	314	313	291.6

9.0 Appendix II. Kinetic Energy Correction

The kinetic energy correction (18) is = $\rho(Vs^2 - Vp^2)$. The quantities Vs and Vp are mean velocities for water and polymer, at the same driving head. In addition, $V_{mean} = \frac{\Delta P R^2}{8\eta L}$. K.E. Correction $= \frac{\rho(\Delta P)^2 R^4}{64L^2}\left\{\frac{1}{\eta_s^2} - \frac{1}{\eta_p^2}\right\}$. For the extreme case of 200 wppm. Coagulant with η_p = 1.06 cp. the K.E. Correction was found to be 9.6 gm./cm.-Sec.^{2}. The average driving head was 9.3 cm. or 9.3 x 981 x 1 = 9123 gm./cm.-Sec.^{2}. Therefore, the K.E. Correction is .001% of the driving head and can be neglected.

10.0 Appendix III. Wall Shear Rate of Capillary Viscometer

The wall shear rate for a Newtonian fluid under laminar capillary flow conditions is given by (26):

$$D = \frac{\Delta PR}{2\eta L}$$

For Cannon-Fenske viscometer, size 50 (26):

P_{avg} = average pressure drop = $h_{avg}\,\rho g$

h_{avg} = average driving fluid head = 9.3 cm.

L = capillary length = 7.3 $\pm$ .3 cm.

R = Radius of capillary = 0.31 $\pm$ 0.2 mm.

η = viscosity of water at 30°C = 0.7975 cp.

Making calculations for water:

$$D = 1216\ (\text{sec.})^{-1}$$

The minimum shear rate occurred at 200 wppm. Coagulant with η = 1.06018 cp. This was found to be 915 $(\text{Sec.})^{-1}$.

11.0 Appendix IV. Data Tables

The following tables summarize the stress decay data discussed in Section 4.0. "Bob Speed Settings" indicated in these tables refer to the rpm's and Newtonian shear rates outlined in Table 1, below

Table 1
Bob Speed Setting for the Rotovisco MV I
Bob and Cup System

Bob Speed Setting	Newtonian Shear Rate (sec^{-1})	Rotational Speed (RPM)
1	1370	582
2	685	291
3	457	194
6	228	97
9	152	64.8
18	76	32.4
27	51	21.6
54	25	10.8
81	16	7.2
162	8.5	3.6

TABLE 2

Stress Decay Data

Polymer lot: WSR 301 (W-1006-A-01)

Concentration (wt. %) 0.24

Time (min)	Bob Speed Setting 1	2	3	6	9	18	27	54	81	162
	Stress (dynes/cm^2)									
0										
.5	250	146	107							
1	247	144	104							
2	238	139	102							
3	229	138	99							
4	219	136	96							
5	212	133	93							
6	207	131	91							
7	199	130	91							
8	195	128	90							
9	192	125	88							
10	188	122	88							
15	179	114	85							
20	171	107	80							
30	161	98	70							
40	153	80	60							
50	147	67	49							
57		62								
60	140		48							
70			49							
80			46							
90			46							

TABLE 3

Stress Decay Data

Polymer lot: WSR 301 (W-1006-A-01)

Concentration (wt. %) 0.36

Time (min)	Bob Speed Setting 1	2	3	6	9	18	27	54	81	162
	Stress (dynes/cm^2)									
0										
0.5		221	165	100	73					
1	343	213	162	96	71					
2	327	204	161	94	70					
3	327	199	158	93	70					
4	327	195	156	93	70					
5	318	192	154	91	68					
6	318	190	151	90	68					
7	302	189	148	88	67					
8	302	185	147	87	67					
9	286	184	144	87	65					
10	286	181	144	85	62					
11	278	178	142	84						
12	273	176	139	84						
13	269	173	139	82						
14	264	170	137	82						
15	261	167	134	80						
16	257	164	131	80						
17	253	161	128	79						
18	249	161	127							
19	244	158	124							
20	241	154	120							
30	216	130	105							
40	198	111	91							
50	179	107	84							
52		105								
58			82							
60	168									
70	164									
80	161									
90	156									
100	153									
110	151									
120	148									
126	148									

TABLE 4

Stress Decay Data

Polymer lot: WSR 301 (W-1006-A-01)

Concentration (wt. %) 0.41

Time (min)	Bob Speed Setting 1	2	3	6	9	18	27	54	81	162
	Stress (dynes/cm^2)									
0										
0.5	414	244	188	114	84					
1	389	233	182	108	82					
2	373	224	176	107	79					
3	365	219	173	107	79					
4	365	216	168	105	79					
5	365	215	165	105	80					
6	357	212	164	104	80					
7	357	209	162	104	79					
8	349	205	162	102	79					
9	341	201	161	101	77					
10	333	196	158	99	74					
11	333	193	158	97	73					
12	325	189	154	97	71					
13	316	184	153	96	70					
14	300	181	151	94	68					
15	297	178	148	94	66					
16	291	173	145	93	66					
17	285	171	145	93	65					
18	280	167	144		65					
19	271	164	141		65					
20	266	164	138							
25	238	150	124							
30	224	141	117							
35	210	130	107							
39	206									
40		122	100							
44		122								
45			96							
50			96							
55			96							

TABLE 5

Stress Decay Data

Polymer lot: WSR 301 (W-1006-A-01)

Concentration (wt. %) 0.63

Time (min)	Bob Speed Setting 1	2	3	6	9	18	27	54	81	162
	Stress (dynes/cm^2)									
0										
.5	600	392	321	204	145					
1	566	351	297	202	151					
2	526	351	292	198	151					
3	502	351	288	195	151					
4	494	343	283	192	148					
5	470	343	277	190	147					
6	462	343	273	187	144					
7	454	334	270	184	142					
8	454	334	267	182	141					
9	454	334	264	178	138					
10	446	334	261	175	140					
11	438	318	260	172	141					
12	421	318	258	170	140					
13	405	302	257	168	140					
14	397	302	253	168	140					
15	389	286	252	168	140					
16	389	286	247	167	140					
17	373	286	244	165	140					
18	357	281	241	164						
19	357	278	238	162						
20	357	275	237	162						
21	357									
25		261	224	156						
28			221							
30		243		148						
35		229								
40		225								

TABLE 6

Stress Decay Data

Polymer lot: WSR-301 (W-1006-A-01)

Concentration (wt. %) 0.91

Time (min)	Bob Speed Setting 1	2	3	6	9	18	27	54	81	162
	Stress (dynes/cm^2)									
0										
0.25		624	510	254	175	138	107	68		
0.5		591	494	300	209	158	121	76		
0.65				309						
0.75		575				168	133	82		
1		575	473	301	230	192	139	85		
1.25						202	142			
1.5						195	144			
1.75						190				
2		550	466	286	220	186	143	93		
2.2								94		
3		542	453	286	216	180	142	91		
4		535	445	276	215	179	142	90		
5		526	430	270	212	179	141	90		
6		519	421	226	210	179	140	90		
7		510	405	262	207	178	139	90		
8		502	405	258	205	176	139			
9		499	405	256	201	176	139			
10		486	405	256	199	175	139			
11		486	389	254	197	173				
12			373	252	196	172				
13			373	252	195	171				
14			373	250	195	170				
15			373	249	195	168				
16				247	194	167				
17				246	194	167				
18				245		166				
19				244	165					
20					165					
21					164					

TABLE 7

Stress Decay Data

Polymer lot: WSR-301 (W-1006-A-01)

Concentration (wt. %) 0.94

Time (min)	Bob Speed Setting 1	2	3	6	9	18	27	54	81	162
	Stress (dynes/cm^2)									
0										
0.25		713		292	239	164	138			
0.3			551							
0.5		673	535	340	264	182	155			
0.75		640	518	365		196	169			
1		624	510	365	289	204	174			
1.25							179			
1.3						212				
1.5							178			
2		600	486	348	286	210	175			
3		592	470	340	282	209	175			
4		583	462	337	279	208	175			
5		575	454	337	277	207	173			
6		567	448	337	274	206	173			
7		559	446	332	272	205	173			
8		551	442	327	270	204	172			
9		551	438	321	267	204	172			
10		543	431	316	266	203	172			
11		538	429	316	264	202	172			
12		535	429	316	263	202	172			
13		535	429	316	263	202				
14			429	316	261	201				
15			426	316	261	201				
16			417	316	260	201				
17			417	316	260					
18			417	316	259					
19				316	259					
20					258					
25					258					
27					258					

TABLE 8

Reproduceability of Stress Decay Data

Polymer lot: WSR-301 (W-1006-A-01)

Concentration (wt. %) 0.36

Time (min)	Bob Speed Setting		
	η(1)	η(2)	η(3)
	Stress (dynes/cm^2)		
0			
.5	359		358
1	351	343	342
2	327	327	334
3	327	327	334
4	327	327	334
5	319	318	334
6	310	318	326
7	294	302	326
8	294	302	310
9	294	286	310
10	294	286	290
11	289	278	284
12	283	273	275
13	277	269	272
14	272	264	267
15	266	261	262
16	261	257	258
17	258	253	253
18	253	249	249
19	250	244	246
20	246	241	242
25	232	229	229
30	216	216	216
35	207	209	
40	196	198	
45	190	189	
50	182	179	
60	170	168	
70	164	164	
80	162	161	
90	159	156	
100	154	153	
110	153	151	
119	150		
120		148	
126		148	

(1) Initial Run
(2) Immediate Repeat Run
(3) Repeat Run 24 Hours Later

TABLE 9

Reproduceability of Stress Decay Data

Polymer lot: WSR-301 (W-1006-A-01)

Concentration (wt. %) 0.41

Time (min)	Bob Speed Setting				
	1(1)	1(2)	3(1)	3(2)	3(3)
	Stress (dynes/cm^2)				
0					
.5	414	379	184	195	188
1	389	363	181	189	182
2	373	363	178	186	176
3	365	363	175	181	173
4	365	355	172	178	168
5	365	355	169	176	165
6	357	347	167	173	164
7	357	339	165	173	162
8	349	330	164	170	162
9	341	330	162	169	161
10	333	322	161	167	159
11	333	314	159	165	158
12	325	314	158	164	154
13	316	306	156	161	153
14	300	298	155	159	151
15	297	290	153	159	148
16	291	282	152	158	145
17	285	282	148	156	145
18	280	274	145	155	144
19	271	266	144	153	141
20	266	263	141	150	138
25	238	233	130	138	124
30	224	217	119	122	117
35	210	206	113	110	107
38			105		
39	206				
40		200			100
45		195			96
50					96
55					96

(1) Initial Run

(2) Immediate Repeat Run

(3) Repeat Run 24 Hours Later

TABLE 10

Stress Decay Data

Polymer lot: WSR 301 (1227-A-01)

Concentration (wt. %) 0.14%

Time (min)	Bob Speed Setting 1	2	3	6	9	18	27	54	81	162
	Stress (dynes/cm^2)									
0										
.5	127	60	42							
1	121	59	40							
2	114	56	39							
3	111	53	39							
4	110	53	38							
5	110	51	37							
6	110	51	37							
7	108									
21	101									
27			32							
53		40								
66			23							
68	88									
92		37								
108	84									
119		35								
125			22							
138	83									
163	80									
167		34								
188	80									
198			22							

TABLE 11

Stress Decay Data

Polymer lot: WSR 301 (1227-A-01)

Concentration (wt. %) 0.41

Time (min)	Job Speed Setting 1	2	3	6	9	18	27	54	81	162
	Stress (dynes/cm^2)									
0										
.5	308	164	121	77						
1	292	154	113	73						
2	276	138	105	68						
3	252	120	98	64						
4	244	114	91	60						
5	235	111	85	59						
6	230	107	82	57						
7	225		81	56						
8	221		81	56						
9	219		79	56						
10	215		79	54						
11	213			54						
12	208									
47	153	87								
68	151									
75		84								
78				45						
97	148									
104		83								
106				45						
122				44						
142			63							
150				44						
189				43						
194	146									
211				43						
255			63							

TABLE 12

Stress Decay Data

Polymer lot: WSR 301 (1227-A-01)

Concentration (wt. %) 0.70

Time (min)	Bob Speed Setting 1	2	3	6	9	18	27	54	81	162
	Stress (dynes/cm^2)									
0										
.5	413	281	229	151						
1	395	269	219	148						
2	358	250	206	142						
3	350	236	195	139						
4	350	227	189	136						
5	342	223	184	130						
6	[illegible]	218	181	128						
7	342	216	178	125						
8	342	215	175	122						
9	342	213	172	121						
10	342	210	167	119						
11		207	166	119						
12		204	165	118						
13		201	164							
14		199	164							
15		198	164							
16		198								
17		196								
18		195								
19		195								
20	302									
30				113						
31	294									
33			155							
42				111						
57		178								
63			146							
77	274			104						
81		175								
95			144							
105		174								
115	269									
120				102						
150			142							
160				100						
166		173								
173	263									
180				97						
183			139							
195				97						
220	259									
229			138							
253	257									
259	25[illegible]									

TABLE 13

Stress Decay Data

Polymer lot: WSR 301 (1227-A-01)

Concentration (wt. %) 1.03

Time (min)	Bob Speed Setting 1	2	3	6	9	18	27	54	81	162
	Stress (dynes/cm^2)									
0										
.5	842	518	348	276						
1	810	502	348	274	212					
2	761	478	334	273	212					
3	745	446	332	270	211					
4	721	437	324	263	208					
5	697	429	316	258	207					
6	693	429	316	254						
7	689	421	316	253						
8	680	413	316	251						
9	664		316	250						
10	648		316	248						
11				246						
12				245						
13				244						
14				244						
15				243						
16				243						
17										
18		389								
20			309							
22			309							
25					193					
26				237	193					
29		373								
30	543									
32			300							
37				234						
40		369			188					
54				227						
70	527									
81				220						
82			277							
88		348								
90					181					
109	527									
117			270							
125					178					
141			269							
160			269	204						
182			264							
186					173					
208			264							
263					167					
291					167					

TABLE 14

Reproduceability of Stress Decay Data

Polymer lot: WSR-301 (W-1227-A-01)

Concentration (wt. %) 0.14

Time (min)	Bob Speed Setting $_1$(1)	Bob Speed Setting $_1$(2)
	Stress (dynes/cm^2)	
0		
0.5	127	128
1	121	122
2	114	117
3	111	114
4	110	113
5	110	113
6	110	113
7	108	113
8		111
9		111
10		111
20		102
21	101	
35		95
68	88	
80		87
108	84	
110		85
120		83
138	83	
163	80	
165		80
178		80
188	80	

(1) Initial Run

(2) Repeat Run 24 Hours Later

TABLE 15

Reproduceability of Stress Decay Data

Polymer lot: WSR-301 (W-1227-A-01)

Concentration (wt. %) 0.41

Time (min)	Bob Speed Setting $2^{(1)}$	Bob Speed Setting $2^{(2)}$
	Stress (dynes/cm^2)	
0		
0.5	164	165
1	154	156
2	138	140
3	120	125
4	114	117
5	117	116
6	107	116
7		114
8		111
9		110
10		108
11		105
12		103
47	87	
68		87
75	84	
104	84	

(1) Initial Run

(2) Repeat Run 24 Hours Later

TABLE 16

Reproduceability of Stress Decay Data

Polymer lot: WSR-301 (W-1227-A-01)

Concentration (wt. %) 0.70

Time (min)	Bob Speed Setting			
	2(1)	2(2)	3(1)	3(2)
	Stress (dynes/cm^2)			
0				
0.5	281	286	229	224
1	269	274	219	216
2	250	255	206	204
3	236	243	195	192
4	227	233	189	181
5	223	227	184	178
6	218	224	181	175
7	216	219	178	173
8	215	216	175	171
9	213	215	172	168
10	210	213	167	165
11	207	212	166	
12	204	210	165	
13	201	210	164	
14	199	209	164	
15	198	209	164	
16	198	208		
17	196	206		
18	195	205		
19	195	203		
20		202		
25		193		
33			155	
57	178			
63			146	
81	175			
95			144	
105	174			
150			142	
166	173			
183			139	
229			138	

(1) Initial Run

(2) Repeat Run 24 Hours Later

12.0 Appendix V. Power Law Analysis of Miscellaneous Preliminary Data

Early in the program a number of preliminary experiments were performed as part of the processes of equipment familiarization and development of analytical techniques. The results of several of these are included here.

Experiments were performed on three samples of concentrated (1% nominal) WSR-301 solutions. These samples are designated as:

Sample A: Prepared in the vortex mixer using ordinary tap water. 72 hours set-up after initial mixing.

Sample B: Boiling water method. Measurements made within two hours.

Sample C: Similar to B, with some variations.

All samples were prepared with powder which was at <u>least</u> one year old. Limiting viscosities over various shear rate ranges were obtained with the three samples. The results are summarized in Figure 59 where shear stress is plotted as a function of shear rate. The liniarity of the curves over the entire shear rate range of about 0.2 to 250 sec^{-1} is further justification of the power-law assumption. The power-law constants thus determined were:

Sample A: $\tau = 7.8D^{0.54}$

Sample B: $\tau = 18.2D^{0.51}$

Sample C: $\tau = 9.8D^{0.54}$

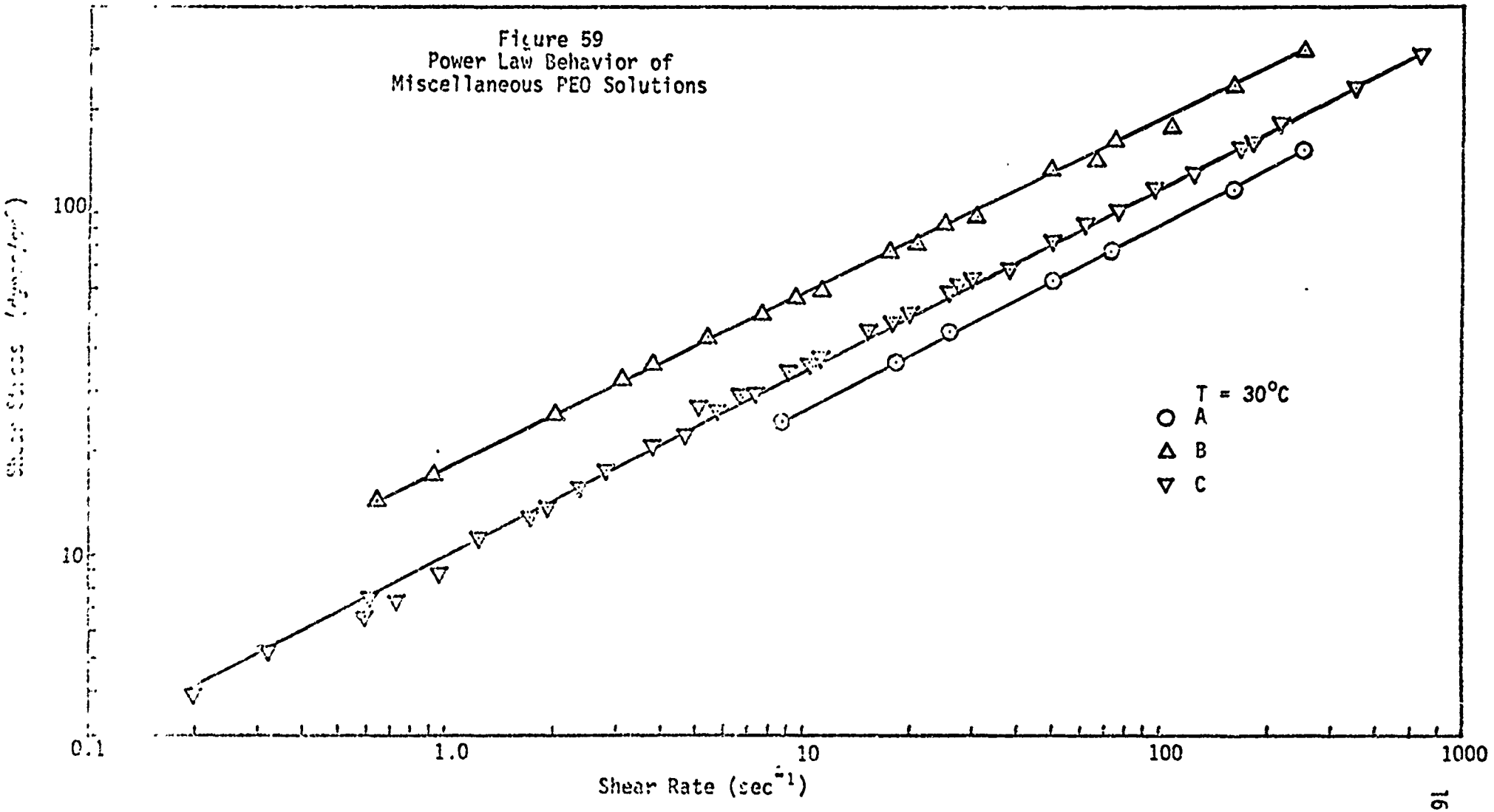

Figure 59
Power Law Behavior of
Miscellaneous PEO Solutions